Dry Deposition of Ozone over Land: Processes, Measurement, and Modeling

Olivia E. Clifton[1], **Arlene M. Fiore**[2], **William J. Massman**[3], **Colleen B. Baublitz**[2], **Mhairi Coyle**[4], **Lisa Emberson**[5], **Silvano Fares**[6], **Delphine K. Farmer**[7], **Pierre Gentine**[8], **Giacomo Gerosa**[9], **Alex B. Guenther**[10], **Detlev Helmig**[11], **Danica L. Lombardozzi**[1], **J. William Munger**[12], **Edward G. Patton**[1], **Sally E. Pusede**[13], **Donna B. Schwede**[14], **Sam J. Silva**[15], **Matthias Sörgel**[16], **Allison L. Steiner**[17], **Amos P. K. Tai**[18]

[1]National Center for Atmospheric Research, Boulder, CO, USA.

[2]Department of Earth and Environmental Sciences, Columbia University, and Lamont-Doherty Earth Observatory of Columbia University, Palisades, NY, USA.

[3]USDA Forest Service, Rocky Mountain Research Station, Fort Collins, CO, USA.

[4]Centre for Ecology and Hydrology, Edinburgh, Bush Estate, Penicuik, Midlothian, UK and The James Hutton Institute, Craigibuckler, Aberdeen, UK.

[5]Stockholm Environment Institute, Environment Department, University of York, York, UK.

[6]Council of Agricultural Research and Economics, Research Centre for Forestry and Wood, and National Research Council, Institute of Bioeconomy, Rome, Italy.

[7]Department of Chemistry, Colorado State University, Fort Collins, CO, USA.

[8]Department of Earth and Environmental Engineering, Columbia University, New York, NY, USA.

[9]Dipartimento di Matematica e Fisica, Università Cattolica del S. C., Brescia, Italy.

[10]Department of Earth System Science, University of California, Irvine, CA, USA.

[11]Institute of Alpine and Arctic Research, University of Colorado at Boulder, Boulder, CO, USA.

[12]School of Engineering and Applied Sciences and Department of Earth and Planetary Sciences, Harvard University, Cambridge, MA, USA.

[13]Department of Environmental Sciences, University of Virginia, Charlottesville, VA, USA.

[14]U.S. Environmental Protection Agency, National Exposure Research Laboratory, Research Triangle Park, NC, USA.

[15]Department of Civil and Environmental Engineering, Massachusetts Institute of Technology, Cambridge, MA, USA.

[16]Max Plank Institute for Chemistry, Atmospheric Chemistry Department, Mainz, Germany.

[17]Department of Atmospheric, Oceanic and Space Sciences, University of Michigan, Ann Arbor, MI, USA.

[18]Earth System Science Programme, Faculty of Science, and State Key Laboratory of Agrobiotechnology, The Chinese University of Hong Kong, Hong Kong SAR, China.

Abstract

Dry deposition of ozone is an important sink of ozone in near surface air. When dry deposition occurs through plant stomata, ozone can injure the plant, altering water and carbon cycling and reducing crop yields. Quantifying both stomatal and nonstomatal uptake accurately is relevant for understanding ozone's impact on human health as an air pollutant and on climate as a potent short-lived greenhouse gas and primary control on the removal of several reactive greenhouse gases and air pollutants. Robust ozone dry deposition estimates require knowledge of the relative importance of individual deposition pathways, but spatiotemporal variability in nonstomatal deposition is poorly understood. Here we integrate understanding of ozone deposition processes by synthesizing research from fields such as atmospheric chemistry, ecology, and meteorology. We critically review methods for measurements and modeling, highlighting the empiricism that underpins modeling and thus the interpretation of observations. Our unprecedented synthesis of knowledge on deposition pathways, particularly soil and leaf cuticles, reveals process understanding not yet included in widely-used models. If coordinated with short-term field intensives, laboratory studies, and mechanistic modeling, measurements from a few long-term sites would bridge the molecular to ecosystem scales necessary to establish the relative importance of individual deposition pathways and the extent to which they vary in space and time. Our recommended approaches seek to close knowledge gaps that currently limit quantifying the impact of ozone dry deposition on air quality, ecosystems, and climate.

Plain Language Summary

The removal of tropospheric ozone at Earth's surface (often called dry deposition) is important for our understanding of air pollution, ecosystem health, and climate. Several processes contribute to dry deposition of ozone. While we have basic knowledge of these processes, we lack the ability to robustly estimate changes in ozone dry deposition through time and from one place to another. Here we review ozone deposition processes, measurements, and modeling, and propose steps necessary to close gaps in understanding. A major conclusion revealed by our review is that most deposition processes can be fairly well described from a theoretical standpoint, but the relative importance of the various processes remains uncertain. We suggest that progress can be made by establishing multiyear measurements of ozone dry deposition at a limited set of sites around the world and coordinating these measurements with laboratory and field experiments that can be integrated with theory through carefully designed modeling studies.

Keywords

1. Introduction

Dry deposition, or removal at the Earth's surface, is a primary sink of ozone in the troposphere where ozone is an air pollutant, greenhouse gas, and central to the atmospheric oxidative capacity. Ozone dry deposition occurring through plant stomata (the pores on

leaves controlling gas exchange) damages plants. While the potential for ozone dry deposition to influence air quality, ecosystems, and crop yields has been recognized for decades (e.g., Hosker & Lindberg, 1982; Reich, 1987; Rich, 1964; Turner et al., 1973), mechanistic understanding of ozone dry deposition is incomplete. Figure 1 illustrates processes contributing to ozone dry deposition and how changes in ozone dry deposition impact tropospheric chemistry, air quality, ecosystems, and climate. In this review, we synthesize knowledge of the controlling processes, review measurement and modeling approaches, and recommend approaches to close knowledge gaps.

To undergo dry deposition, atmospheric turbulence transports ozone close to a given surface and then ozone must move through the quasi-laminar boundary layer around that surface. The rate of ozone uptake by a particular surface depends on the surface's properties. Ozone dry deposition occurs not only through stomatal uptake (Rich et al., 1970), but also through other nonstomatal deposition pathways including uptake by leaf cuticles (Rondón et al., 1993; Sun, S., Moravek, Trebs, et al., 2016), soil (Garland & Penkett, 1976; Turner et al., 1974), snow (Helmig, Bocquet, Cohen et al., 2007; Helmig, Ganzeveld, Butler, et al., 2007), water (Gallagher et al., 2001; Helmig et al., 2012), and man-made surfaces (Shen & Gao, 2018). Both surfaces with high-destruction rates (e.g., vegetation) and spatially-extensive surfaces with low destruction rates (e.g., snow, water) are relevant to the tropospheric ozone budget and large-scale ozone pollution (Clifton, 2018; Ganzeveld et al., 2009; Hardacre et al., 2015; Helmig, Ganzeveld, Butler, et al., 2007).

Quantifying stomatal ozone uptake is not only important for estimating ozone removal, but also for understanding the plant response to ozone. Stomatal ozone uptake injures plants by generating reactive oxygen species that can induce cell death and lesions and thus accelerate senescence (Ainsworth et al., 2012; Fiscus et al., 2005). Reactive oxygen species also impair photosynthetic enzyme activities, enhance respiration, and interfere with carbon allocation (Ainsworth et al., 2012; Fiscus et al., 2005). Ozone injury to plants alters terrestrial carbon and water cycling (Arnold et al., 2018; Franz et al., 2017; Hoshika et al., 2015; Lombardozzi et al., 2015; Oliver et al., 2018; Sadiq et al., 2017; Sun, G., et al., 2012; Yue & Unger, 2014), which influences boundary-layer meteorology (Li, J., Mahalov, & Hyde, 2016, 2018; Sadiq et al., 2017; Super et al., 2015) and climate (Kvalevåg & Myhre, 2013; Sitch et al., 2007) and increases surface ozone due to a reduced stomatal ozone sink (Li, J., Mahalov, & Hyde, 2016, 2018; Sadiq et al., 2017; Zhou, S. S., et al., 2018).

Numerical simulations of tropospheric ozone, including high ozone pollution episodes and background ozone levels, are sensitive to model descriptions of ozone dry deposition (Anav et al., 2018; Beddows et al., 2017; Bela et al., 2015; Campbell et al., 2019; Clifton, 2018; Emberson et al., 2013; Falk & Søvde Haslerud, 2019; Helmig, Ganzeveld, Butler, et al., 2007; Hogrefe et al., 2018; Huang et al., 2016; Lin, J.-T., et al., 2008; Lin, M., et al., 2017, 2019; Matichuk et al., 2017; Silva & Heald, 2018; Solberg et al., 2008; Tang et al., 2011; Val Martin et al., 2014; Vautard et al., 2005; Vieno et al., 2010; Walker, 2014; Wild, 2007; Wong, A. Y. H., et al., 2019). However, many widely used ozone dry deposition schemes do not represent processes mechanistically or capture observed spatiotemporal variations (Clifton et al., 2017; Kavassalis & Murphy, 2017; Pleim & Ran, 2011; Silva & Heald, 2018; Silva et al., 2019; Travis & Jacob, 2019). Among models, differences are two- to three-fold

in estimates of ozone dry deposition for a given location (Hardacre et al., 2015; Schwede et al., 2011; Wu, Z., et al., 2018; Wong, A. Y. H., et al., 2019) and in estimates of the global annual tropospheric ozone loss through dry deposition (Hardacre et al., 2015; Stevenson et al., 2006; Wild, 2007; Young et al., 2013, 2018). Understanding of the contribution of individual deposition pathways to ozone dry deposition is incomplete, but key for building mechanistic representation in the large-scale models used to quantify the effects of ozone dry deposition across earth systems from hourly to centennial time scales.

Below, we address the following questions:

1.   What approaches are currently used to measure and model ozone dry deposition?

2.   What is current understanding of the processes controlling ozone dry deposition based on theory, observations, and modeling?

3.   What major knowledge gaps and uncertainties exist with respect to (1) and (2)?

4.   How can we most rapidly advance knowledge of ozone dry deposition and its impacts on air quality, vegetation, and climate?

We examine stomatal, leaf cuticular, soil, and snow deposition pathways, as well as turbulent transport and fast ozone loss through ambient chemistry. Not only is fast chemistry important for building understanding of ozone dry deposition from ozone flux measurements, but it also leads to formation of secondary aerosol precursors (e.g., Bouvier-Brown et al., 2009; Kurpius & Goldstein, 2003). To limit the scope of our review, we do not cover transport through the quasi-laminar boundary layer adjacent to surfaces. However, the magnitude of the quasi-laminar transport can widely vary among model parameterizations, and thus uncertainty in this process may be nonnegligible (e.g., Brutsaert, 1979; Schuepp, 1993; Massman, 1999, 2004). Differences across models (e.g., Choudhury & Monteith, 1988; Jensen & Hummelshøj, 1995, 1997; Massman, 1999; Wesely & Hicks, 1977), the impacts of canopy structure, turbulence, and leaf properties (e.g., aerodynamics, morphology, presence of water) on transport (e.g., Cook & Viskanta, 1968; Daudet et al., 1999; Stokes et al., 2006), and scaling from leaf to canopy should be emphasized in future research. While in this review we discuss the deposition pathways considered to be most important for terrestrial ozone dry deposition impacts on tropospheric chemistry, air quality, and vegetation, we emphasize that better understanding of ozone dry deposition to other terrestrial surfaces, such as urban surfaces, lakes, rivers, branches, and leaf litter, is needed.

2.   Measuring Ozone Dry Deposition

2.1   History of Measurements and Survey of Current Datasets

Methods for field measurement of ozone dry deposition have been available since the 1950s (e.g., Regener, 1957). In the 1950s and 1960s, ozone dry deposition was typically measured using gradient methods during short campaigns (e.g., Galbally, 1971). By the 1970s, the eddy covariance (EC) approach – the preferred approach for measuring turbulent fluxes (Hicks et al., 1989; Meyers & Baldocchi, 2005) – became possible with fast ozone analyzers deployed on masts and towers (e.g., Wesely et al., 1978) and aircraft (e.g., Lenschow et al., 1980). Growing recognition of the importance of biogeochemical cycles led to workshops in

the late 1970s and 1980s recommending research priorities for fluxes of ozone, carbon dioxide, and other constituents (Georgii, 1989; Hicks et al., 1980; Hosker & Lindberg, 1982; Lenschow & Hicks, 1989). In particular, a 1987 workshop on trace gas and particle fluxes recommended that future studies "span both diurnal and seasonal cycles" and investigate "surfaces of importance to global budgets" (Lenschow & Hicks, 1989).

Likely as the result of momentum in the research community and support from funding agencies, the number of sites with ecosystem-scale ozone fluxes increased from the late 1980s into the next decade (Figure 2). The first annual record of continuous hourly ozone and carbon dioxide EC began in the early 1990s at Harvard Forest in the northeastern United States (Munger et al., 1996; Wofsy et al., 1993). Emphasis on ozone dry deposition in the community waned around the millennium, as evident from stabilizing number of sites with measurements after the mid-1990s (very low numbers after 2014 may reflect the time needed to report and analyze data).

Sites with ozone fluxes primarily reside in Europe and North America (Figure 2), indicating a paucity of knowledge on ozone dry deposition for most parts of the world. More consistent emphasis on ozone fluxes in Europe (Figure 2) may reflect regional initiatives to quantify the impact of ozone on ecosystems. While the observational record captures a variety of land use/land cover (LULC) types, most data are for crops and forests (Figure 3) and the datasets for particularly undersampled LULC types tend to be very short term (i.e., days) (Table A1).

Synthesizing knowledge and testing hypotheses across ozone flux datasets are fundamental to advancing understanding of ozone dry deposition. However, current knowledge does not reflect a meta-analysis of all, or even the majority, of datasets in Table A1. While Table A1 provides a record for future studies to identify potentially available ozone flux data, the lack of a central archive limits efforts to analyze multiple records. Differences in instrumentation, a lack of coordinated protocols across datasets, and in some cases missing complementary measurements also limit the utility of older data and meaningful syntheses across records.

Despite the common emphasis in the 1970s and 1980s on the need to establish long-term flux observations for gases like ozone and carbon dioxide, ozone flux data lag far behind carbon dioxide flux data in the number, dataset length, and diversity of sites. Carbon dioxide fluxes are available for around 900 sites for over 7000 combined site years of data, including many sites with more than a decade of data (Chu et al., 2017). In contrast, only 114 sites have ozone fluxes, only 11 sites have more than 5 years of data, and none exceed 15 years (Table A1). There are likely different needs in terms of carbon dioxide versus ozone flux data, but gaining a robust understanding of interannual variability and trends in ozone dry deposition and accurately interpreting the observational anomalies challenging current understanding require long-term data. The recent National Academies of Sciences, Engineering, and Medicine (NASEM) report on "*The Future of Atmospheric Chemistry Research*" also emphasizes the need for long-term fluxes of reactive gases and aerosols (NASEM, 2016).

One issue impeding ozone EC measurements is the fast ozone analyzers meeting the stringent criteria of the EC technique are generally resource intensive to operate. The lack of

simple reliable analyzers may in part explain why ozone EC measurements have been limited to research groups with atmospheric chemistry and physics expertise while the ecological community widely adopted carbon dioxide EC, catalyzing the development of a larger network. Motivating the development of new measurement techniques and an observational network is also challenging for an interdisciplinary subject such as ozone dry deposition.

A misconception that the mechanisms controlling ozone dry deposition are well understood may have also contributed to ozone flux measurements losing luster. While the literature widely states that stomatal uptake governs ozone dry deposition over physiologically active vegetation (e.g., Baldocchi et al., 1987; Bauer et al., 2000; Erisman et al., 1994; Mills et al., 2018; Potier et al., 2015), observationally based estimates of the stomatal fraction of ozone dry deposition show a co-dominant role for deposition through nonstomatal pathways (Figure 4) with stomatal uptake as 45% of the total on average.

Not only is nonstomatal uptake nonnegligible, but it is also highly variable. Observationally based studies illustrate unexpected variations in nonstomatal deposition in diel cycles (Coe et al., 1995; Rondón et al., 1993) including over soil and snow (Fumagalli et al., 2016; Helmig, Cohen, Bocquet, et al., 2009; Stella, Loubet, Lamaud, et al., 2011; Stella et al., 2019), year-to-year variability (Clifton et al., 2017; Rannik et al., 2012), after rain and dew (Fuentes et al., 1992; Potier et al., 2015), and spatially (Clifton et al., 2019; Godowitch, 1990; Lenschow et al., 1981; Mahrt et al., 1995; Wolfe et al., 2015). Measurements also show that ambient chemistry with unmeasured biogenic volatile organic compounds (BVOCs) influences ozone flux observations (Goldstein et al., 2004; Kurpius & Goldstein, 2003; Wolfe et al., 2011).

Unconstrained variations in ozone dry deposition challenge the ability to attribute changes in tropospheric ozone to other processes (e.g., sources) accurately. Capturing unexpected variability with ozone flux records allows the community to build hypotheses about controlling processes, target laboratory and field measurements (Altimir et al., 2006; Fuentes & Gillespie, 1992; Fumagalli et al., 2016; Pleijel et al., 1995; Potier et al., 2017; Sun, S., Moravek, Trebs, et al., 2016; Sun, S., Moravek, von der Heyden, et al., 2016), and build mechanistic models (e.g., Potier et al., 2015).

Mechanistic modeling is fundamental for interpreting observed ozone fluxes because the ozone flux integrates many different processes, and techniques to isolate individual processes are limited. For example, isolating nonstomatal deposition and fast in-canopy chemistry from the ozone flux strongly relies on residual analysis, leading to uncertainty in variations and the relative importance of a given process. Together with the statistical power provided by long-term data, mechanistic modeling is also instructional in informing ozone dry deposition schemes, which currently rely heavily on poorly constrained empirical relationships (e.g., Tuovinen et al., 2004; Wesely, 1989; Zhang, L., et al., 2002).

2.2   Measurement Techniques

Here we review approaches for measuring ozone dry deposition. We discuss EC, flux gradient, and modified Bowen Ratio techniques, and chamber and isotopic methods. We

detail the fast ozone analyzers needed for EC because their cost, maintenance requirements, and limited availability may thwart efforts to measure dry deposition through ozone EC, the most fundamental and direct method for measuring turbulent exchange (e.g., Hicks et al., 1989; Meyers & Baldocchi, 2005).

2.2.1   Micrometeorological Approaches—We start with the Reynolds-averaged mass continuity equation for ozone at a given location under turbulent conditions (e.g., Stull, 1988) to elucidate the strengths and limitations of a vertical turbulent ozone flux measurement representing ozone dry deposition.

$$
\frac{\partial \overline{O_3}}{\partial t} = -\left(\overline{u}\frac{\partial \overline{O_3}}{\partial x} + \overline{v}\frac{\partial \overline{O_3}}{\partial y} + \overline{w}\frac{\partial \overline{O_3}}{\partial z} \right) - \left(\frac{\partial \overline{u'O_3'}}{\partial x} + \frac{\partial \overline{v'O_3'}}{\partial y} + \frac{\partial \overline{w'O_3'}}{\partial z} \right) + \overline{P}_{O_3} - \overline{L}_{O_3} \\
- \overline{Dep}_{O_3}
\tag{1}
$$

$\overline{O_3}$ is ozone concentration; u, v, and w are wind velocity in longitudinal (x), lateral (y), and vertical (z) directions; $\overline{P}_{O_3}$ is chemical production of ozone; $\overline{L}_{O_3}$ is chemical loss of ozone; $\overline{Dep}_{O_3}$ is dry deposition of ozone. Overbars represent temporal averages and primes represent fluctuations from the temporal average.

In the absence of both subsidence ($\overline{w} = 0$) and horizontal advection of ozone ($\overline{u}\frac{\partial \overline{O_3}}{\partial x} = \overline{v}\frac{\partial \overline{O_3}}{\partial y} = 0$), equation (1) simplifies to:

$$
\frac{\partial \overline{O_3}}{\partial t} = -\frac{\partial F_{O_3, z}}{\partial z} + \overline{P}_{O_3} - \overline{L}_{O_3} - \overline{Dep}_{O_3}
\tag{2}
$$

We now refer to the vertical turbulent flux of ozone ($\overline{w'O_3'}$) as $F_{O_3, z}$. Integrating equation (2) from the ground to the height of measurement (h) yields:

$$
\int_0^h \frac{\partial \overline{O_3}}{\partial t} dz = -\int_0^h \frac{\partial F_{O_3, z}}{\partial z} dz + \int_0^h \overline{P}_{O_3} dz - \int_0^h \overline{L}_{O_3} dz - \int_0^h \overline{Dep}_{O_3} dz
\tag{3}
$$

where

$$
\int_0^h \frac{\partial F_{O_3, z}}{\partial z} dz = (F^h_{O_3, z} - F^0_{O_3, z})
$$

$F^h_{O_3, z}$ represents the ozone flux at h and $F^0_{O_3, z}$ represents ozone flux at the ground. The community frequently assumes that $F^h_{O_3, z}$ represents ozone dry deposition beneath h:

$$
F^h_{O_3, z} = F^0_{O_3, z} - \int_0^h \overline{Dep}_{O_3} dz
\tag{4}
$$

For this assumption to be valid, equation (3) demonstrates two additional conditions need to be satisfied (or the contributions from each term quantified adequately).

The first condition is negligible ambient ozone chemistry below h $\left(\int_0^h \overline{P}_{O_3} dz = \int_0^h \overline{L}_{O_3} dz = 0\right)$. This is not always true; we further discuss this in section 4.5.

The second condition is stationary ozone concentration on the time frame of the averaging operator $\left(\int_0^h \frac{\partial \overline{O_3}}{\partial t} dz = 0\right)$. Storage, or ozone temporarily accumulating within the canopy (i.e., between the ground surface and h), violates this condition. Estimating storage requires ozone concentration measurements at different heights in the canopy (the number of heights needed depends on how much ozone changes vertically). An assumption inherent to using one concentration profile is that the location represents the ecosystem sampled by the vertical turbulent flux measurement. This assumption has been shown to be limited for carbon dioxide (e.g., Nicolini et al., 2018).

Storage is considered to be nonnegligible in forest canopies. Not many studies give estimates of ozone storage, but storage tends to overestimate ozone dry deposition in forests during morning and underestimate during evening, with the influence averaging out over a day (e.g., Finco et al., 2018; Munger et al., 1996; Rummel et al., 2007). Specifically, the bias is <20% at Harvard Forest (Munger et al., 1996) and Bosco Fontana in Italy (Finco et al., 2018), but may be ~50% at a tropical forest in Reserva Biológica Jarú (Rummel et al., 2007).

2.2.1.1   Eddy Covariance: Ozone EC systems are usually custom built by research groups and require atmospheric chemistry and physics expertise (e.g., Weinheimer, 2006). Because there is no formal recipe for their design, we present necessary considerations for ozone and refer the reader to previous reviews on EC (e.g., Aubinet et al., 2012; Lee et al., 2004).

A first consideration is to measure the vertical wind velocity and ozone concentration at a frequency high enough to resolve the full range of eddies contributing to vertical transport. In particular, the ozone analyzer has to be sufficiently accurate to resolve concentration variability due to turbulence (10–60 Hz) but also ambient chemistry, which may require a faster measurement. Instrument frequency responses can be evaluated by comparing spectra and co-spectra for ozone with those for heat and momentum. Derivation of transfer functions based on the co-spectra enables correction for any loss of high-frequency contributions (e.g., Aubinet et al., 2012; Lee et al., 2004).

Current ozone analyzers used for EC are based on chemiluminescence, or light production via chemical reaction, due to their fast response times. While there is a method to correct ozone fluxes measured with an ultraviolet (UV) photometric ozone analyzer, the empirical correction is large and random uncertainty in the daytime ozone flux is 60% (Wohlfahrt, Hörtnagl, Hammerle, et al., 2009). Reported frequency response corrections from fast ozone analyzers typically range from 5–30% (Bauer et al., 2000; Keronen et al., 2003; Horváth et al., 2017; Munger et al., 1996; Plake, Stella, Moravek et al., 2015; Zhu et al., 2015).

A second consideration is that duration of the averaging interval must be long enough to sample the slowest turbulent eddies contributing to exchange, but short enough that ozone concentration remains stationary. Sampling or random error may be an important contribution to uncertainty in ozone EC. For example, the sampling error ranges from 23 to 33% for one analyzer during different time periods at five sites in the eastern United States (Finkelstein & Sims, 2001) and from 10 to 20% with another analyzer at Hyytiälä in southern Finland (Keronen et al., 2003; Rannik et al., 2009).

Third, there are not currently open-path fast-response ozone analyzers. High instrument flow rates are thus needed to minimize residence time in measurement volumes and ozone loss in the sample stream due to reaction with walls or other compounds, as well as achieve a turbulent flow, which reduces attenuation in the tubing (Lenschow & Raupach, 1991). When the required flow rate is too high for the analyzer to accommodate, excess flow can be pulled through a bypass pump. For pressure-sensitive analyzers (e.g., when the reaction required to detect ozone is sensitive to pressure), linking the bypass flow to a pressure controller may be necessary to maintain constant pressure at the analyzer inlet.

Chemiluminescence analyzers vary by reagent phase: gas, solid ("dry"), and liquid ("wet"). While chemiluminescence analyzers have fast response times and high sensitivity, they can be expensive (gas) or need frequent maintenance and calibration (dry and wet), adding labor costs and down time. Gas chemiluminescence leverages the reactions between ozone and ethene (e.g., Desjardins et al., 1995; Droppo, 1985; Duyzer et al., 1983; Munger et al., 1996) or nitric oxide (NO) (e.g., Bariteau et al., 2010; Eastman & Stedman, 1977; Pearson, 1990; Stedman et al., 1972). While several gas chemiluminescence analyzers were commercially available in the past, to our knowledge there is only one currently available (Table 1).

Dry chemiluminescence uses a solid dye that emits light upon reaction with ozone. Not requiring toxic (e.g., NO) or flammable (e.g., ethene) compressed gases, dry chemiluminescence is advantageous over gas chemiluminescence. Dry analyzers also can be smaller and only require low power due to the physical configuration of their electronic components and the pumps or fans used to sample air. A coumarin solid dye, which emits a blue light upon reaction with ozone, is typically used for dry chemiluminescence (e.g., Muller et al., 2010). The photomultiplier tubes for detection of blue light are less expensive than the ones for red light needed for other common gas or dry chemiluminescence techniques. A dry analyzer used to be offered by Gesellschaft Für Angewandte Systemtechnik (GFAS) (Güsten et al., 1992; Güsten & Heinrich, 1996). Several groups made or used GFAS clones (e.g., Bauer et al., 2000; Coyle, 2005; Coyle et al., 2009; Cros et al., 2000; Finco et al., 2018; Kurpius et al., 2002; Mészáros, Horváth, Weidinger, et al., 2009). Currently, there are three dry analyzers commercially available, including one GFAS clone (Table 1).

Disadvantages of dry chemiluminescence include degradation of dye-impregnated discs (i.e., loss of ozone sensitivity) such that they need regular replacement (e.g., every few days). There is a 12% daily mean difference between ozone fluxes from a GFAS and a GFAS clone at Easter Bush in southern Scotland (Muller et al., 2010), suggesting analyzer performance and disc stability may be sources of uncertainty in ozone flux data. A new disc preparation

method extending disc field stability is described in Ermel et al. (2013) who show high ozone sensitivity can be maintained over threefold more disc ozone uptake. An extended disc stability means measurements can proceed either for longer without maintenance or in higher ozone environments with similar maintenance.

A second ozone analyzer, which can be a commonly used UV absorbance instrument, is always necessary in dry chemiluminescence setups to account for the changing disc sensitivity. Different techniques to calculate an absolute signal can lead to substantially different ozone fluxes, as shown by measurements at Easter Bush (Muller et al., 2010) and a Chinese wheat field (Zhu et al., 2015).

Wet chemiluminescence employs organic liquid dye that emits light upon reaction with ozone (e.g., Drummond et al., 1991; Keronen et al., 2003; Ray et al., 1986; Zona et al., 2014). In principle, wet chemiluminescence is a relative measurement (because the dye degrades), but with a substantial amount of liquid reagent in the bottle used for measurement, it can be considered absolute. The dye does need to recirculate (usually via a peristaltic pump), however, and recirculation often fails when the bottle is not close to full (Keronen et al., 2003). Depending on ozone concentration at the site, the bottle may only need to be refilled every few months to keep it near full though (Keronen et al., 2003).

The need for long-term ambient ozone concentration measurements not requiring much maintenance has driven the market towards instruments inherently too slow for EC. More robust and economical fast analyzers not requiring frequent maintenance or involving toxic or flammable consumables or compressed gases will enable more ozone EC measurements and thus faster progress towards improved understanding of ozone dry deposition.

2.2.1.2 Flux Gradient: The flux gradient technique requires determining the eddy diffusivity for ozone and the ozone concentration at two heights above a surface. Commonly-used slower ozone instruments (e.g., UV absorbance) are adequate for this technique, likely making the technique more affordable and simpler than ozone EC. However, the flux gradient method has several limiting assumptions. For example, it assumes K-theory and often eddy diffusivity for ozone (K_{o3}) equals eddy diffusivity for sensible heat. K-theory (or, first-order closure; e.g., Stull, 1988) assumes transport only occurs down the local mean gradient, but organized turbulent motions can transport material up- (or counter-) gradient.

$$F_{O_3}^h = -K_{o3}\frac{\partial \overline{O_3}}{\partial z}$$

(5)

The eddy diffusivity for sensible heat can be calculated by employing Monin-Obukhov Similarity Theory (MOST) (Businger et al., 1971; Högström, 1988). However, MOST does not hold in the roughness sublayer above vegetation (Raupach, 1979), which can extend higher than double the vegetation height (e.g., Cellier & Brunet, 1992; Harman & Finnigan, 2007; Thom, 1975). Most observed gradients are located below this height. Additionally, ozone is reactive and ambient chemistry may perturb the ozone gradient so assuming the

eddy diffusivity for ozone is equal to that for heat is not always valid (Fitzjarrald & Lenschow, 1983; Lenschow, 1982; Vilá-Guerau de Arellano & Duynkerke, 1992).

Using a single analyzer with switching or moveable inlets to sequentially sample concentrations at different heights for the ozone gradient measurement is preferred over separate analyzers for the different heights because the latter requires effort to eliminate biases between the analyzers. However, when the measurements are not simultaneous (i.e., one analyzer is used at multiple heights), then the gradient needs to be stable over the time required to obtain measurements at both heights. Otherwise there needs to be a correction for sequential sampling.

Inferring accurate ozone fluxes using the flux gradient technique is also challenging because ozone differences between the two heights may be very small and challenge the resolution and accuracy of the instrument (Businger, 1986). Maximizing the vertical distance between top and bottom heights to get larger differences helps (Arya, 2001), but both measurements must be in the surface layer with comparable footprints. Comparison of ozone EC and gradient fluxes over several ecosystems suggests fluxes and v_d from the flux gradient technique may be biased and not represent variations accurately (Duyzer & Westrate, 1995; Loubet et al., 2013; Mikkelsen et al., 2000; Muller et al., 2009; Wu, Z. Y., et al., 2015).

2.2.1.3 Modified Bowen Ratio: The approach commonly called the modified Bowen Ratio technique (Businger, 1986) is also used to infer ozone fluxes from an ozone concentration gradient (e.g., Leuning, Neumann, & Thurtell, 1979; Leuning, Unsworth, Neumann, et al., 1979; Mayer et al., 2011). The Bowen Ratio approach assumes similar turbulent diffusivities of ozone and of a reference quantity (i.e., another scalar, such as carbon dioxide) so the ozone flux can be calculated by a simple scaling of the flux of the reference quantity ("*ref*"):

$$F_{O_3}^h = F_{Ref}^h \frac{\frac{\partial \overline{O_3}}{\partial z}}{\frac{\partial \overline{C_{ref}}}{\partial z}} \tag{6}$$

The concentrations of ozone and the reference quantity ($\overline{C_{ref}}$) are from measurements at the same heights in the surface layer. The modified Bowen Ratio technique may be advantageous over the flux gradient technique because the modified Bowen Ratio technique does not directly require turbulent diffusivity estimates. While commonly used ozone UV absorbance instruments are likely adequate for this technique, this method requires detection of likely small gradients in ozone and the reference quantity. Previous work suggests substantial biases (50–100%) in ozone fluxes estimated with the modified Bowen Ratio technique with carbon dioxide fluxes relative to ozone EC at Harvard Forest (Wu, Z. Y., et al., 2015).

2.2.2 Chamber Methods—Chamber methods are employed to isolate ozone uptake to foliage, soil, water, and other surfaces in the field (Almand-Hunter et al., 2015; Altimir et al., 2002; Fumagalli et al., 2016; Gut et al., 2002; Horváth et al., 2006; Kaplan et al., 1988;

Kirkman et al., 2002; Meixner et al., 1997; Pilegaard, 2001; Remde et al., 1993; Tong et al., 2011; Unsworth et al., 1984; Wieser et al., 2012). However, previous work largely focuses on soil NO emissions (e.g., Gut et al., 2002; Horváth et al., 2006; Kaplan et al., 1988; Kirkman et al., 2002; Meixner et al., 1997; Remde et al., 1993) or plant response to ozone (e.g., Tong et al., 2011; Wieser et al., 2012) rather than ozone deposition processes.

For an open chamber, air is generally drawn into the chamber and the ozone concentration difference between the inlet and outlet is measured with a slow ozone instrument. The uptake rate to the surface is determined from the concentration difference, the known flow rate into the chamber, and volume of the chamber.

We emphasize the value of chamber methods for gaining mechanistic understanding of ozone dry deposition (e.g., Altimir et al., 2006; Fumagalli et al., 2016). However, we note that chamber footprint is small (i.e., on the order of a meter or less), chambers modify microclimate, and ozone chemistry may occur in the chamber air or with chamber walls and tubing (Breuninger at al., 2012; Pape et al., 2009). In the field, multiple chambers are necessary to account for inhomogeneity across a wider area (e.g., the footprint of a flux tower) as well as understand the robustness of observed dependencies on environmental conditions.

The strength in using chamber measurements to separate the canopy portion of the ozone flux from the ground ozone uptake (see equation (4)) (e.g., Duyzer et al., 2004; Finco et al., 2018; Rummel et al., 2007) or to serve as a surrogate to ozone EC (Almand-Hunter et al., 2015; Plake, Stella, Moravek, et al., 2015) hinges on the ability to obtain an estimate spatially representative of the ecosystem, to remove the effects of turbulent transport modified by the chamber, and to estimate in-canopy turbulent transport and the contribution from fast ambient chemistry to the ecosystem-scale ozone fluxes.

2.2.3   Isotopic Methods—Isotopic experiments in the laboratory and field may be able to pinpoint the primary sites of ozone surface reactions and thus improve understanding of ozone deposition pathways (Subke et al., 2009; Toet et al., 2009). Subke et al. (2009) present a method for adding ^{18}O into an electric discharge ozone generator and using a silica gel to separate ^{18}O ozone from ^{18}O O_2. However, ^{18}O from the generated ozone leads to ^{18}O enriched water vapor as well as other gases (e.g., O_2) that do not necessarily remain on a surface, complicating estimates of deposited ozone (Toet et al., 2009). The authors conclude that better understanding of the reactions determining loss of ^{18}O ozone into other gases is needed for this technique to be useful for constraining ozone deposition pathways.

3.   Modeling Ozone Dry Deposition using Resistance Networks

We present common resistance network approaches for parameterizing ozone dry deposition in models considering vegetation as one big leaf and in models considering vertical variation in plant canopy structure. In general, resistance network approaches have many strengths. For example, resistance approaches are appropriate for modeling at different scales, are simple and adaptable, and allow for representing individual processes.

For big-leaf models, we describe both single- and dual-surface models. Dividing the negative ozone flux at height h $\left(F_{O_3}^h\right)$ by the ozone concentration at that height (O_{3h}) gives the ozone deposition velocity (v_d), a simple measure of the efficiency of ozone dry deposition:

$$v_d = -\frac{F^h{}_{O_3}}{O_{3h}} \tag{7}$$

The simplest possible resistance network for v_d is the single-surface big-leaf model (Figure 5a), which lumps all surfaces to which ozone deposits into a single surface:

$$v_d = (r_a + r_b + r_c)^{-1} \tag{8}$$

r_a is the bulk aerodynamic resistance; r_b is the bulk quasi-laminar boundary-layer resistance; r_c is the bulk surface resistance for the single-surface model. Due to the need to separate stomatal from nonstomatal deposition for modeling ozone impacts on plants, r_c in a single-surface big-leaf model is typically modeled in the following way, with the assumption that stomatal and the bulk nonstomatal surfaces are at the same height in the canopy:

$$r_c = \left(\frac{1}{r_{stom} + r_{meso}} + \frac{1}{r_{ns}}\right)^{-1} \tag{9}$$

r_{stom} is the resistance to uptake of ozone through diffusion into stomata; r_{meso} is the resistance to ozone reaction inside the leaf; r_{ns} is the resistance to all nonstomatal deposition pathways. Often, a residual r_{ns} is inferred using ozone fluxes and complementary micrometeorological measurements (i.e., to infer r_a, r_b, and r_{stom}) with this single-surface big-leaf approach.

The dual-surface big-leaf model (Figure 5b) considers two surfaces for dry deposition. In the context of a plant canopy, the two surfaces represented are typically leaves and soil, with all leaves considered to be at one height.

$$v_d = \left(r_a + \left(\frac{1}{r_{b,leaf} + r_{stom} + r_{meso}} + \frac{1}{r_{b,leaf} + r_{cut}} + \frac{1}{r_{ac} + r_{b,soil} + r_{soil,}}\right)^{-1}\right)^{-1} \tag{10}$$

$r_{b,leaf}$ is the resistance associated with transfer in the quasi-laminar boundary layer around leaves; r_{stom} and r_{meso} are defined for the single-surface big-leaf model; r_{cut} is the leaf cuticular resistance to ozone uptake; r_{ac} is the resistance associated with atmospheric transport through the canopy air space; $r_{b,soil}$ is the resistance in the quasi-laminar boundary layer around soil; r_{soil} is the resistance to ozone uptake by soil.

The big-leaf resistance network structure varies across different dry deposition schemes. For example, Wesely (1989) consider a bulk quasi-laminar boundary layer resistance for soil and leaves, which is added in series with the bulk r_a whereas Massman (2004) consider different quasi-laminar boundary layer resistances for soil versus leaves.

One big-leaf modeling shortcoming is no consideration of vertical variation in leaf properties and functioning (e.g., in response to canopy attenuation of solar radiation). Multilayer resistance models (Figure 5c) – where surface resistance (r_{surf}) is calculated at each level of the canopy (z) below canopy height (h_c) – are designed to address this issue:

$$r_{surf}(z) = \left(\frac{1}{r_{b,leaf}(z) + r_{stom}(z) + r_{meso}(z)} + \frac{1}{r_{b,leaf}(z) + r_{cut}(z)} \right)^{-1} \; if \; z \leq h_c \quad (11)$$

$$r_{surf}(0) = \left(\frac{1}{r_{b,\,soil} + r_{soil}} \right)^{-1} \; if \; z = 0 \quad (12)$$

To calculate v_d with this approach, the above r_{surf} parameterization needs to be embedded into a model considering ozone turbulent transport among canopy layers and between h_c and h. Turbulent transport could be simulated with a resistance approach or more explicitly.

Most ozone dry deposition schemes deployed in regional and global models use big-leaf approaches. Multilayer resistance approaches exist (e.g., Duyzer et al., 2004; Fares et al., 2019; Ganzeveld et al., 2002; Launiainen et al., 2013; Meyers et al., 1998; Potier et al., 2015; Wolfe & Thornton, 2011; Zhou, P. T., et al., 2017), but mostly are used in single-point models for interpreting field observations rather than modeling regional-to-global ozone dry deposition. An advantage of the multilayer approach is the ozone continuity equation can be calculated at every height and thus the influence of in-canopy chemistry (e.g., Ashworth et al., 2015; Wolfe et al., 2011) or turbulence (e.g., Chang et al., 2018; Patton et al., 2016; Pyles et al., 2000) explicitly resolved. We refer to the approach where the ozone mass continuity equation is solved at each height as a multilayer canopy model. To our knowledge, in-canopy chemistry has never been explicitly considered in a big-leaf framework although empiricism in model development may have led to implicit inclusion (Wolfe et al., 2011).

4. Theory, Models, and Observations of Terrestrial Ozone Deposition Pathways and Related Processes

We review ozone dry deposition to plant stomata (section 4.1), leaf cuticles (section 4.2), soil (section 4.3), and snow-covered surfaces (section 4.6). We also review turbulent transport (section 4.4) and ambient chemistry (section 4.5), presenting these sections before the section on deposition to snow-covered surfaces due to our focus on turbulence and chemistry in plant canopies. In all sections, we discuss modeling and measurement techniques. For sections on deposition to cuticles, soil, and snow-covered surfaces, we synthesize understanding of these processes based on laboratory and field observations and theory. For sections on stomatal deposition, turbulence, and fast ambient chemistry, we highlight advances in understanding pioneered by the fields of plant physiology/ecology, boundary-layer meteorology, and atmospheric chemistry, respectively, and identify steps needed to advance knowledge of the process as related to ozone dry deposition.

4.1 Stomata

Stomata are the pores on plant leaves regulating gas exchange between the atmosphere and vegetation. Accurate estimates of the stomatal ozone flux (F_{stom}) are key for interpreting ozone flux observations and assessing ozone plant damage. F_{stom} is estimated by dividing the ambient ozone concentration outside the leaf (O_{3leaf}) by the sum of several resistances:

$$F_{stom} = \frac{O_{3leaf}}{r_{b,leaf} + r_{stom} + r_{meso}} \tag{13}$$

$r_{b,leaf}$ is the resistance to transport through the quasi-laminar boundary layer between the leaf and outside air; r_{stom} is the resistance to gaseous diffusion through stomatal pores; r_{meso} is the resistance to ozone reaction inside the leaf. The inverse of r_{stom} is stomatal conductance (g_s). While a mesophyll resistance (i.e., r_{meso}) is the conventional way of describing that reactions destroying ozone within the leaf may limit F_{stom}, ozone is not primarily destroyed inside the leaf by reactions with the mesophyll tissue. Despite r_{meso} being a misnomer, we retain the terminology for consistency with previous work (e.g., Wesely, 1989).

Observational approaches and prognostic models for r_{stom} are typically for water vapor. To obtain an estimate of the resistance to ozone diffusion through stomatal pores, r_{stom} for water vapor is multiplied by the ratio of the diffusivity of water vapor in air to the diffusivity of ozone in air. The current estimate of this ratio is 1.61 (Massman, 1998). The assumption inherent to this approach is proportionality between ozone diffusing inward through stomata and water vapor diffusing outward. Collisions between ozone and water vapor molecules may lead to an error of 4–10% in estimates of the stomatal ozone flux (Uddling et al., 2012).

A widely used assumption is reactions inside the leaf do not limit stomatal ozone uptake (i.e., negligible r_{meso}). While some laboratory studies (Laisk et al., 1989; Omasa et al., 2000; Sun, S., Moravek, von der Heyden, et al., 2016; Wang et al., 1995) and the modeling study of Plöchl et al. (2000) suggest this assumption holds, the findings of other laboratory studies and the modeling study of Tuzet et al. (2011) suggest otherwise. In particular, laboratory findings of nonlinear relationships between stomatal uptake of water vapor and stomatal uptake of ozone (Eller & Sparks, 2006; Fares et al., 2007; Fares, Park, Ormeno, et al., 2010; Loreto & Fares, 2007; Tuzet et al., 2011) imply nonnegligible resistance to ozone reaction inside the leaf. Nonetheless, separating ozone destruction inside the leaf from g_s, cuticular ozone uptake, and gas-phase ozone loss is challenging. We recommend future studies further investigate ozone destruction inside the leaf and its influence on stomatal ozone uptake.

In the rest of this section, we highlight common observational constraints on g_s (section 4.1.1) and prognostic g_s models (section 4.1.2). We discuss leaf, tree, and ecosystem-scale observational approaches. Note we say observational constraints or approaches because g_s is not typically measured directly. For prognostic g_s modeling, common mechanistic and empirical approaches are highlighted. We also review how the stomatal ozone sink may influence itself through ozone plant damage (section 4.1.3).

4.1.1 Measuring Stomatal Conductance at Leaf, Tree, and Ecosystem Scales

—Leaf-level observational constraints typically inform mechanistic and empirical prognostic g_s models. Leaf-level g_s is inferred from a leaf diffusion porometer or gas exchange system, which record changes in humidity or maintains constant water vapor to infer transpiration. To obtain g_s, transpiration is divided by the vapor pressure deficit between the substomatal cavity of the leaf and porometer chamber. To calculate vapor pressure deficit, the air inside the leaf is assumed to be saturated. A recent study using carbon and water isotopes challenges this assumption, finding subsaturation in two conifer species under moderate to high atmospheric vapor pressure deficit and a resulting bias in the inferred g_s (Cernusak et al., 2018). Whether subsaturation inside the leaf occurs more broadly is unknown.

Ecosystem-scale observational g_s constraints are often used for directly interpreting ozone turbulent flux measurements and estimate the ecosystem-scale stomatal ozone uptake. We discuss multiple methods of inferring ecosystem-scale g_s because we recommend using multiple independent approaches to quantify ecosystem-scale g_s due to uncertainties across approaches. Ideally, agreement among approaches would be used to draw robust conclusions.

The first ecosystem-scale method employs water vapor EC fluxes and is the most popular method for estimating the ecosystem-scale stomatal ozone uptake. In this method, water vapor fluxes are inverted assuming Fick's law to obtain a surface conductance for water vapor. The intricacies of this method, described below, result in several ways of applying it (e.g., Gerosa et al., 2007).

The surface conductance for water vapor is not exactly g_s because surface conductance includes contributions from in-canopy turbulent transport of water vapor (Baldocchi et al., 1987; Baldocchi et al., 1991; Paw U & Meyers, 1989; Raupach & Finnigan, 1987) and evaporation from soil and vegetation (Baldocchi et al., 1987; Baldocchi & Meyers, 1998; Raupach & Finnigan, 1987) in addition to g_s. The contribution of evaporation is undesirable in estimating stomatal ozone uptake because evaporation is not directly related to ozone dry deposition. While advances with respect to the ecosystem-scale transpiration fraction of evapotranspiration (e.g., Stoy et al., 2019) will help estimates of surface conductance more strictly represent g_s, there is still the issue that surface conductance includes the contribution of turbulent transport of water vapor through the canopy. Assuming similar in-canopy concentration profiles of ozone and water vapor, the contribution of in-canopy turbulence to the surface conductance may be desirable in an ecosystem-scale estimate of g_s. However, the safety of the assumption of similar ozone and water vapor in-canopy profiles and thus transport needs to be evaluated.

Inverting the water vapor EC flux via Fick's law for surface conductance requires an ecosystem-scale estimate of water vapor inside the leaf. The assumption for estimating this is that leaf air is saturated, which may be problematic as suggested by leaf level measurements (e.g., Cernusak et al., 2018), and requires an estimate of ecosystem-scale leaf temperature (more commonly, canopy skin temperature). Because canopy skin temperature constraints are not usually available, most inversion approaches include an approximation

depending on sensible heat flux, which can be (and previously had to be) inferred from the surface energy budget (i.e., by subtracting the ground heat flux and latent heat flux from net radiation). Not only does the lack of surface energy balance closure in EC measurements (Foken et al., 2010; Wilson & Baldocchi, 2000) suggest errors in inferring sensible heat flux from the energy balance, but including latent heat flux in an equation for latent heat flux introduces circularity (Wohlfahrt, Haslwanter, Hörtnagl, et al., 2009). Modern sensible heat flux measurements avoid the need to estimate sensible heat flux, and thus methods that incorporate the measured sensible heat flux should be used. New canopy skin temperature measurements (e.g., Kim et al., 2016) may lead to even more accurate estimates of surface conductance.

Ecosystem-scale fluxes of other gases should be used to complement ecosystem-scale g_s estimates from water vapor fluxes (e.g., Clifton et al., 2019). Carbon dioxide fluxes can be used to constrain g_s through empirical or semi-empirical modeling (see section 4.1.2), but require uncertain estimates of respiration (e.g., Wehr et al., 2016) to infer net photosynthesis. Carbonyl sulfide fluxes (e.g., Whelan et al., 2018) are used to validate an empirical g_s model for Harvard Forest (Wehr et al., 2017; Wehr & Saleska, 2015) based on findings that they represent ecosystem-scale g_s (Commane et al., 2015). Whether this approach transfers readily from Harvard Forest to other locations remains to be established.

Sap flow measurements on individual trees can also be useful for estimating the stomatal ozone flux (Goldstein, 2003; Matyssek et al., 2004; Nunn et al., 2010; Wieser et al., 2003, 2006; Fares et al., 2012) because sap flow isolates transpiration's contribution to the total water vapor flux. However, constraining ecosystem-scale g_s with sap flow requires nontrivial scaling from individual trees to the ecosystem. At a mixed forest in Europe, the stomatal fraction of the ozone flux from sap measurements is 42% lower than inverting ecosystem-scale water vapor fluxes (Nunn et al., 2010). While differences may be due to evaporation from foliage and soil influencing the inversion of ecosystem-scale water vapor flux, uncertainties in sap flow measurements and scaling techniques (e.g., Poyatos et al., 2016) may also contribute to differences between approaches.

4.1.2 Modeling Stomatal Conductance—The most popular prognostic g_s models in dry deposition schemes are empirical and closely adhere to the Jarvis (1976) multiplicative approach (e.g., Emberson, Simpson, Tuovinen, et al., 2000; Wesely, 1989). In the Jarvis approach, a prescribed maximum g_s is multiplied by several factors and each factor is a function of a particular environmental condition. The conditions may be meteorological or biophysical (e.g., soil moisture, leaf age). The Jarvis type of model is informed by leaf-level and sometimes ecosystem-scale observational g_s constraints (e.g., Büker et al., 2007, 2012; Kelliher et al., 1995).

An increasingly common method for prognostic g_s modeling is coupling g_s with net photosynthesis (A_{net}) (hereafter, A_{net}-g_s model), providing an estimate of carbon dioxide exchange across stomata driven by the carbon supply and demand for photosynthesis. In an A_{net}-g_s model, g_s is modeled according to a relationship with A_{net} (Miner et al., 2017; Wong, S. C., et al., 1979) that varies with some metric of humidity, as constrained by leaf-level data (Ball et al., 1987; Leuning, 1995; Medlyn et al., 2011). Recent work assigns a

physical basis to this relationship by reconciling mechanistic and empirical approaches with optimization theory for maximizing carbon gain and minimizing water loss (Cowan & Farquhar, 1977; Lin, Y. S., et al., 2015; Medlyn et al., 2011). However, whether stomata function optimally as assumed under this particular theory is uncertain (e.g., Buckley & Mott, 2013; Lin, C., et al., 2018; Sperry et al., 2017; Wolf et al., 2016; Zhou, S., et al., 2013).

In general, whether modeled through empirical or mechanistic prognostic approaches, g_s is calculated for a single leaf and scaled to the ecosystem by multiplying leaf-level g_s by leaf area index (LAI), or using canopy scaling factors or a multilayer canopy or resistance model. It is currently uncertain which scaling approach best estimates g_s.

While some dry deposition schemes employ A_{net}-g_s models (Charusombat et al., 2010; Clifton, 2018; Lin, M., et al., 2019; Hollaway et al., 2016; Ran et al., 2017; Val Martin et al., 2014), the Jarvis type of model remains ubiquitous (e.g., Emberson, Simpson, Tuovinen et al., 2000; Hardacre et al., 2015). A_{net}-g_s models are more closely based on physiological principles, but the simplicity, adaptability, and computation efficiency of the Jarvis approach makes it attractive for many applications. However, the Jarvis approach requires tuning for the ecosystems and environmental conditions represented and its success is limited by dearth of data for many ecosystems (e.g., tropical forests) and conditions. Nonetheless, A_{net}-g_s models are semi-empirical in that they require one to a few parameters to be defined (Franks et al., 2018; Lin, Y. S., et al., 2015; Medlyn et al., 2011; Miner et al., 2017). Both model types are typically tuned with leaf-level data due the historical lack of ecosystem-scale data. Recent efforts to tune models with ecosystem-scale measurements (e.g., Li, J., Duan, Wang, et al., 2018; Raoult et al., 2016), such as latent heat and carbon dioxide fluxes, can complement leaf-level approaches by allowing for insight into what happens at larger scales.

To evaluate the strengths and weaknesses of prognostic g_s models in simulating stomatal ozone uptake, the community would benefit from better understanding of model sensitivities to parameters and variables as well as their physiological realism. For example, connections between g_s and soil moisture and the ability of models to capture such connections (e.g., Anderegg et al., 2017; Bonan et al., 2014; Kennedy et al., 2019; Verhoef & Egea, 2014; Zhou, S., et al., 2013) may be critical for capturing stomatal ozone uptake.

4.1.3 Ozone Damage to Plants, as Relevant for Stomatal Uptake of Ozone—

Ozone damage to plants may lead to myriad ecosystem responses. Here we focus on the direct influence of ozone on g_s and thus stomatal ozone dry deposition.

Stomatal ozone uptake changes g_s through both short-term and long-term responses. In the short term, stomatal ozone uptake decreases g_s by changing guard cell turgor pressure and signaling pathways (Freer-Smith & Dobson, 1989; Hassan et al., 1994; Maier-Maercker & Kock, 1991; Manes et al., 2001; Mills et al., 2009; Torsethaugen et al., 1999).

In the long term, the mean g_s response to stomatal ozone uptake across plant physiological studies is a decrease (Lombardozzi et al., 2013). However, both g_s increases and decreases are observed. For example, stomatal ozone uptake can lead to reduced photosynthetic efficiency, which increases internal carbon dioxide and signals stomatal closure (Calatayud

et al., 2007; Farage et al., 1991; Herbinger et al., 2007; Manes et al., 2001; Noormets et al., 2001; Paoletti & Grulke, 2005; Reich, 1987).

On the other hand, stomatal ozone uptake can lead to g_s increases in the long term through decreased sensitivity to abscisic acid (Mills et al., 2009), which alters stomatal cell ion exchange (Manes et al., 2001; Torsethaugen et al., 1999), and the collapse of epidermal cells surrounding guard cells (Hassan et al., 1994), which can lead to sluggish stomatal responses to external stimuli (Freer-Smith & Dobson, 1989; Maier-Maercker & Koch, 1991; Manes et al., 1998, 2001; McLaughlin et al., 2007; Paoletti, 2005; Paoletti & Grulke, 2010). Stomatal ozone uptake may also cause early and a more rapid onset of senescence (e.g., Ainsworth et al., 2012), which reduces g_s through growing season length and physiologically active LAI.

Two types of model parameterization allow for stomatal ozone uptake to influence itself. In the first type, a response integrated across several physiological processes is used to parameterize impact of ozone on a single physiological process (Clark et al., 2011; Sitch et al., 2007; Yue & Unger, 2014). For example, the observed effect of stomatal ozone uptake on plant biomass or crop yield may be equated to the ozone impact on photosynthesis in models and parameterized accordingly, and thus any impact on stomatal ozone uptake is due to ozone's parameterized impact on photosynthesis (e.g., Sitch et al., 2007).

The second type of model considers the ozone impact on the same physiological process considered in the observational evidence (Ewert & Porter, 2000; Deckmyn et al., 2007; Lombardozzi, Levis, Bonan, et al., 2012; Lombardozzi, Sparks, Bonan, et al., 2012; Lombardozzi et al., 2015; Martin et al., 2001; Tao et al., 2017). For example, Lombardozzi et al. (2013) investigate the effects of cumulative stomatal ozone uptake on g_s versus photosynthesis with a meta-analysis of published chamber data. Finding differing observed effects on the two processes, consistent with other work (e.g., Koch et al., 1998; Paoletti & Grulke, 2010), Lombardozzi et al. (2013) parameterize the effect of the cumulative stomatal ozone uptake on each process separately.

Another difference across models parameterizing ozone damage with stomatal ozone uptake is whether damage is tied to the instantaneous or cumulative stomatal ozone uptake. There are a few models, most commonly for crops, considering both instantaneous and cumulative stomatal uptake (Emberson et al., 2018; Ewert & Porter, 2000; Tao et al., 2017). Plant damage is often assumed more closely related to cumulative, rather than instantaneous, stomatal ozone uptake (Massman et al., 2000; Matyssek et al., 2004; Ducker et al., 2018).

The stomatal ozone uptake does not account for plant abilities to cope with the oxidative stress that ozone causes (i.e., detoxify). Detoxification ability controls the plant sensitivity to ozone and thus determines the ozone plant injury (e.g., Matyssek et al., 2008; Musselman et al., 2006). Detoxification is often simulated by assuming a constant threshold of stomatal ozone uptake below which damage does not occur due to detoxification. Detoxification is highly uncertain and may vary with environmental variables and come at a cost to the plant (U.S. EPA, 2006; Musselman et al., 2006; Matyssek et al., 2008; Ainsworth et al., 2012; Ainsworth, 2017).

Current knowledge of the effects of stomatal ozone uptake on g_s at large scales (e.g., ecosystem, region) is largely based on scaling up leaf-level effects (Massman et al., 2000; Matyssek et al., 2008). Limited leaf-level data (e.g., most data are for temperate species) and lack of clear response across existing datasets (e.g., Lombardozzi et al., 2013) limit the fidelity of given empirical parameterization. In general, large-scale responses to stomatal ozone uptake are poorly understood and not widely evaluated given the paucity of observational constraints on ozone damage at larger scales. Understanding ecosystem abilities to detoxify is sorely needed to pinpoint stomatal ozone uptake's influence on itself.

4.1.4 Main Takeaways

- Water vapor EC fluxes are typically used to constrain ecosystem-scale g_s, but multiple independent observational approaches are needed and ideally agreement among them would be used to draw robust conclusions.

- A_{net}-g_s models represent current mechanistic understanding, but how much A_{net}-g_s models improve g_s estimates over widely used empirical approaches is uncertain.

- Identification of the key parameters to which prognostic g_s models are most sensitive, as well as the physiological realism of modeled sensitivities, is needed.

- Ecosystem-scale constraints on stomatal ozone uptake and the ecosystem's ability to detoxify are needed to understand the influence of stomatal ozone uptake on itself.

4.2 Leaf Cuticles

4.2.1 Controls on Ozone Dry Deposition to Leaf Cuticles: Field, Modeling, and Laboratory Evidence—The following synthesis suggests aqueous heterogeneous chemistry is the primary mechanism controlling ozone dry deposition to leaf cuticles. Direct constraints on cuticular ozone uptake are slim, but insightful. For example, ozone and carbon dioxide leaf uptake measured with chambers at Hyytiälä provide strong evidence for a dependence of cuticular ozone uptake on relative humidity (Altimir et al., 2006). A laboratory study that induced stomatal closure in young trees by treating leaves with abscisic acid also shows increases in ozone uptake with relative humidity (Sun, S., Moravek, Trebs, et al., 2016) (Figure 6). Increases in cuticular uptake with humidity suggest aqueous ozone-destroying chemistry on the cuticle; liquid surface films form when humidity increases because there is absorption of water to the leaf surface, capillary condensation, or deliquescence of deposited particles (Burkhardt & Eiden, 1994; Burkhardt & Hunsche, 2013; Eiden et al., 1994).

Several field studies report increases in inferred nonstomatal uptake over vegetation with relative humidity, providing evidence that aqueous surface chemistry on leaves may be important at ecosystem scales (Altimir et al., 2006; Clifton et al., 2019; Lamaud et al., 2009; Li, Q., et al., 2018; Neirynck & Verstraeten, 2018; Rannik et al., 2012; Zhang, L., et al., 2002). However, at some field sites, nonstomatal uptake increases with humidity at high humidity, but decreases with humidity at low humidity (Coyle et al., 2009; Hogg et al., 2007). This diverging behavior may reflect a change in the mechanism controlling cuticular

uptake with thermal decomposition dominating at lower humidity (Coyle et al., 2009; Grøntoft et al., 2004; Pöschl & Shiraiwa, 2015).

In general, the degree to which ecosystem-scale nonstomatal uptake estimates represent cuticular uptake is uncertain because other processes, such as ozone uptake by soil and ambient chemistry, cannot always be discounted. Additionally, imperfect estimates of stomatal deposition and transport imply at least some error in residual nonstomatal deposition estimates.

A recent review of ozone dry deposition to building surfaces concludes the influence of relative humidity on ozone uptake is uncertain (Shen & Gao, 2018). It may be that only some ozone-destroying surface reactions are expedited in water films and that water films only form easily on some surfaces. Increased cuticular uptake at higher humidity may also be associated with stomatal exudation of reactive compounds when leaves are wet (Potier et al., 2017). For example, water around stomata can act as a bridge into saturated stomatal pores (Burkhardt, 2010) and stomata may leach ascorbate compounds into the water on the cuticle. If ozone destruction on cuticles is limited by ascorbate flowing out of stomata when leaves are wet, then a fundamental question is how much leakage occurs.

In their laboratory study examining ozone uptake to aluminum, stainless steel, beeswax and hydrocarbon wax, Cape et al. (2009) find an Arrhenius-like dependence of ozone uptake on temperature and suggest a role for thermal decomposition of ozone when ozone deposits to leaf cuticles. There is some field evidence for this hypothesis in dry conditions, as discussed above. However, increases in temperature only lead to small increases in ozone uptake to building surfaces (Shen & Gao, 2018). In general, thermal decomposition of ozone on a given surface depends on the surface area and activation energy, which varies across materials (e.g., Cape et al., 2009). Whether thermal decomposition plays a role in governing cuticular ozone uptake needs to be better understood.

While light-mediated ozone destruction on cuticles received attention in previous reviews on ozone dry deposition (e.g., Ganzeveld et al., 2015; Fowler et al., 2009; Tuovinen et al., 2009), evidence for the importance and occurrence of this pathway is minimal. In brief, Coe at al. (1995) find a diel cycle in nonstomatal deposition inferred from field measurements. The hypothesis that photochemistry on the leaf surface causes this diel cycle is given attention on the basis of Rondón (1993), an unpublished laboratory study. A more recent laboratory study finds similar cuticular ozone uptake for light and dark conditions (Sun, S., Moravek, Trebs, et al., 2016), suggesting cuticular uptake is unlikely to be related to photochemistry.

High v_d after rain and dew observed in field studies is often attributed to increases in cuticular uptake (Altimir et al., 2006; Finkelstein et al., 2000; Fuentes et al., 1992; Grantz et al., 1995, 1997; Lamaud et al., 2002; Potier et al., 2015; Turnipseed et al., 2009). Increases in ozone dry deposition on wet leaves in the laboratory (Fuentes & Gillespie, 1992) and in a field chamber experiment after spraying the grass in the chamber with water (Pleijel et al., 1995) are also attributed to increases in cuticular uptake. While there are fairly consistent increases in v_d over vegetation after rain and dew across field studies (Table 2), whether

observed responses truly indicate changes in cuticular uptake remains an open question. For example, there may be changes in g_s after rain (e.g., Clifton et al., 2019) or emissions of highly reactive species (e.g., Altimir et al., 2006; Clifton et al., 2019; Turnipseed et al., 2009).

4.2.2   Composition of the Leaf Cuticle—Composition of the cuticular surface likely determines ozone reactivity. Cuticular composition and thus reactivity may reflect deposited aerosols, the cuticular wax itself, and/or compounds exuded from the plant, but the relative importance of each source of reactivity is uncertain and may vary in space and time. Different wetting mechanisms may alter cuticular composition and thus ozone uptake. For example, rain may wash leaves of compounds (e.g., Xu et al., 2017; Zhang, L., et al., 2019) with which ozone can react. Deliquescent salts on cuticles may also increase ozone solubility compared to pure water (e.g., Rischbieter et al., 2000). Below we discuss evidence for each source (deposited aerosols, cuticular wax, and exuded compounds) contributing to ozone reactivity. We find that the dominant reactivity sources on cuticles needs to be established.

Depending on leaf size and shape, up to 50 μg cm^{-2} of aerosols can accumulate on leaves (Burkhardt, 2010; Popek et al., 2013; Sæbø et al., 2012). In the laboratory study of Sun, S., Moravek, Trebs, et al. (2016), ozone uptake is highest for leaves either exposed to outdoor air or sprayed with a solution containing major inorganic components of typical continental aerosols relative to the other treatments (Figure 6), suggesting cuticular uptake through reaction with deposited aerosols may be important. However, evidence from kinetic studies on soot, mineral dust, and proxies for organic aerosols shows rapid declines in ozone uptake after high initial uptake (Chapleski et al., 2016; Disselkamp et al., 2000; Hanisch & Crowley, 2003; Karagulian & Rossi, 2006; McCabe & Abbatt, 2009), implying persistent ozone uptake requires sustained aerosol deposition to cuticles. The exception is uptake by organic photosensitizers (e.g., humic acid) in light (D'Anna et al., 2009; Jammoul et al., 2008).

Cuticular waxes mostly contain compounds derived from long-chain fatty acids unreactive with ozone, but can contain unsaturated compounds (Buschhaus & Jetter, 2012; Jetter et al., 2006; Yeats & Rose, 2013) reactive with ozone. Clean cuticles have low but nonnegligible ozone uptake at relative humidity higher than 40% (Figure 6), but there is negligible cuticular uptake on the same species for lower humidity (Sun, S., Moravek, Trebs, et al., 2016) as well as on different species at 65% relative humidity (Omasa et al., 2000). While Fares et al. (2007) suggest negligible cuticular uptake by two tree species in their laboratory study, stomatal uptake does not fully explain ozone uptake for one of the species. Whether some species' waxes provide substantial ozone sinks, and whether this changes with environmental conditions like humidity, is unclear.

Compounds exuded by the plant, whether the compounds are sorbed BVOCs or organic compounds leached out of stomata, may contribute to ozone reactivity on the cuticle. Ascorbate leaching through stomata on wet leaves may be an important contributor to ozone reactivity for some plant species and phenological states (Potier et al., 2015, 2017). Laboratory studies show conflicting evidence as to whether sorbed BVOCs may be an

effective cuticular ozone sink. For example, high cuticular uptake due to reaction with sorbed a-pinene on waxes is not supported by Cape et al. (2009), but exuded terpenoids efficiently react on the cuticle with ozone in Jud et al. (2016).

4.2.3   Modeling Ozone Dry Deposition to Leaf Cuticles—Models for ozone dry deposition to cuticles are largely empirical and stem from sparsely available laboratory and field measurements. Many models include only LAI and a tuning factor (e.g., Massman, 2004). Several models distinguish deposition between wet and dry cuticles, but there are differences across models in the direction of the simulated response. For example, Wesely (1989) prescribes a lower cuticular deposition when leaves are wet, but L. Zhang et al. (2002) prescribe higher cuticular deposition when leaves are wet. Some models include a dependence on relative humidity (Altimir et al., 2004; Clifton, 2018; Lamaud et al., 2009; Stella, Personne, Loubet, et al., 2011; Zhang, L., et al., 2002), which may represent the effect of thin water films on leaves.

We use mechanistic modeling to explore strengths and weaknesses of the simple approaches outlined above. The mechanistic equation for resistance to deposition through heterogeneous reaction of ozone on dry cuticles ($r_{cut,dry}$) [s m^{-1}] in a big-leaf approach follows:

$$r_{cut,dry} = \frac{1}{\frac{1}{4}K_d\sqrt{\frac{8RT_{leaf}}{\pi M_{O_3}}}f_{dry}LAI}$$

(14)

K_d is the cuticular deposition coefficient [unitless], which is a measure of the probability that ozone reacts upon contact with the cuticle; R is the universal gas constant [8.314 J mol^{-1} K^{-1}]; T_{leaf} is leaf temperature [K]; M_{O_3} is the ozone molecular mass [0.048 kg mol^{-1}]; f_{dry} is the dry fraction of the leaf [unitless]; LAI is leaf area index.

The model expressed by equation (14) simulates collision and reaction of a gas with a surface analogously to heterogeneous chemistry in the atmosphere (e.g., Jacob, 2000). While K_d is challenging to infer at the ecosystem scale, the model expressed by equation (14) is structurally simple and relatable to existing approaches [m^2 m^{-2}].

For the resistance to deposition to wet cuticles ($r_{cut,wet}$ [s m^{-1}]; either thin water films or droplets from rain or dew), Potier et al. (2015) present a physically-based model based on the diffusion-reaction equation. We derive a form of this model in Appendix B and review its physical underpinnings. The following model represents ozone dissolution in the water on a cuticle and reaction with compounds in the water in a big-leaf approach:

$$r_{cut,wet} = \frac{1}{k_H^{CC}\Gamma_{aq}D_{O_3,aq}\tanh\left(\Gamma_{aq}\delta_d\right)\left(1-f_{dry}\right)LAI}$$

(15)

k_H^{cc} is the dimensionless Henry's law constant for ozone; $\Gamma_{aq} = \sqrt{\frac{\kappa^{aq}}{D_{O_3,aq}}}$; κ^{aq} is the first-order reaction rate of ozone in the water mixture on the leaf [s^{-1}]; $D_{O_3,aq}$ is the ozone diffusivity in water [m^2 s^{-1}]; δ_d is the thickness of the wetness on the cuticle [m].

As is, this model's utility to represent ozone uptake by wet cuticles at large scales hinges on whether input variables can be estimated adequately (e.g., δ_d, κ^{aq}). We recommend exploring the model parameter space (e.g., $r_{cut,wet}$ sensitivity to different inputs).

For both dry and wet cuticular deposition modeling, whether one or two-sided LAI should be used depends on the source of wetness and reactivity as well as whether the plant has stomata on a single side of the leaf or both sides.

Representation of reactivity on a cuticle is likely critical to model cuticular ozone dry deposition accurately. The fastest gain in understanding will likely happen when knowledge from studies on plant physiology and aerosol dry deposition is leveraged for information about cuticular composition (e.g., cuticular wax, deposited aerosols, compounds exuded from stomata) and changes in time and space.

Ozone destruction on cuticles may decrease stomatal ozone uptake (Jud et al., 2016; Kanagendran et al., 2018), and thus there may be interactions between stomatal and cuticular deposition. While the theoretical modeling of Jud et al. (2016) indeed shows cuticular ozone uptake reduces stomatal ozone uptake, the theoretical modeling of Altimir et al. (2008) shows stomatal ozone uptake is only reduced by unrealistically high cuticular ozone uptake. Because interactions between stomatal and cuticular uptake challenge assumptions underlying current modeling frameworks representing pathways as independent (e.g., Altimir et al., 2008; Jud et al., 2016), a better understanding of such interactions is warranted.

4.2.4 Main Takeaways

- Most field and laboratory studies support aqueous heterogeneous chemistry dominating cuticular ozone uptake, but there may be a role for thermal decomposition of ozone on cuticles, especially at low humidity.

- The observed dependence of cuticular uptake on relative humidity likely represents surface water films promoting aqueous chemistry.

- Representation of reactivity on a cuticle is likely critical to model cuticular ozone dry deposition accurately.

- We derive a model for mechanistic representation of ozone dry deposition to cuticles.

- We recommend further exploration of this mechanistic wet cuticular deposition model and its ability to represent uptake at large scales.

4.3 Soil

4.3.1 Controls on Ozone Dry Deposition to Soil: Field, Modeling, and Laboratory Evidence—While a dominant pathway for ozone dry deposition to soil is considered to be reaction with unsaturated carbon bonds in soil organic material (e.g., Sorimachi & Sakamoto, 2007), mean daytime v_d of ~0.1 cm s^{-1} from a short-term field campaign in the Sahara Desert suggests ozone reaction with soil organic material is not the only soil deposition pathway (Güsten et al., 1996). It is possible thermal decomposition of

ozone occurs on soil surfaces or gas-phase loss of ozone in soil pore spaces occurs through reaction with NO or BVOCs.

Evidence from eight field studies (Table 3), including one field chamber study (Fumagalli et al., 2016), and four laboratory-based studies (Aldaz, 1969; Sorimachi & Sakamoto, 2007; Toet et al., 2009; Turner et al., 1973) suggests soil moisture inhibits ozone uptake by limiting diffusion through soil pore spaces. Decreases in soil ozone uptake with increasing soil moisture suggest moisture reduces surface area available for reaction with ozone, overriding any effect of moisture promoting heterogeneous chemistry (e.g., as observed on leaf cuticles). Indeed, employing the isotopic method discussed in section 2.2.3 to constrain ozone uptake by soil versus soil pore water, Toet et al. (2009) show ozone deposition to soil pore water is a substantial fraction of soil ozone uptake at 60% soil moisture, but much lower than ozone uptake by soil at 30% soil moisture where it is only a small fraction of the total (>10%).

Short-term observed ozone EC fluxes above bare agricultural soils and a semi-arid plain in Europe show an exponential decrease in soil ozone uptake with near-surface relative humidity (Stella et al., 2019) stronger than the relationship with soil water content for at least one of the sites (Stella, Loubet, Lamaud, et al., 2011). Stella, Loubet, Lamaud, et al. (2011) hypothesize surface relative humidity better indicates the water molecules on the ground preventing ozone from entering soil, relative to soil water content at a shallow depth.

Stella et al. (2019) suggest variation among the six sites examined is caused by soil clay content because clay is a structural indicator of available surface area (e.g., Hillel, 1980) and clay modifies the amount of water in soil. In particular, regression analysis suggests the magnitude of soil uptake increases with soil clay content, but soil uptake decreases more quickly with surface relative humidity in soils with more clay content (Stella et al., 2019). Whether these findings hold more generally needs to be established.

4.3.2   Modeling Ozone Dry Deposition to Soil—Ozone dry deposition to soil is often constant in large-scale models, sometimes varying by LULC type and season (e.g., Wesely, 1989). Massman (2004) compiles resistances to ozone dry deposition to soil (r_{soil}) inferred from observations, suggesting 100 s m^{-1} for dry soil and 500 s m^{-1} for wet soil. Later site-specific work defines similar empirical models (Bassin et al., 2004; Clifton et al., 2019; Fares et al., 2012, 2014; Mészáros, Horváth, Weidinger, et al., 2009) but studies more directly isolating r_{soil} support stronger dependencies on soil moisture (Fumagalli et al., 2016) or surface relative humidity (Stella, Loubet, Lamaud, et al., 2011; Stella et al., 2019).

Most studies creating models for soil ozone dry deposition use short-term data. Whether simple models accurately capture r_{soil} magnitude and variability on a variety of scales is uncertain. Uncertainty may stem in part from a lack of observational constraints on r_{soil} spatiotemporal variability.

To better understand processes governing soil ozone uptake and provide a roadmap for more robust empirical modeling, we present a more mechanistic model of r_{soil} (derivation in

Appendix B). The model represents ozone reaction with surfaces in soil and gases in soil pore spaces:

$$r_{soil} = \left[\left(A K_d \frac{1}{4} \sqrt{\frac{8RT_{soil}}{\pi M_{O_3}}} + \sum_i K_{X_i, O_3} X_{i, soil} \right) \left((\eta - \theta) \tau D_{O_3} \right) \right]^{-\frac{1}{2}} \qquad (16)$$

A is surface area on which ozone dry deposition occurs per unit volume of the porous media [$m^2\ m^{-3}$]; K_d is a measure of the probability that an ozone molecule reacts once it comes into contact with the surface [unitless]; R is the universal gas constant [$8.314\ J\ mol^{-1}\ K^{-1}$]; T_{soil} is soil temperature [K]; M_{O_3} is the ozone molecular mass [$0.048\ kg\ mol^{-1}$]; K_{X, O_3} is the rate coefficient [$ppmv\ s^{-1}$] for chemical ozone destruction in soil pore spaces by gas species X_{soil} [ppmv]; η is the volumetric air-filled soil pore space when completely dry [$m^3\ m^{-3}$]; θ is volumetric soil moisture [$m^3\ m^{-3}$]; τ is the soil tortuosity factor [$0 < \tau < 1$; unitless] (a measure of how many paths ozone can take in soil); D_{O_3} is ozone diffusivity in air [$m^2\ s^{-1}$].

The utility of this model in representing soil ozone uptake hinges on whether (i) all relevant processes are represented accurately and (ii) model input variables can be estimated adequately. In terms of (i), the model assumes neither obstruction to transport into soil nor any thermal decomposition or aqueous ozone reaction in soil. Based on mechanistic modeling, we suggest the contribution of thermal decomposition may be important (see Appendix B). The results of Toet et al. (2009) also imply aqueous ozone reaction in soil at low soil moisture may dominate.

In terms of (ii), most of the inputs likely require a fair amount of parameterization and thus are uncertain. We should be able to leverage understanding of some input variables and parameters from the fields of soil physics and chemistry. We recommend sensitivity analyses with the model expressed in equation (16) to identify the parameters and variables driving modeled variations under different conditions.

We also recommend more measurements of soil ozone uptake to constrain the observed driver(s) of soil ozone uptake under a given environmental condition and further parameterize and evaluate the model expressed in equation (16). Our synthesis indicates capturing ozone's ability to diffuse into and through soil pore spaces is key. Models should thus consider soil moisture as a limiting factor. Useful constraints on soil ozone uptake include ozone EC fluxes at heights in the lower canopy and over bare soil and chambers on the ground (e.g., Finco et al., 2018; Launiainen et al., 2013; Stella et al., 2019).

4.3.3 Main Takeaways

- Observations suggest soil moisture decreases ozone uptake by soil, hindering ozone's ability to diffuse into soil and through soil pore spaces.

- The dominant pathway for soil ozone uptake is likely reaction with organic matter, but the contributions of thermal decomposition, aqueous chemistry, and reaction with gaseous compounds in soil cannot currently be discounted.

- We derive a model for mechanistic representation of ozone dry deposition to soil.

- We recommend reconciling mechanistic and empirical modeling approaches and additional observational constraints on soil ozone uptake both in terms of longer datasets and representation of more ecosystems.

4.4 Turbulence

Atmospheric turbulence is generated by either shear or buoyancy forces, and complex surface elements (e.g., vegetation) drive stronger and more variable turbulence enhancing contact between air parcels and surfaces. Turbulence moves air and transports ozone-rich air parcels towards the surface, and thus is fundamental to ozone's ability to deposit. Correlations between friction velocity and v_d or ozone flux (El-Madany et al., 2017; Fares et al., 2014; Lamaud et al., 2002; Neirynck et al., 2012; Van Pul & Jacobs, 1994) indeed suggest turbulent transport is an important, and sometimes limiting, driver of ozone dry deposition.

Over vegetation, turbulent eddies of size similar to the canopy drive most of the exchange between the canopy and atmosphere, as well as among canopy layers (e.g., Gao et al., 1989; Patton & Finnigan, 2013). Fluid flow interacting with a canopy is hydrodynamically unstable, which produces eddies observed as combinations of sweeps of air from above the canopy penetrating into the canopy and bursts of air ejecting canopy air into the atmospheric surface layer above (e.g., Finnigan et al., 2009; Raupach et al., 1996). These bursts and sweeps facilitate uptake of trace gases and also lead to segregation of air masses in the canopy (e.g., Dupont & Patton, 2012; Steiner et al., 2011; Thomas & Foken, 2007; Patton et al., 2016).

Transfer of trace gases from the surface layer to the surface is typically modeled with MOST, an empirical formation based on dimensional analysis that accounts for atmospheric stability influences on near-surface turbulence and holds in the inertial sublayer. Different empirical formulations of MOST may contribute to differences among air quality models in simulated v_d under stable conditions (Toyota et al., 2016).

There are substantial limitations to modeling approaches utilizing MOST to simulate canopy-atmosphere exchange. The underlying assumptions of MOST fail in the roughness sublayer above a plant canopy that can extend up to 2–3 canopy heights (e.g., Cellier & Brunet, 1992; Harman & Finnigan, 2007; Thom, 1975). Recent observations at the Amazon Tall Tower Observatory suggest the roughness sublayer above the forest merges directly into the mixed layer and does not even form the inertial sublayer where MOST is valid (Dias-Júnior et al., 2019). Another issue is many forest canopies reside in hilly or mountainous terrain, but MOST assumes horizontal homogeneity.

Multilayer canopy models are typically limited in simulating vertical exchange among canopy layers, but simulated turbulence in these models influences the canopy distribution of ozone and thus dry deposition and ambient chemistry. Most multilayer canopy models employ K-theory (Ashworth et al., 2015; Bryan et al., 2012; Ganzeveld et al., 2002; Stroud et al., 2005; Wolfe & Thornton, 2011; Zhou, P. T., et al., 2017), which does not realistically simulate turbulence in a complex canopy environment. Some multilayer canopy models

(Stroud et al., 2005; Wolfe & Thornton, 2011; Bryan et al., 2012) include near-field approximations (Makar et al., 1999), which leverage the Lagrangian perspective of dispersion in a canopy outlined by Raupach (1989). However, near-field parameterizations are designed for neutral stability conditions and their utility hinges on whether observed wind profiles and turbulence statistics can be prescribed (Harman & Finnigan, 2008).

The multilayer canopy model described by Bonan et al. (2018) with the Harman and Finnigan (2007, 2008) analytic roughness sublayer mixing scheme shows potential for prognostic simulation of canopy vertical exchange. While the Harman and Finnigan (2007, 2008) scheme relies on K-theory, its introduction of a length scale associated with the turbulent eddies produced by wind shear at the canopy top incorporates the influence of counter-gradient transport. Bonan et al. (2018) find that the Harman and Finnigan (2007, 2008) scheme improves simulation of friction velocity and ambient temperature at several forest and grassland sites. With a multilayer canopy large eddy simulation (LES) model explicitly resolving turbulence above and in a forest canopy, Patton et al. (2016) show atmospheric stability exerts a control on vertical exchange at the top of the canopy through the structure of the atmospheric boundary layer, suggesting roughness sublayer parameterizations consider the effect.

The representation of in-canopy turbulence is also limited in big-leaf dry deposition schemes. For example, in the Wesely (1989) scheme, there are two resistances to in-canopy turbulence, one for lower-canopy deposition and the other for soil uptake. Wesely (1989) defines a simple model based on solar radiation and slope of the terrain for the former and prescribes constants that vary with LULC type and season for the latter.

Later big-leaf schemes (e.g., Clifton, 2018; Emberson, Simpson, Tuovinen, et al., 2000; Erisman et al., 1994; Paulot et al., 2018; Pleim & Ran, 2011; Zhang, L., et al., 2002, 2003) do not include deposition to the lower canopy, and adopt or modify a model employing LAI, friction velocity, and canopy height based on six days of afternoon ozone fluxes over a corn field (Van Pul & Jacobs, 1994) for turbulent transport to the ground. As mentioned, several studies indeed find friction velocity as a driver of variation in ozone dry deposition (Lamaud et al., 2002; El-Madany et al., 2017; Fares et al., 2014; Neirynck et al., 2012). However, a site-specific model like Van Pul and Jacobs (1994) may not capture variability in the resistance to canopy turbulence across different landscapes and boundary-layer conditions. For example, daytime transport timescales near the ground over a grassland constrained with radon and thoron isotopes are 50% too low with the Van Pul and Jacobs (1994) model (Plake & Trebs, 2013). In general, multilayer canopy LES models offer an opportunity to explore how turbulent transport influences ozone dry deposition and refine parameterizations.

While most observational constraints on canopy turbulence are from sonic anemometers above the canopy, some recent studies employ sonic anemometers at multiple vertical or horizontal locations (e.g., Fuentes et al., 2016; Patton et al., 2011) to advance understanding of canopy turbulence and its impact on vertical exchange of trace gases. For example, using profile measurements of ozone concentrations and turbulence statistics at a tropical forest, Freire et al. (2017) suggest the ozone concentration profile is primarily a function of turbulent mixing, although the authors only consider a single depositional sink for the entire

canopy. Isotopic measurements of thoron and radon also offer constraints on turbulent transport near the ground in a plant canopy (Plake & Trebs, 2013), which may be useful in interpreting ozone flux measurements (e.g., separating ozone dry deposition to soil from canopy sinks).

4.4.1   Main Takeaways

- Turbulence is inherently fundamental to ozone's ability to deposit.

- Constraints on turbulent transport are useful for interpreting observed ozone fluxes and establishing the relative importance of a given deposition pathway.

- The magnitude and variability in turbulent transport simulated by current models used to estimate or interpret measurements of ozone fluxes are uncertain.

- Explicitly resolving above- and in-canopy turbulence in models such as LES should be used to improve current turbulent transport parameterizations.

4.5   Fast Ambient Chemistry

While ambient chemistry is not technically ozone dry deposition, fast ambient chemistry influences observed ozone fluxes. We emphasize fast here because the time scale over which ambient chemistry operates is central to its influence on ozone fluxes. The rule of thumb is chemical reactions below the measurement height (hereafter, "in canopy") must occur on timescales equivalent to or faster than the canopy residence time determined by turbulent transport to influence the ozone flux.
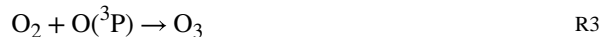
Timescales for turbulent transport (τ_{trans}) and chemical reactions (τ_{chem}) can be compared via the Damköhler number (D_a; Damköhler, 1940; Lenschow, 1982; Lenschow & Delany, 1987; Vilá-Guerau de Arellano, 2003; Vilá-Guerau de Arellano & Duynkerke, 1992):

$$D_a = \frac{\tau_{trans}}{\tau_{chem}} \tag{17}$$

If D_a is greater than 1 then chemistry should be a major influence on observed ozone fluxes; if D_a is between 0.1 and 1 then the influence of chemistry should be moderate while if D_a is less than 0.1 then turbulent transport dominates and the influence of chemistry should be negligible. If $D_a = 1$ then segregation (i.e., the spatial separation of reactants in the canopy by organization in turbulence) becomes a factor depending on the source (and likely sink) distributions of the reactants (e.g., Patton et al., 2001).

D_a does not always present an accurate picture of chemistry's influence on ozone fluxes; multilayer canopy modeling shows chemistry slower than turbulence (e.g., $D_a = 0.03$) still alters the ozone flux (Wolfe et al., 2011). Nonetheless, D_a helps to establish which reactive gases are involved in chemistry relevant to interpreting ozone fluxes.

In considering fast ozone loss through reaction with NO, it is important to consider NO-NO_2-O_3 chemistry, which occurs on the timescale of turbulence (Van Aalst, 1982; Duyzer et al., 1983) and consists of the following reactions:

$$O_3 + NO \rightarrow NO_2 + O_2 \hspace{4cm} \text{R1}$$

$$NO_2 + h\nu \rightarrow NO + O(^3P) \hspace{3cm} \text{R2}$$

$$O_2 + O(^3P) \rightarrow O_3 \hspace{4cm} \text{R3}$$

Reaction with NO leads to a permanent ozone sink when NO_2 is oxidized to higher nitrogen oxides (Min et al., 2012, 2014; Turnipseed et al., 2006; Wolfe et al., 2009) or taken up by stomata (Delaria et al., 2018; Bakwin et al., 1990; Plake, Stella, Moravek, et al., 2015; Rummel et al., 2002) and serves as a temporary reservoir if NO_2 is photolyzed and ozone is reformed. In a shaded forest canopy, photolysis of NO_2 (i.e., R2) is expected to be low.

In general, the effects of R1 on ozone fluxes are usually small (Kramm et al., 1995; Plake, Sörgel, Stella, et al., 2015; Rannik et al., 2009; Stella et al., 2012; Vuolo et al., 2017) because there is typically much more ozone than NO_x (= NO + NO_2). However, some studies suggest R1 accounts for a nonnegligible influence on observed ozone fluxes (Dorsey et al., 2004; Finco et al., 2018; Lamaud et al., 2009; Neirynck & Verstraeten, 2018; Rummel et al., 2007), especially at night when there is relatively high NO_x.

The contribution of NO-NO_2-O_3 chemistry to observed ozone fluxes can be estimated with ozone, NO, and NO_2 fluxes at two heights (Finco et al., 2018; Fitzjarrald & Lenschow, 1983; Lenschow & Delany, 1987; Vilá-Guerau de Arellano et al., 1993). An empirical technique only requiring flux measurements at one height (Duyzer et al., 1995) has also been used (e.g., Plake, Sörgel, Stella, et al., 2015; Stella et al., 2012; Vuolo et al., 2017). This empirical technique assumes flux divergences of NO, NO_2 and ozone are logarithmic with height, but the theoretical basis for this assumption is lacking. Both techniques may be limited with respect to key assumptions: first-order closure and negligible influence from other in-canopy chemical reactions. More explicitly resolving interactions between in-canopy turbulence and ambient chemistry (e.g., through LES modeling) will allow for stronger constraints on the influence of fast chemistry on ozone fluxes.

Some sesquiterpenes, such as β-caryophyllene and α-humulene, and monoterpenes, such as α-terpinene, react very quickly with ozone (Calogirou et al., 1999; Shu & Atkinson, 1994; Yee et al., 2018) and constitute a permanent ozone sink. Reactions of these compounds with ozone may account for a nonnegligible fraction of the observed ozone flux (Bouvier-Brown et al., 2009; Fares, McKay, Holzinger, et al., 2010; Fares et al., 2012; Goldstein et al., 2004; Holzinger et al., 2005; Helmig et al., 2006; Kurpius & Goldstein, 2003; Jardine et al., 2011; Wolfe et al., 2011). However, the ability to constrain the relative contribution of chemistry is limited by a lack of comprehensive isomer-resolved BVOC measurements and uncertainty in rates for reaction with ozone (Bouvier-Brown et al., 2009; Goldstein et al., 2004; Shu & Atkinson, 1994; Yee et al., 2018). Sesquiterpenes are difficult to measure due to their low volatility, which leads to underestimates from the loss on sampling lines and instrument

surfaces, and to their low concentrations, which require sensitive detection and/or lower time resolution methods.

Supporting evidence for the influence of highly reactive BVOCs on observed ozone fluxes is largely based on observations and modeling at Blodgett Forest in the Sierra Nevada Mountains of California. Evidence includes (i) a dependence of observed ozone fluxes on air temperature consistent with monoterpene emissions from vegetation (Kurpius & Goldstein, 2003; Fares, McKay, Holzinger, et al., 2010), (ii) similar enhancements in ozone fluxes and monoterpene concentrations following forest thinning (Goldstein et al., 2004), (iii) direct measurements of oxidation products (Holzinger et al., 2005), and (iv) multilayer canopy modeling (Wolfe et al., 2011). Constraints on highly reactive chemistry at other sites, in combination with large-scale modeling, are needed to understand the large-scale impact of ambient ozone loss through reaction with highly reactive BVOCs on observed ozone fluxes.

Substantial soil emissions of highly reactive sesquiterpenes are observed at an Amazonian forest (Bourtsoukidis et al., 2018). While measurements at other locations are needed to understand whether this phenomenon occurs elsewhere, neglecting a soil source of highly reactive BVOCs in interpreting ozone fluxes may lead to an overemphasis of the role of other processes.

In-canopy ambient chemistry impacts not only ozone, but also other molecules. Reactions between ozone and highly reactive BVOCs may account for observed emission of oxidized organic species from the canopy (Alwe et al., 2019; Choi et al., 2010; Holzinger et al., 2005; Schobesberger et al., 2016) and subsequent secondary organic aerosol formation (Bouvier-Brown et al., 2009; Buzorius et al., 1998; Farmer et al., 2011; Goldstein et al., 2009; Wolfe et al., 2011), production of the hydroxyl radical (Faloona et al., 2001; Kurpius & Goldstein, 2003), and emission of reactive nitrogen oxides (Farmer & Cohen, 2008; Wolfe et al., 2009). Fluxes of oxidized organic and inorganic compounds may provide observational constraints on the location and mechanism of chemical influences on observed ozone fluxes.

4.5.1   Main Takeaways

- Fast ambient chemistry confounds ozone dry deposition estimates from ozone flux observations.

- Observed co-located fluxes of ozone and highly reactive compounds and models resolving their in-canopy distributions and fluxes are needed to estimate the influence of fast chemistry on ozone fluxes.

- Analytical challenges and uncertain reaction rates limit knowledge on the contribution of highly reactive BVOCs to observed ozone fluxes.

4.6   Snow-Covered Surfaces

Ozone deposition velocities over snow are typically low relative to the other terrestrial surfaces considered in this review, but are highly uncertain. The range of observed v_d over snow from both field and laboratory studies is −3.6 to 1.8 cm s^{-1} with most of the data from 0 to 0.1 cm s^{-1} (Figure 7).

The slowest observed v_d are over polar snowpack (both glacial and sea ice), suggesting ozone uptake to snow-covered landscapes is not primarily controlled by snow presence. While ozone destruction by snow grains may be slow, the transport of air through snowpack (a porous medium with high surface area) to the bottom (Helmig, Bocquet, Cohen, et al., 2007) occurs on timescales of minutes to hours, allowing ozone destruction through reaction with surfaces within or underneath the snowpack. Snow-covered forests exhibit the fastest v_d relative to other snow-covered surfaces, followed by snow-covered grassland and soils (Figure 7).

Hypothesized or identified pathways for ozone dry deposition over snow-covered surfaces include reaction with organic or humic trace impurities, black carbon (Albert et al., 2002), and halogens (Peterson & Honrath, 2001). Based on snowpack chemical and transport modeling, reaction with bromine (Thomas et al., 2011) and formic acid in the aqueous phase (Murray et al., 2015) may be ozone deposition pathways for snow on glacial ice. In environments where vegetation protrudes from the snow, ozone uptake by biological materials may be the determining ozone sink.

For seasonally deep snowpack at midlatitudes, snowpack insulates the ground, promoting relatively warm and moist soil conditions that foster soil microbial processes resulting in a steady production and emission of NO. For example, interstitial air is enriched in NO by a factor of up to ~100 compared to the air above the surface at Niwot Ridge (Helmig, Seok, Williams, et al., 2009). Snowpack reaction between ozone and NO under low light conditions when NO_2 photolysis does not occur may be a primary route for ozone loss in this type of environment. Currently, there are no observations of ozone dry deposition over snow-covered permafrost soils. Such observations may help establish v_d over snow-covered soils without the contribution of ozone reaction with NO.

Ozone deposition velocity over snow-covered surfaces also exhibits a diel cycle, with maximum values in the afternoon (Helmig, Cohen, Bocquet, et al., 2009; Neirynck & Verstraeten, 2018). The processes driving the diel cycle are uncertain.

Most models apply a constant resistance for ozone dry deposition to snow regardless of environmental conditions and the substrate underneath the snowpack. As evident from v_d variability for snow-covered surfaces (Figure 7), a single resistance will not describe ozone dry deposition over myriad snow-covered environments accurately. A more comprehensive parameterization likely requires accounting for dependencies on snow conditions, chemical snow properties, and substrate underneath snowpack. Variability in observed v_d for a given LULC type also emphasizes the need for more observational constraints.

A range of approaches has been used to study ozone fluxes over snow, including observing ozone decay in chambers filled with snow (Aldaz, 1969; Galbally & Roy, 1980), the flux gradient technique (Bocquet et al., 2011; Colbeck & Harrison, 1985; Helmig, Cohen, Bocquet, et al., 2009; Neirynck & Verstraeten, 2018; Wu, Z., et al., 2016), EC (Stocker et al., 1995; Zeller & Hehn, 1996; Zeller & Nikolov, 2000), and near-surface vertical profiles measured with an automated elevator system (Van Dam et al., 2010).

Low snowpack ozone fluxes challenge instrument resolution and thus uncertainty needs to be considered. The lack of turbulence over snow and snow cover promoting thermal inversions limit micrometeorological techniques. Methods for measuring ozone in air withdrawn from snowpack are highly sensitive and promising for constraining the controls on and strength of ozone snowpack sinks (Bocquet et al., 2007; Helmig, Bocquet, Cohen, et al., 2007; Seok et al., 2015; Van Dam et al., 2015).

Several studies report consistently negative v_d over snow-covered surfaces, suggesting emission from the surface (Galbally & Allison, 1972; Zeller & Hehn, 1996; Zeller & Nikolov, 2000). Relatively large negative v_d in earlier work has not been reproduced recently (Figure 7), bringing up the question of whether older findings are influenced by earlier experimental approaches with higher uncertainty. We recommend emphasizing newer relative to older measurements due to the improvement of EC instrumentation and refinement of data-analysis protocols.

Recent high-resolution ozone flux measurements show consistently negative (but relatively small) nighttime v_d at Summit in Greenland with increasingly negative values towards summer (Helmig, Cohen, Bocquet, et al., 2009). Snowpack is not a location of ozone production: ozone in snowpack interstitial air is generally depleted compared to above the surface (Albert et al., 2002; Bocquet et al., 2007; Helmig, Bocquet, Cohen, et al., 2007; Peterson & Honrath, 2001; Seok et al., 2015) and ozone is always destroyed in snow chamber experiments (Aldaz, 1969; Bottenheim et al., 2002). However, ozone production in the poorly mixed layer right above snow may occur following the accumulation of ozone precursor emissions from the snowpack and enhanced irradiance from snow (e.g., Crawford et al., 2001; Cristofanelli et al., 2018; Helmig et al., 2008; Legrand et al., 2009; 2016).

4.6.1 Main Takeaways

- There is strong variability in observed v_d over snow-covered surfaces.

- Accurate modeling of ozone dry deposition to snow-covered surfaces requires better understanding of dependencies on underlying substrate, snow conditions, and meteorology.

- We recommend emphasizing relatively newer measurements due to the improvement of EC instrumentation and refinement of data-analysis protocols.

5. Simulating Ozone Dry Deposition in Regional and Global Models

Most ozone dry deposition schemes used in regional and global models employ resistance networks (section 3) and rely on lookup tables for component resistances and changes with season and LULC type (e.g., Simpson et al., 2001; Wesely, 1989; Zhang, L., et al., 2002). While environmental conditions (e.g., temperature, surface wetness) sometimes modify lookup values, there is rarely mechanistic representation of processes in dry deposition schemes. Incomplete process representation limits the fidelity of these schemes in simulating ozone dry deposition impacts on air pollution, ecosystems, and climate.

Wesely (1989) is the basis of many large-scale models' dry deposition schemes. The Wesely (1989) scheme was designed to represent regional and seasonal average conditions. However, observations from very short time periods at only a few field sites informed Wesely (1989) as well as later schemes (e.g., L. Zhang et al. (2002)), calling into question whether climatological v_d is represented accurately in these schemes. There is also hardly an emphasis on v_d variations on different timescales (e.g., daily, interannual) in past scheme development.

Despite the similar structure of commonly used dry deposition schemes, v_d varies strongly across models (Bela et al., 2015; Herwehe et al., 2011; Hardacre et al., 2015; Park et al., 2014; Wu, Z., et al., 2011). For example, monthly v_d varies by ±20% across models in the Task Force on Hemispheric Transport of Air Pollution (HTAP) ensemble (Figure 8). Because most HTAP models identify as employing Wesely (1989), substantial intermodel variation emphasizes the need to critically assess the implementation of a given scheme as well as input uncertainty (e.g., LULC distribution). Strong v_d variability across models leads to uncertainty in the tropospheric ozone budget (Wild, 2007) as well as model estimates of ozone pollution (e.g., Hogrefe et al., 2018; Walker, 2014) and plant damage.

Substantial v_d differences also occur among different ozone dry deposition schemes (Schwede et al., 2011; Wu, Z., et al., 2018; Wong, A. Y. H., et al., 2019). For example, there are two- to three-fold v_d differences among five schemes all driven by the same forcing data at Borden Forest in Canada (Figure 9). There are also large differences in summer interannual variability and 30-year trends in v_d across four schemes implemented in one global atmospheric chemistry model (Wong, A. Y. H., et al., 2019). Studies comparing schemes in depth (Schwede et al., 2011; Wu, Z., et al., 2018) illustrate a variety of processes and parameters contributing to intermodel differences.

Improved understanding of parameter and process uncertainty in individual dry deposition schemes (Charumsombat et al., 2010; Cooter & Schwede, 2000; Mészáros, Zsély, Gy, et al., 2009; Silva & Heald, 2018; Simpson et al., 2003; Tuovinen et al., 2001; Tuzet et al., 2011) is needed, and will inform v_d differences and similarities across models. We recommend archival of model diagnostics oriented towards processes and LULC types (see Figure 10) in multimodel comparison efforts because such diagnostics allow pinpointing the causes of intermodel similarities and differences.

Model ozone dry deposition evaluation typically consists of comparing simulated and observed seasonal v_d averages or diel cycles with observations at sites with ozone fluxes (Centoni, 2017; Clifton, 2018; Hardacre et al., 2015; Silva & Heald, 2018; Val Martin et al., 2014; Wu, Z., et al., 2018). Some observed climatological features are captured by current schemes. For example, the modified Wesely (1989) scheme in GEOS-Chem captures diel cycles and seasonality at various sites relatively well but does not capture the v_d spatial distribution (Silva & Heald, 2018). However, in general, skill varies by model and site, and there is poor understanding of the processes leading to similarities and differences between models and observations (Centoni, 2017; Hardacre et al., 2015; Silva & Heald, 2018; Val Martin et al., 2014; Wu, Z., et al., 2011).

Ozone flux datasets used for model evaluation typically span a couple of months at maximum. However, v_d varies by a factor of two across eleven years of observations at Harvard Forest, which is not captured by the modified Wesely (1989) scheme in GEOS-Chem (Clifton et al., 2017). Strong unreproducible v_d interannual variability suggests model evaluation with a single year of observations is inadequate. We recommend emphasizing multiyear averages from long-term ozone flux datasets over short-term datasets for climatological v_d evaluation.

Ozone flux datasets are limited to homogeneous terrain (e.g., Wesely & Hicks, 2000) so models are unconstrained for complex terrain. Given that the theories underpinning current parameterizations assume horizontal heterogeneity, models likely perform poorly over complex landscapes.

Future work should evaluate model performance not only in terms of climatological seasonal and diel cycles of v_d, but also spatiotemporal variability and relationships with meteorological and biophysical parameters. For example, observations suggesting a weak dependence on LAI (Clifton et al., 2017, 2019; Mahrt et al., 1995; Wolfe et al., 2015) may imply the strong LAI sensitivity in many models (Charusombat et al., 2010; Schwede et al., 2011; Silva & Heald, 2018) is exaggerated. However, whether observations generally suggest a weak dependence on vegetation density is unknown; some work suggests a strong dependence (e.g., MacPherson et al., 1995). The most insightful model evaluation relies on process-oriented relationships yet to be identified from a meta-analysis of observations.

Only a few studies probe the roles of deposition processes driving model biases (e.g., Tuovinen et al., 2004; Wu, Z., et al., 2018). Most studies largely assume stomatal uptake drives variations in v_d. We emphasize the contribution of nonstomatal deposition (Figure 4) should be considered in model evaluation. We recommend developing and archiving model diagnostics oriented towards processes (see Figure 10). Isolating simulated v_d for a specific LULC type from the grid-box average (Figure 10), which combines multiple LULC types, is also helpful for more direct comparison with observations (e.g., Silva & Heald, 2018; Paulot et al., 2018). For evaluation with such diagnostics to be most instructional, a firm grasp on the relative roles of individual ozone deposition pathways and the mechanisms responsible for differences across LULC types as gleaned from observations is needed.

In general, differences between site and model environmental variables (e.g., meteorology, soil moisture) and observational uncertainty confound model evaluation (Cooter & Schwede, 2000; Schwede et al., 2001; Silva & Heald, 2018; Tuovinen et al., 2001; Wu, Z., et al., 2018). To reduce the impact of differences between site and model variables on model evaluation and thus separate input uncertainty from process and parameter uncertainty (e.g., Z. Wu et al., 2018), we recommend driving standalone schemes with observed variables representative of the flux-tower footprint. Given more observational constraints on the processes controlling observed v_d, driving models with flux-tower data will allow identification of realistic schemes. Otherwise, as is the case for modeling at regional-to-global scales, agreement with observations may stem from incorrect contributions from the various deposition pathways.

6.   Remaining Gaps and Recommendations for Future Work

Ozone dry deposition intersects multiple fields, including atmospheric chemistry, plant physiology/ecology, and boundary-layer meteorology, all with distinct research questions on the subject (e.g., Hosker & Lindberg, 1982). While ecologists aim to quantify stomatal ozone uptake and understand the ensuing damage to plants, atmospheric chemists aim to quantify ozone deposition velocity over different surfaces and understand the impact of ozone dry deposition on tropospheric chemistry and composition. Identifying current measurement techniques, modeling, and available data as well as assessing and advancing knowledge on ozone dry deposition requires bridging across distinct research communities.

Current understanding of ozone dry deposition is largely based on only a few ozone flux datasets, many of which only span short time intervals. It is generally uncertain which aspects of observed ozone dry deposition are specific to a given site versus represent the broader region or land use/land cover type, or are climatological versus episodic. Our top recommendation is establishing key field sites with long-term ozone eddy covariance fluxes. The highest priority complementary measurements depend on the specific question ranked as most important (Table 4). If robust evaluation of variability across sites is a desired outcome of future field studies, then a coordinated approach across sites is needed to ensure consistency across measurements.

We also recommend that older datasets be revisited in order to build on the deeper mechanistic understanding revealed by our synthesis here. Our efforts to document ozone flux records since 1985 identifies over 100 sites with measurements. A central archive of ozone fluxes along with complementary data would facilitate broad synthetic meta-analyses and hasten progress towards robust scientific advances. Quantifying uncertainty in data, particularly with respect to random and systematic errors associated with measurement technique, is essential when synthesizing information across datasets. We suggest holistic examinations of older datasets will lead to new knowledge of the processes and conditions driving ozone dry deposition on different temporal and spatial scales.

Because there are only a handful of sites with long-term ozone flux records and many no longer measure ozone fluxes, we emphasize that continued support of current and past sites and establishment of new long-term sites are fundamental to advance knowledge. Because ozone dry deposition is closely related to carbon and water exchange and associated conditions (e.g., ambient humidity, soil organic content), science will progress most rapidly when ozone fluxes are added to sites already well-characterized in terms of carbon and water cycling and boundary-layer meteorology.

For both future short-term campaigns and long-term monitoring, we recommend measuring ozone flux through ozone eddy covariance. That the fast ozone analyzers required for ozone eddy covariance either require frequent maintenance or are expensive and require toxic or flammable compressed gases is a potential roadblock. We emphasize the importance of developing new analytical methods for fast ozone measurement. An effort to coordinate across research groups measuring ozone fluxes is sorely needed and should promote best practices learned from the carbon dioxide flux community in calculating fluxes, filtering

datasets, and sharing data. Such an effort should also include validation and intercomparison of different fast ozone analyzers.

While our review offers an unprecedented synthesis of process-based knowledge of ozone deposition pathways, the relative importance of individual depositional pathways remains uncertain. In particular, we emphasize large uncertainty in the partitioning of ozone dry deposition occurring through pathways other than through plant stomata. Our synthesis of observationally based estimates of the stomatal fraction of ozone dry deposition across peer-reviewed literature shows on average the stomatal fraction over physiologically active vegetation is 45%, underscoring the importance of nonstomatal deposition.

Process-oriented investigation of spatiotemporal variations and trends in ozone fluxes is necessary to quantify the relative importance of various deposition pathways, and will inform the degree of complexity needed to model deposition of ozone at large scales. If coordinated with short-term field intensives, laboratory studies, and mechanistic modeling, measurements from a few long-term sites as described in Table 4 would bridge the molecular to ecosystem scales needed to establish the relative importance of various deposition pathways and the extent to which they vary in space and time.

Advancing understanding of dry deposition of ozone is also relevant for dry deposition of other reactive trace gases that alter atmospheric chemistry, climate, and ecosystems because similar physical and chemical processes govern their uptake. Process knowledge of dry deposition for ozone can be translated to any trace gas reacts with surfaces (e.g., nitrogen dioxide, oxygenated volatile organic compounds). Additionally, models frequently parameterize dry deposition of other reactive trace gases by using ozone and sulfur dioxide as end members. Specifically, a gas's oxidizing ability is scaled to ozone dry deposition while a gas's solubility is scaled to sulfur dioxide given ozone is an oxidant but insoluble and sulfur dioxide is not an oxidant but soluble. Building on the mechanistic framework for ozone dry deposition outlined in this review should inform the strengths and limitations of such a parameterization.

The optimal parameterization for ozone dry deposition remains elusive, but the process understanding synthesized in this review lays the groundwork for one. Representation of most deposition processes in current models should be regarded as insufficient. While current parameterizations capture some of the main observed features of ozone dry deposition, the underlying brazen empiricism of these schemes hinders a full mechanistic understanding of the influence of ozone dry deposition on air pollution, ecosystems, and climate.

Acknowledgements

Appendix A

Table A1

Ecosystem-Scale Ozone Flux Datasets from 1985 Onwards.

Site name	Region	Latitude	Longitude	Length of observational dataset	Measurement Type	Land use/ land cover	Previous literature
Alice Holt	England	51.1667452°N	0.8658308°W	July-August 2005	EC	oak forest	
Amazon Tall Tower Observatory (ATTO)	Brazil	2.1459°S	59.00°W	December 2015, March 2016-present	EC	tropical forest	
Auchencorth Moss	Scotland	55°47'30"N	3°14'20"W	1995–1998	gradient	moorland	Fowler et al., 2001; Tuovinen et al., 2004
Beaufort	Southeast US	34.88°N	−76.62°W	10 June to 01 August 1993	EC	crop	Finkelstein et al., 2000; Meyers et al., 1998
Beijing	China	39.98°N	116.39°E	August-November 2016, May-June 2017	EC	urban	
Bergamo	Italy	45°36'51'N	9°40'22'E	May-June 2001	EC	wheat field	Gerosa et al., 2003
Bily Kriz	Czech Republic	49°33'N	18°32'E	gradient: July-August 2008, 2012–2017; EC: summer 2017	gradient, EC	Norway spruce forest, established in 1981 by planting four-year-old seedlings in rows	Jurá et al., 2019; Zapletal et al., 2011
Blodgett Forest	California	38.9°N	120.63°W	June-September 1997, May-November 1998, June 1999 to June 2000, January 2001 to December 2006	EC	ponderosa pine plantation	Bauer et al., 2000; Fares, McKay, Holzinger, et al., 2010; Goldstein et al., 2003, 2004; Kurpius et al., 2002; Kurpius & Goldstein, 2003; Wolfe et al., 2011
Bondville	Midwest US	40.05°N	88.37°W	18 August to 1 October 1994	EC	corn	Finkelstein et al., 2000; Finkelstein, 2001; Meyers et al., 1998; Wu, Y., et al., 2003;

Site name	Region	Latitude	Longitude	Length of observational dataset	Measurement Type	Land use/ land cover	Previous literature
							Zhang, L., et al., 2002
Bosco Fontana	Italy	45°12'02"N	10°44'44"E	12 June to 11 July 2012	EC	mixed oak-hornbeam forest	Finco et al., 2018
Braunschweig	Germany	53°18'N	10°26'E	20 May to 15 June 2000	EC	intensively managed grassland	Bassin et al., 2004; Mészáros, Horváth, Weidinger, et al., 2009
Bruneck	Italy	46°49'N	11°55'E	December 1999	EC	snow-covered mountain valley	Cieslik, 2009
Bugacpuszta	Hungary	46.69°N	19.60°E	August 2012 to January 2014	EC	semi-natural semi-arid sandy grassland	Horváth et al., 2017
Bukit Atur	Malaysia	4°58'49.10"N	117°51'19.12"E	7 April to 24 July 2008	EC, gradient	tropical forest	Fowler et al., 2011
Burriana	Spain	39°55'N	0°03'W (0.04'W for last campaign)	16–29 July 1995, 28 April to 3 May 1996, 2–16 June 1997	EC	orange grove	Cieslik, 2004
Cala Violina	Italy	42°55'N	10°30'E	June-December 2005, July-September 2006	EC	mixed oak forest in complex terrain	Cieslik, 2009; Gerosa et al., 2007
Camp Borden	Canada	44°19'N	79°56'W	July-August 1988 (EC), March-April 1990 (EC), May 2008 - April 2013 (gradient)	EC, gradient	temperate mixed forest	Fuentes et al., 1992; Padro, 1993, 1994; Padro et al., 1991; Wu, Z., et al., 2016, 2018
Castelporziano	Italy	41.42°N	12.21°E	June 1993, May 1994	EC	Mediterranean pseudo steppe	Cieslik, 2004; Cieslik & Labatut, 1997
Castelporziano	Italy	41.42°N	12.21°E	August-September 2003, June-November 2004, June-October 2003, 2011–2015	EC	Holm oak forest	Gerosa et al., 2005, 2007, 2009b; Fares et al., 2013, 2014; Hoshika et al., 2017; Rydsaa et al., 2017; Savi & Fares, 2014; Vitale et al., 2005

Site name	Region	Latitude	Longitude	Length of observational dataset	Measurement Type	Land use/ land cover	Previous literature
Castile and Leon	Spain	42°1'N	4°32'W	5, 6, and 8 May 1994, six days in July 1995	gradient	semi-arid steppe on a plateau covered in barley	De Miguel & Bilbao, 1999; Sánchez et al., 1997
Central Plains Experimental Range	western US	40°28'23"N	104°45'15"W	5 March to 2 August 1988, 24 January to 21 February 1989, 7 June to 10 July 1989	EC	bare patches of soil and dead or senescent vegetation or snow	Massman, 1993; Stocker et al., 1993, 1995
Chinese Research Academy of Environmental Sciences	Beijing			September and November 2000, 10 days each	gradient	grassland	Sorimachi et al., 2003
CODE cotton	California	36°48'50"N	120°40'38"W	8 July to 6 August 1991	EC	cotton	Grantz et al., 1997; Massman et al., 1994; Padro, Massman, Shaw, et al., 1994; Padro, 1996
CODE grassland	California	37°02'N	119°48'30"W	30 days during summer 1991	EC	grassland	Massman et al., 1994; Padro, Massman, Shaw, et al., 1994; Padro, 1996
CODE vineyard	California	36°51'36"N	120°6'7"W	11 July to 1 August 1991, 8 July to 6 August 1991	EC	grape	Grantz et al., 1995; Massman et al., 1994; Padro, Massman, Den Hartog, et al., 1994; Padro, 1996
Colt Park	England	54.19°N	2.34°W	August to October 2005	EC	semi-natural grassland	
Comun Nuovo	Italy	45°37'N	9°40'E	May-June 2001, July-September 2001, May-June 2002	EC	wheat, soybean, or barley	Bassin et al., 2004; Cieslik, 2009; Gerosa et al., 2003; Tuovinen et al., 2004; Rydsaa et al., 2017
Cuatro Vientos	Spain	40°40'N	3°56'W	2–13 May 1997	EC	low vegetation	Cieslik, 2004
Dakhla Oasis	Egypt			23 March to 9 April 1993	EC	Saharan desert	Güsten et al., 1996

Site name	Region	Latitude	Longitude	Length of observational dataset	Measurement Type	Land use/ land cover	Previous literature
Diepoholz	Germany	52°39'8"N	8°39'12"E	30 June to 4 August 2014	EC	peatland	El-Madany et al., 2017
Duke Forest	southeast US			spring 2017 to 2019	EC	bottomland mixed hardwood forest along urban to rural gradient	
Duke Forest Blackwood Division	southeast US	35.97°N	79.13°W	15 April to 15 May 1996	EC	Loblolly pine plantation	Finkelstein et al., 2000; Meyers et al., 1998
Easter Bush	Scotland			August 2007	EC	grasslands with predominately perennial rye-grass with grazing in adjacent fields	Muller et al., 2009, 2010
Flanders	Belgium	51°18'N	4°31'E	2000–2015	gradient	mixed forest in a suburban area	Neirynck et al., 2012; Neirynck & Verstraeten, 2018
Gilchriston Farm	Scotland	55.9°N	2.8°W	one month in summer 2006	EC	potato canopy	Coyle et al., 2009
GLEES Brooklyn Lake	Western US	41°22'N	106°14.5'W	14–27 April, 6–19 May, June, and 2–9 July 1992, 15–26 January 1993, 30 July to 8 August 1996	EC	subalpine coniferous forest	Zeller, 2000; Zeller & Hehn, 1995; 1996; Zeller & Nikolov, 2000
GLEES Brooklyn Lake	Western US	41°22'N	106°14.5'W	24 April to 3 May 1994, 7–21 June, 2–10 August 1994	EC	open meadow	Zeller & Hehn, 1995
Grignon	France	48.84422°N	1.95191°E	19 June to 7 October 2002, 26 July to 1 October 2002, 2004–2009, 7 August 2012 to 13 March 2013	EC	crop (sometimes bare soil, maize, winter wheat)	Lamaud et al., 2009; Loubet et al., 2013; Stella, Loubet, Lamaud, et al., 2011; Stella, Personne, Loubet, et al., 2011; Stella et al., 2012, 2013, 2019; Tuzet et al., 2011; Vuolo et al., 2017
Halvergate Trace Gas Exchange Experiment	England			15 September 1989	gradient	drained marshland pasture	Hargreaves et al., 1992; Kramm et al., 1991

Site name	Region	Latitude	Longitude	Length of observational dataset	Measurement Type	Land use/ land cover	Previous literature
Hartheim	Germany	47°56'N	7°37'E	17–20 May 1992	gradient	Scots pine plantation	Joss & Graber, 1996
Harvard Forest	Northeast US	42.53°N	72.18°W	1990–2000	EC, gradient	temperate deciduous forest	Clifton et al., 2017, 2019; Munger et al., 1996; Wu, Z. Y., et al., 2015
Hesse	France	48°0'27"N	7°03'52"E	September 2010 to March 2011	EC	European beech	Le Morvan-Quéméner et al., 2018
Hohenpeissenberg	Germany	47°48'N	11°02'E	29 August to 20 September 2005	EC	meadow, pre-alpine landscape	Stella et al., 2013
Horsepool	Western US			25 January to 2 April 2013	EC	dry, sandy soil and low-lying sage brush	
Hortobágy	Hungary			19–30 June 1993, 5 May to 21 June 1994, 13–30 September 1994	gradient	grassland	Hórvath et al., 1997
Hurdal	Norway			1 July 2000 to 31 March 2003	gradient	Norway spruce forest	Hole et al., 2004
Hyytiälä	Finland	61.85°N	24.28°E	2001–2013	EC	coniferous forest	Altimir et al., 2006; Launiainen et al., 2013; Rannik et al., 2009, 2012; Zhou, P. T., et al., 2017
Ispra forest	Italy	45.8126°N	8.6336°E	2013–2015	EC	deciduous forest	
Ispra grassland	Italy	44°48'N	8°38'E	September 1997	EC	grassland	Cieslik, 2009
Kaamanen	Finland	69°08'N	27°17'E	September 1995	EC	open fark fen (ridges and open water pools)	Tuovinen et al., 1998, 2004
Kane Experimental Forest	Northeast US	41.595°N	78.766°W	29 April to 23 October 1997	EC	deciduous forest	Finkelstein et al., 2000; Finkelstein, 2001; Meyers et al., 1998; Zhang, L., et al., 2001, 2002
Keenly Fell	England	54°53'49.0"N	2°19'26.6"W	June 2007 to December 2011	EC	semi-natural grassland	

Site name	Region	Latitude	Longitude	Length of observational dataset	Measurement Type	Land use/ land cover	Previous literature
Klippeneck	Germany	48°10'N	8°45'E	10–22 September 1992		grassland	Cieslik, 2004
Konza Praire Research Natural Area	Central US			26 May to 6 June 1987, 25 June to 11 July, 6–21 August 1987, 5–16 October 1987	EC	predominately big bluestem grass; surface materials above ground southwest of tower removed recently by fire	Gao et al., 1992
Kranzberger Forst	Germany	48°25'N	11°39'E	2–29 July 2007	EC	mixed forest	Nunn et al., 2010
La Barben	France	43°35'N	5°15'E	29 June to 13 July 2001	EC	Mediterranean shrubland, mostly *Quercus coccifera*	Michou et al., 2005
La Cape Sud	France	44°24'N	0°38'W	26 July 2007 to 4 March 2008	EC	crop	Stella, Personne, Loubet, et al., 2011; Stella et al., 2019
La Crau	France	43°34'N	4°49'E	20 April to 31 May 2001	EC	semi-arid part of the La Crau plain; totally flat, uniform, almost bare soil with mainly pebbles	Michou et al., 2005; Stella et al., 2019
Lake Kinisheo	Canada			late June to July 1990		lichen bogs and small conifer shrubs	Fuentes et al., 1994
Lake Kuivajärvi	Finland	61°50'N	24°17'E	August to September 2012	EC	boreal lake	Fung, 2018
Lamasquére	France	43°49'N	1°23'W	2008–2010	EC	crop	Stella, Personne, Loubet, et al., 2011; Stella et al., 2019
Le Bray	France	44°34'33.24"N	0°46'33.72"W	May to August 2007, May to August 2008	EC	stand of maritime pines planted in 1970	Le Morvan-Quéméner et al., 2018
Le Dézert	France	44°05'N	0°43'W	16–18 April 1997	EC	coniferous forest	Cieslik, 2004
Les Landes	France	44°12'N	0°42'W	June 1994, 21 June to 3 July 1997, 21–24 February 1997, June 1996, October 1996	gradient, EC	mixed forest	Lamaud et al., 2002; Sánchez et al., 1997

Site name	Region	Latitude	Longitude	Length of observational dataset	Measurement Type	Land use/ land cover	Previous literature
Lincove	California	36.36°N	119.09°W	October 2009 to November 2010	EC	orange orchard	Fares et al., 2012
Lochristi	Belgium	51°06'44"N	3°51'02"E	2010–2016	EC	short-rotation coppice poplar plantation	Zenone et al., 2016; Zona et al., 2014
London	England	51.52°N	0.14°W	October 2011 to August 2013	EC	urban	
Lusignan	France	46°24'N	0°07'E	17 March to 5 May 2011	EC	crop	Stella et al., 2019
Lusignan	France	46°26'08"N	0°07'25"E	August to September 2010	EC	meadow	Le Morvan-Quéméner et al., 2018
Manaus	Brazil	3°S	60°W	at most a couple of days in July - August 1985	gradient	tropical forest	Kirchhoff et al., 1988
Mea Moh	Thailand	18.28°N	99.72°E	January-April 2002, January-August 2004	gradient	teak forest	Matsuda et al., 2005, 2006
Mekrijärvi	Finland	62°52'N	30°55'E	July 1995	EC	low Scots pine forest on border of southern and middle boreal zones	Tuovinen et al., 2001, 2004
Meyrargues	France	43°39'N	5°32'E	12–28 June 2001	EC	maize	Michou et al., 2005
Monmeyan	France	43°39'N	6°05'E	10–26 June 2001	EC	Mediterranean forest (95% *Quercus Pubescens*)	Michou et al., 2005
Nashville/ Keysburg	Southeast US	36.65°N	87.03°W	22 June to 11 October 1995	EC	soybean	Finkelstein et al., 2000; Finkelstein 2001; Meyers et al., 1998; Pleim et al., 2001; Wu, Y., et al., 2003; Zhang, L., et al., 2002
Neustift	Austria	47°07'N	11°19'E	11 July to 20 October 2008	gradient; EC	temperate mountain meadow	Wohlfahrt, Hörtnagl, Hammerle, et al., 2009
Niwot Ridge	Western US	40.03°N	105.55°W	6 June to 31 August 2002; 1 April to 19 November 2003; 21 May to 30 June 2004; 20 May to 31 August 2005	EC	coniferous sub-alpine forest	Turnipseed et al., 2009

Site name	Region	Latitude	Longitude	Length of observational dataset	Measurement Type	Land use/ land cover	Previous literature
Norwood Park	England			25–28 July 1994	EC	fruit orchard	Walton, Gallagher, Choularton, et al., 1997; Walton, Gallagher, & Duyzer, 1997
Nyírjes	Hungary			5–30 September 1991, 20 March to 16 April 1992, 28 January to 17 February 1993, 8 July to 29 August 1993, 15 July to 6 August 1994	gradient	Norway spruce forest	Hórvath et al., 1997
Oshiba Highland	Japan	32°52'N	137°58'E	April-September 2001	gradient	red pine forest	Zhang, S., et al., 2005
Palatinate	Germany	49.16°N	8.28°E	April-September 1992	EC	barley or flat harvested field	Güsten et al., 1997
Petsikko	Finland	69°52'N	27°14'E	beginning of June to August 18 1996	EC	subarctic mountain birch	Tuovinen et al., 2001
Plymouth	Southeast US	35.70°N	76.80°W	15 July to 15 August 1996	EC	soybean	Finkelstein et al., 2000; Meyers et al., 1998; Wu, Y., et al., 2003
Polder Piloto de Sarazola	Portugal	40°42'N	8°37'W	November 1994 to October 1995	gradient	meadow	Pio & Feliciano, 1996; Pio et al., 2000; Tuovinen et al., 2004
Ramat Hanadiv Nature Park	Israel	32°33'19.87"N	34°56'50.23"E	31 July to 30 September 2015, 1 February to 31 March 2016, 1 June to 7 July 2016, 2 August to 17 September 2016, 5 January to 22 May 2017, 12 June to 2 July 2017	EC	shrub 3.6 km away from eastern Mediterranean seashore	Li, Q., et al., 2018
Reserve Adolfo Ducke	Amazonia	2°57'S	59°57'W	22 April to 8 May 1987	EC	tropical forest	Fan et al., 1990
Rhine Valley	Germany			September 1992	gradient	short sparse wheat	Horváth et al., 1998
Rhineland-Palatinate	Germany	49.9685°N	8.1481°E	July-October 2011	EC	natural nutrient-poor	Ermel et al., 2013;

Site name	Region	Latitude	Longitude	Length of observational dataset	Measurement Type	Land use/ land cover	Previous literature
						steppe-like grassland; occasionally subject to management in past	Plake, Stella, Moravek, et al., 2015
Rivox	Scotland	55°19'57"N	3°31'43"W	May 1992	EC	Sitka spruce plantation	Coe et al., 1995
Rondonia	Amazonia	10°04'55'S	61°55'48"W	4–22 May 1999, 21 September to 20 October 1999	EC	wet and dry season, la Niña year	Rummel et al., 2007
Rondonia	Amazonia	10°45'44"S	62°21'27"W	30 April to 17 May 1999, 24 September to 27 October 1999	EC	pasture; transition seasons "wet-dry" and "dry-wet", la Niña year	Kirkman et al., 2002; Rummel et al., 2007
S. Pietro Capofiume	Italy	44°39'N	11°37'E	2–11 June 1993	EC	beet	Cavicchioli et al., 1997; Cieslik, 2004, 2009
Sabah	Malaysia	5°14'58.69"N	118°27'15.76"E	4–11 June 2008	EC	crop	Fowler et al., 2011
San Rossore	Italy	43°43′55′′N	10°17′27′′E	20 January to 10 February 2013, 22 April to 12 May 2013, 8–27 July 2013, 9–29 September 2013	EC	coniferous forest (*Pinus pinea*)	Hoshika et al., 2017
Sand Flats State Forest	Northeast US	43.565°N	75.238°W	12 May to 20 October 1998	EC	mixed forest	Finkelstein et al., 2000; Finkelstein 2001; Meyers et al., 1998; Zhang, L., et al., 2001, 2002
Sand Mountain	Southeast US	34.29°N	85.97°W	15 April to 13 June 1995	EC	grassland	Finkelstein et al., 2000; Finkelstein, 2001; Meyers et al., 1998; Wu, Y., et al., 2003; Zhang, L., et al., 2002
Schachtenau	Germany			June to September 1987, 18–28 September 1989	EC	coniferous forest	Enders, 1992; Enders et al., 1992
Schefferville	Canada	54°50'N	66°40'W	July to August 1990	EC	spruce woodland	Munger et al., 1996

Site name	Region	Latitude	Longitude	Length of observational dataset	Measurement Type	Land use/ land cover	Previous literature
Scherzheim	Germany			11–22 September 1992	EC	harvested and harrowed wheat field with re-grown wheat	Pilegaard et al., 1998
Sinderhoeve	Netherlands	51.58°N	5.42°E	30 June 1988, 6, 19, 25, and 28 July 1988, 12 and 28 August 1988, 12 and 22 September 1988, 4 October 1988	EC	maize	Van Pul & Jacobs, 1994
Speulderbos	Netherlands			nine months in 1993	EC	Douglas fir plantation	Dorsey et al., 2004; Duyzer et al., 1995
Summit	Greenland	72.34°N	38.29°W	19–30 July 2003, 22 March to 14 August 2004, 17 March to 28 April 2005	gradient	polar snowpack on glacial ice	Helmig, Bocquet, Cohen, et al., 2007; Helmig, Cohen, Bocquet, et al. 2009
Toolik Lake	Alaska	68.6°N	149.6°N	May-August 2011	EC	tundra	Van Dam et al., 2016
Turro	Italy	44°59'N	9°42'E	March-April 2014	EC	crop	Stella et al., 2019
Ulborg	Denmark	56°17'N	8°25'E	EC: 7 days in April 1995, 10 days in June 1994, 7 days in August 1997, 5 days in September 1995, May-June 1995, 2003; gradient: 1994–2000	EC, gradient	mixed forest (mostly Norway spruce)	Mikkelsen et al., 2000, 2004; Pilegaard et al., 1995; Ro-Poulsen et al., 1998; Tuovinen et al., 2004
UMBS Prophet	Midwest US	45.5°N	84.7°W	27 June to 28 September 2002, 7 August to 15 October 2003, 15 June to 15 September 2004, 15 June to 3 September 2005	EC	mixed forest (Bigtooth aspen, white pine, red oak, red maple, paper birch)	Hogg et al., 2007; Hogg, 2007
Viols-en-Laval	France	43°41'N	3°47'E	16–24 July 1998	EC	Mediterranean shrub	Cieslik, 2004
Virginia Forest Research Facility	Southeast US	37.92°N	78.27°W	July 2019-present	EC	mixed forest	
Voghera	Italy	45°01'N	9°00'E	May-July 2003	EC	onion	Cieslik 2009; Gerosa et al., 2007

Site name	Region	Latitude	Longitude	Length of observational dataset	Measurement Type	Land use/ land cover	Previous literature
Yucheng Comprehensive Experimental Station of the Chinese Academy of Sciences	China	36°50'N	116°34'E	9 August to 28 September 2011, 2 March to 6 June 2012	EC	corn, wheat	Zhu et al., 2014; Zhu, 2019
Yukon Delta National Wildlfie Refuge	Alaska	61°05.41'N	162°00.92'W	14 July to 12 August 1988	EC	tundra	Jacob et al., 1992
Zegveld	Netherlands			6 September 1994	gradient	Dutch pasture	Galmarini et al., 1997

Appendix B

Mechanistic Modeling of Ozone Dry Deposition to Leaf Cuticles

Here we derive and review the Potier et al. (2015) physically-based model for ozone dry deposition to wet leaves. We begin with the steady-state diffusion/reaction equation for aqueous ozone ($O_{3,aq}$) [mol m^{-3}]:

$$-D_{O_{3,aq}}\left(\frac{d^2 O_{3,aq}}{dz^2}\right) = L_{O_{3,aq}} \tag{B1}$$

$D_{O_{3,aq}}$ [m^2 s^{-1}] is ozone diffusivity in water; z is distance from the leaf surface ($z = 0$ at the leaf surface); $L_{O_{3,aq}}$ is the aqueous ozone chemical sink. With a first order rate constant κ^{aq} [s^{-1}] such that $L_{O_{3,aq}} = -\kappa^{aq} O_{3,aq}$, we have:

$$\frac{d^2 O_{3,aq}}{dz^2} = \left(\frac{\kappa^{aq}}{D_{O_{3,aq}}} O_{3,aq}\right) \equiv \Gamma_{aq}^2 O_{3,aq} \tag{B2}$$

We now derive the resistance for aqueous ozone uptake ($r_{cut,aq}$) [s m^{-1}] by water droplets and films on a leaf surface. The boundary condition at the upper surface of the water (i.e., the air-water interface) is $O_{3,aq}(\delta_d)$ where δ_d is the thickness of the film or droplet. The boundary condition at the lower surface of the water (i.e., the leaf-water interface) is:

$$D_{O_{3,aq}}\frac{\partial O_{3,aq}}{\partial z} = \frac{O_{3,aq}(0)}{r_{cut}} \tag{B3}$$

r_{cut} [m s^{-1}] is the resistance to aqueous ozone uptake by cuticle underneath the water. Defining $\gamma = \left(r_{cut}\Gamma_{aq}D_{O_{3,aq}}\right)^{-1}$, the solution to equation (B2) is:

$$O_{3,\,aq}(z) = O_{3,\,aq}(\delta_d)\left(\frac{\left(1-\gamma\right)e^{-\Gamma_{aq}z} + \left(1+\gamma\right)e^{\Gamma_{aq}z}}{\left(1-\gamma\right)e^{-\Gamma_{aq}\delta_d} + \left(1+\gamma\right)e^{\Gamma_{aq}\delta_d}}\right) \tag{B4}$$

$$\frac{dO_{3,\,aq}}{dz} = O_{3,\,aq}(\delta_d)\Gamma_{aq}\left(\frac{-\left(1-\gamma\right)e^{-\Gamma_{aq}z} + \left(1+\gamma\right)e^{\Gamma_{aq}z}}{\left(1-\gamma\right)e^{-\Gamma_{aq}\delta_d} + \left(1+\gamma\right)e^{\Gamma_{aq}\delta_d}}\right) \tag{B5}$$

Then, we have:

$$D_{O_{3,\,aq}}\frac{dO_{3,\,aq}}{dz}\bigg|_{z\,=\,\delta_d} = \frac{O_{3,\,aq}(\delta_d)}{r_{cut,\,aq}} \tag{B6}$$

which yields:

$$r_{cut,\,aq} = \frac{1}{\Gamma_{aq}D_{O_{3,\,aq}}}\left(\frac{\left(1-\gamma\right)e^{-\Gamma_{aq}\delta_d} + \left(1+\gamma\right)e^{\Gamma_{aq}\delta_d}}{-\left(1-\gamma\right)e^{-\Gamma_{aq}\delta_d} + \left(1+\gamma\right)e^{\Gamma_{aq}\delta_d}}\right) \tag{B7}$$

However, the definition of the resistance to ozone uptake on wet cuticles is usually defined relative to the gas phase, not the aqueous phase. We therefore replace equation (B6) with:

$$D_{O_{3,\,aq}}\frac{dO_{3,\,aq}}{dz}\bigg|_{z\,=\,\delta_d} = \frac{O_3(\delta_d)}{r_{cut,\,wet}} \tag{B8}$$

$O_3(\delta_d)$ [mol m^{-3}] is gaseous ozone concentration at the surface of the water; $r_{cut,wet}$ [s m^{-1}] is the resistance to gaseous ozone uptake by wet cuticles. Fully specifying $r_{cut,wet}$ requires a relationship between O_3 and $O_{3,aq}$, and the simplest approach is assuming O_3 and $O_{3,aq}$ are in equilibrium with Henry's law:

$$O_3\left(\delta_d\right) = \frac{O_{3,\,aq}\left(\delta_d\right)}{k_H^{cc}} \tag{B9}$$

k_H^{cc} is the dimensionless Henry's law constant (e.g., Sander, 1999, 2015). Then, we have:

$$r_{cut,\,wet} = \frac{r_{aq}}{k_H^{cc}} = \frac{1}{k_H^{cc}\Gamma_{aq}D_{O_{3,\,aq}}}\left(\frac{\left(1-\gamma\right)e^{-\Gamma_{aq}\delta_d} + \left(1+\gamma\right)e^{\Gamma_{aq}\delta_d}}{-\left(1-\gamma\right)e^{-\Gamma_{aq}\delta_d} + \left(1+\gamma\right)e^{\Gamma_{aq}\delta_d}}\right) \tag{B10a}$$

This $r_{cut,wet}$ expression is the same as Potier et al. (2015) equation (A5) except for our using the dimensionless form of Henry's law constant.

Given that ozone diffusion through water is slow and the underlying cuticle may not be very reactive with ozone, we may be able to assume the lower boundary condition is zero. This gives us a simpler expression for $r_{cut,wet}$:

$$r_{cut, wet} = \frac{1}{k_H^{CC}\Gamma_{aq}D_{O_3, aq}\tanh\left(\Gamma_{aq}\delta_d\right)} \tag{B10b}$$

Mechanistic Modeling of Ozone Dry Deposition to Soil

Here we derive a mechanistic model for the resistance to ozone uptake by soil (r_{soil}), generalizing the approach of Tuzet et al. (2011) who analytically solve the steady-state equation of mass conservation for ozone within soil pore spaces ($O_{3,soil}$) to obtain r_{soil}. We begin with the steady-state diffusion-only mass conservation equation for $O_{3,soil}$:

$$\frac{d}{dz}(F_{O_3, soil}) = Dep_{O_3, soil} + L_{O_3, soil} \tag{B11}$$

z refers to depth below the soil surface; $Dep_{O_3, soil}$ [ppbv s^{-1}] is the soil ozone depositional sink; $L_{O_3, soil}$ [ppbv s^{-1}] is the chemical sink within soil pore space. $F_{O_3, soil}$ [ppbv m s^{-1}] is the ozone vertical diffusive flux within soil (e.g., Hillel, 1980) and follows:

$$F_{O_3, soil} = -(\eta - \theta)\tau D_{O_3}\frac{dO_{3, soil}}{dz} \tag{B12}$$

η is volumetric air-filled soil pore space when completely dry [m^3 m^{-3}]; θ is volumetric soil moisture [m^3 m^{-3}]; τ is the soil tortuosity factor [$0 < \tau < 1$; unitless] (a measure of the how many paths ozone can take in soil); D_{O_3} is ozone diffusivity in air [m^2 s^{-1}].

To insure equation (B11) is amenable to analytical solution, we approximate:

$$\frac{d}{dz}(F_{O_3, soil}) = -(\eta - \theta)\tau D_{O_3}\frac{d^2 O_{3, soil}}{dz^2} \tag{B13}$$

However, soils vary vertically in terms of η, τ, θ, and temperature (T_{soil}), which may influence variables such as D_{O_3}.

The next steps are to construct $L_{O_3, soil}$ and $Dep_{O_3, soil}$. We parameterize $L_{O_3, soil}$ as $-\sum_i K_{X_i, O_3}O_{3, soil}X_{i, soil}$ where K_{X, O_3} [ppmv s^{-1}] is the rate coefficient for ozone chemical destruction in soil pore spaces by some gas species X_{soil}.

For porous media, the basic approach for a sink term (S^*) associated with dry deposition is to assume $S^* = AF^*$ where A [m^2 m^{-3}] is the surface area on which dry deposition occurs per unit volume of the porous media and F^* [ppmv m s^{-1}] is the net flux to that surface. Following this approach and Morrison and Nazaroff (2002) for ozone dry deposition to carpet, we parameterize F* analogously to heterogeneous chemistry in the atmosphere (e.g., Jacob, 2000):

$$\text{F*} = \frac{1}{4}K_d \upsilon O_{3,\,soil} \tag{B14}$$

K_d is the surface deposition coefficient [unitless], which provides a measure of the probability that an ozone molecule reacts once it comes into contact with the surface; $\upsilon = \sqrt{\frac{8RT_{soil}}{\pi M_{O_3}}}$; R is the universal gas constant [8.314 J mol^{-1} K^{-1}]; M_{O_3} is ozone molecular mass [0.048 kg mol^{-1}].

We now have:

$$(\eta - \theta)\tau D_{O_3}\frac{d^2 O_{3,\,soil}}{dz^2} = AK_d\frac{1}{4}\sqrt{\frac{8RT_{soil}}{\pi M_{O_3}}}O_{3,\,soil} + \sum_i K_{X_i,\,O_3}O_{3,\,soil}X_{i,\,soil} \tag{B15}$$

The solution to equation (B15) is:

$$O_{3,\,soil}(z) = ae^{-\sqrt{\Gamma}z} + be^{\sqrt{\Gamma}z} \tag{B16}$$

$$F_{O_3,\,soil}(z) = -(\eta - \theta)\tau D_{O_3}\sqrt{\Gamma}(-ae^{-\sqrt{\Gamma}z} + be^{\sqrt{\Gamma}z}) \tag{B17}$$

where

$$\Gamma = \frac{\left(AK_d\frac{1}{4}\sqrt{\frac{8RT_{soil}}{\pi M_{O_3}}} + \sum_i K_{X_i,\,O_3}X_{i,\,soil}\right)}{(\eta - \theta)\tau D_{O_3}} \tag{B18}$$

a and b are constants determined by the boundary conditions. The upper boundary condition (at $z = 0$) is $F_{O_3,\,soil}(0) = \frac{O_{3,\,soil}(0)}{r_{soil}}$, assuming ozone flux is continuous across the soil surface (this assumption is not valid when diffusion into soil is blocked).

A general lower boundary condition follows from noting $O_{3,soil}(z)$ should remain bounded for all soil depths (i.e., $\lim_{z \to -\infty} O_{3,\,soil}(z) = 0$). Because $z \leq 0$, a bounded lower boundary condition can be assured unconditionally by requiring $a \equiv 0$.

Combining $a \equiv 0$ with $O_{3,soil}(0)$ and $F_{O_3,\,soil}(0)$ yields the following expression for r_{soil}:

$$\begin{aligned} r_{soil} &= \frac{1}{(\eta - \theta)\tau D_{O_3}\sqrt{\Gamma}} \\ &\equiv \left[\left(AK_d\frac{1}{4}\sqrt{\frac{8RT_{soil}}{\pi M_{O_3}}} + \sum_i K_{X_i,\,O_3}X_{i,\,soil}\right)((\eta - \theta)\tau D_{O_3})\right]^{-1/2} \end{aligned} \tag{B19}$$

Incorporating Thermal Decomposition into Mechanistic Modeling of Ozone Dry Deposition to Soil

We construct a similar mechanistic model for ozone dry deposition to soil as above, but one that includes thermal decomposition of ozone on soil surfaces in order to explore the role of this process. We generalize the approach outlined by Seinfeld and Pandis (2006) for thermal decomposition, assuming as they do that thermal decomposition follows first-order chemical kinetics:

$$Dep_{O_3, soil}^{therm} = \frac{A}{4}\left(K_0^{therm} e^{-\frac{E_a^{therm}}{RT_{soil}}}\right)\sqrt{\frac{8RT_{soil}}{\pi M_{O_3}}} \tag{B20}$$

K_0^{therm} is a proportionality parameter related to the probability of ozone colliding with a molecule on the soil surface [unitless]; E_a^{therm} [J mol^{-1}] is the activation energy required for thermal decomposition to occur as a result of collision.

Following the same steps as before, the basic model for the ozone concentration profile within soil is:

$$(\eta - \theta)\tau D_{O_3}\frac{d^2 O_{3, soil}}{dz^2} = AK_* \frac{1}{4}\sqrt{\frac{8RT_{soil}}{\pi M_{O_3}}}O_{3, soil} + \sum_i K_{X_i, O_3}O_{3, soil}X_{i, soil} \tag{B21}$$

where $K_* = K_d + K_0^{therm} e^{-\frac{E_a^{therm}}{RT_{soil}}}$.

Equation (B21) yields the following:

$$r_{soil} \equiv \left(\left[\frac{A}{4}K_*\sqrt{\frac{8RT_{soil}}{\pi M_{O_3}}} + \sum_i K_{X_i, O_3}X_{i, soil}\right](\eta - \theta)\tau D_{O_3}\right)^{-1/2} \tag{B22}$$

To estimate whether ozone dry deposition via thermal decomposition on soil surfaces may be important, we present r_{soil} assuming soil dry deposition only occurs through thermal decomposition:

$$r_{soil} = \left(\left[\frac{A}{4}K_0^{therm} e^{-\frac{E_a^{therm}}{RT_{soil}}}\sqrt{\frac{8RT_{soil}}{\pi M_{O_3}}}\right](\eta - \theta)\tau D_{O_3}\right)^{-1/2} \tag{B23}$$

Previous studies infer E_a^{therm} using regression analyses, assuming the resistance to uptake (r_i) is $r_i = ae^{\frac{b}{RT}}$ where a and b are empirical coefficients. For sandy-loam soil at Ispra forest in Italy, b is 40,000 J mol^{-1} (Fumagalli et al., 2016). For aluminum, stainless steel, beeswax and paraffin wax (Cape et al., 2009), b is 16,000 to 30,000 J mol^{-1}. To estimate r_{soil} from equation (B23), we use b = 25,000 J mol^{-1} which corresponds to E_a^{therm} = 50,000 J mol^{-1}

because equation (B23) is analogous to $r_i = ae^{\frac{b}{2RT}}$. If $E_a^{therm} = 50,000$ J mol^{-1} and T_{soil}

$=15°$C, then $r_{soil} = \dfrac{9.5x10^5}{\sqrt{AK_0^{therm}(\eta - \theta)\tau}}$.

Depending on the magnitude of A, K_0^{therm}, and $(\eta - \theta)\tau$, thermal decomposition of ozone on surfaces could be an important contribution to ozone dry deposition. For example, A ranges from 3×10^7 to 1×10^9 m^2 m^{-3} for various clay minerals (Kabata-Pendias, 2004), assuming a bulk density of 1.3 g cm^{-3} (Warrick & Nielsen, 1980). If we assume the unity upper bounds of K_0^{therm} and $(\eta - \theta)\tau$, then this range in A leads an upper bound of r_{soil} from thermal decomposition as 30 to 170 s m^{-1}, connoting efficient ozone removal.

Appendix C

Table C1

Participants at a Workshop on Ozone Dry Deposition at Lamont Doherty Earth Observatory of Columbia University in October 2017.

In-person participants	Affiliation
Alex Guenther	University of California Irvine
Allison Steiner	University of Michigan
Anthony Y. H. Wong	Boston University
Arlene Fiore	Lamont Doherty Earth Observatory/Columbia University
Ashok Luhar	Commonwealth Scientific and Industrial Research Organisation (CSIRO) Climate Science Centre, Australia
Barry Lefer	NASA
W. J. Massman	United States Forest Service
J. W. Munger	Harvard University
Catherine Hardacre	UK Met Office
Christopher Holmes	Florida State University
Colette Heald	Massachusetts Institute of Technology
Colleen Baublitz	Lamont Doherty Earth Observatory/Columbia University
Delphine Farmer	Colorado State University
Dennis Baldocchi	University of California Berkeley
Detlev Helmig	INSTAAR - University of Colorado
Donna Schwede	United States Environmental Protection Agency (EPA)
Dylan Jones	University of Toronto
Dylan Millet	University of Minnesota
Elena McDonald-Buller	University of Texas at Austin
Erin Delaria	University of California Berkeley
Garry Hayman	Centre for Ecology & Hydrology, Wallingford, UK
Giacomo Gerosa	Università Cattolica del Sacro Cuore, Brescia, Italy
Glenn Wolfe	NASA GSFC and UMBC

Jason Ducker	Florida State University
Jennifer Murphy	University of Toronto
Jingqiu Mao	University of Alaska Fairbanks
Joanna Joiner	NASA GSFC
Katie Travis	Massachusetts Institute of Technology
Kenneth Mooney	NOAA Climate Program Office
Kevin Griffin	Columbia University
Larry Horowitz	GFDL/NOAA
Leiming Zhang	Environment and Climate Change Canada
Lisa Emberson	Stockholm Environment Institute, University of York
Maria Val Martin	University of Sheffield
Matthias Sörgel	Max Planck Institute for Chemistry
Meiyun Lin	Princeton University & NOAA GFDL
Mhairi Coyle	NERC Centre for Ecology and Hydrology (CEH) Edinburgh
Monika Kopacz	NOAA/UCAR
Olivia Clifton	Lamont Doherty Earth Observatory/Columbia University
Peter Zoogman	Minerva Schools at KGI
Phil Stevens	Indiana University
Sally Pusede	University of Virginia
Sam Silva	Massachusetts Institute of Technology
Sarah Kavassalis	University of Toronto
Stefano Galmarini	European Commission/JRC
Xiaomeng Jin	Lamont Doherty Earth Observatory/Columbia University
Zhiyong Wu	United States Environmental Protection Agency (EPA)
Remote participants	**Affiliation**
Amos Tai	Chinese University of Hong Kong
Amanda Cole	Environment and Climate Change Canada
Andrew Langford	NOAA ESRL Chemical Sciences Division
Christian Hogrefe	United States Environmental Protection Agency (EPA)
Eiko Nemitz	Centre for Ecology and Hydrology (CEH) Edinburgh
Frank Dentener	European Commission
Jeff Geddes	Boston University
Gabriele Pfister	National Center for Atmospheric Research (NCAR)
Jonathan Pleim	United States EPA
Kenneth Mooney	NOAA Climate Program Office
Liji David	Departments of Chemistry and Atmospheric Science, Colorado State University
Louisa Emmons	National Center for Atmospheric Research (NCAR)
Nadine Unger	University of Exeter
William Porter	University of California Riverside

References

Ainsworth EA (2017). Understanding and improving global crop response to ozone pollution. The Plant Journal, 90, 886–897. [PubMed: 27739639]

Ainsworth EA, Yendrek CR, Sitch S, Collins WJ, & Emberson LD (2012). The effects of tropospheric ozone on net primary productivity and implications for climate change. Annual Reviews of Plant Biology, 63, 637–661. 10.1146/Annurev-Arplant-042110-103829

Albert MR, Grannas AM, Bottenheim J, Shepson PB, & Perron FE (2002). Processes and properties of snow-air transfer in the high Arctic with application to interstitial ozone at Alert, Canada. Atmospheric Environment, 36, 2779–2787. 10.1016/s1352-2310(02)00118-8

Aldaz L (1969). Flux Measurements of Atmospheric Ozone over Land Water. Journal of Geophysical Research, 74. 10.1029/JC074i028p06943

Almand-Hunter BB, Walker JT, Masson NP, Hafford L, & Hannigan MP (2015). Development and validation of inexpensive, automated, dynamic flux chambers. Atmospheric Measurement Techniques, 8, 267–280. 10.5194/amt-8-267-2015

Altimir N, Kolari P, Tuovinen J-P, Vesala T, Bäck J, Suni T, Kulmala M, & Hari P (2006). Foliage surface ozone deposition: a role for surface moisture? Biogeosciences, 3, 209–228. 10.5194/bgd-2-1739-2005

Altimir N, Tuovinen J-P, Vesala T, Kulmala M, & Hari P (2004). Measurements of ozone removal by Scots pine shoots: calibration of a stomatal uptake model including the non-stomatal component. Atmospheric Environment, 38(15), 2387–2398.

Altimir N, Vesala T, Aalto T, Bäck J and Hari P (2008). Stomatal-scale modelling of the competition between ozone sinks at the air-leaf interface. Tellus Series B: Chemical and Physical Meteorology. 10.1111/j.1600-0889.2008.00344.x

Altimir N, Vesala T, Keronen P, Kulmala M, & Hari P (2002). Methodology for direct field measurements of ozone flux to foliage with shoot chambers. Atmospheric Environment, 36(1), 19–29.

Alwe HD, Millet DB, Chen X, Raff JD, Payne ZC, & Fledderman K (2019). Oxidation of Volatile Organic Compounds as the Major Source of Formic Acid in a Mixed Forest Canopy. Geophysical Research Letters, 46(5), 2940–2948. 10.1029/2018GL081526 [PubMed: 31068737]

Anav A, Proietti C, Menut L, Carnicelli S, De Marco A, & Paoletti E (2018). Sensitivity of stomatal conductance to soil moisture: implications for tropospheric ozone. Atmospheric Chemistry and Physics, 18, 5747–5763. 10.5194/acp-18-5747-2018

Anderegg WRL, Wolf A, Arango-Velez A, Choat B, Chmura DJ, Jansen S et al. (2017). Plant water potential improves prediction of empirical stomatal models. PLoS ONE, 12, e0185481. 10.1371/journal.pone.0185481 [PubMed: 29023453]

Arnold SR, Lombardozzi D, Lamarque J-F, Richardson T, Emmons LK, Tilmes S, et al. (2018). Simulated global climate response to tropospheric ozone-induced changes in plant transpiration. Geophysical Research Letters, 45, 13070–13079. 10.1029/2018GL079938

Arya SP (2001). Introduction to Micrometeorology, Second Edition. San Diego, CA: Academic Press.

Ashworth K, Chung SH, Griffin RJ, Chen J, Forkel R, Bryan AM, & Steiner AL (2015). FORest Canopy Atmosphere Transfer (FORCAsT) 1.0: a 1-D model of biosphere-atmosphere chemical exchange. Geoscientific Model Development, 8, 3765–3784. 10.5194/gmd-8-3765-2015

Aubinet M, Vesala T, & Papale D (Eds.). (2012). Eddy covariance: a practical guide to measurement and data analysis. Springer Science & Business Media

Bakwin PS, Wofsy SC, Fan SM, Keller M, Trumbore SE, & Costa JMD (1990). Emission of nitric oxide (NO) from tropical forest soils and exchange of NO between the forest canopy and atmospheric boundary layers. Journal of Geophysical Research: Atmospheres, 95(D10), 16755–16764. 10.1029/JD095iD10p16755

Baldocchi DD, Hicks BB, & Camara P (1987). A canopy stomatal resistance model for gaseous deposition to vegetated surfaces. Atmospheric Environment, 2(1), 91–101.

Baldocchi DD, Luxmoore RJ, & Hatfield JL (1991). Discerning the forest from the trees: an essay on scaling canopy stomatal conductance. Agricultural and Forest Meteorology, 54, 197–226.

Baldocchi D, & Meyers T (1998). On using eco-physiological, micrometeorological and biogeochemical theory to evaluate carbon dioxide, water vapor and trace gas fluxes over vegetation: a perspective. Agricultural and Forest Meteorology, 90, 1–25.

Ball JT, Woodrow IE, & Berry JA (1987). A model predicting stomatal conductance and its contribution to the control of photosynthesis under different environmental conditions. In: Biggens J (Ed.), Progress in Photosynthesis Research (pp. 221–224). The Hague: Martinus Nijhoff

Bariteau L, Helmig D, Fairall CW, Hare JE, Hueber J, & Lang EK (2010). Determination of oceanic ozone deposition by ship-borne eddy covariance flux measurements. Atmospheric Measurement Techniques, 3(2), 441–455.

Bassin S, Calanca P, Weidinger T, Gerosa G, & Fuhrer J (2004). Modeling seasonal ozone fluxes to grassland and wheat: model improvement, testing, and application. Atmospheric Environment, 38, 2349–2359. 10.1016/j.atmosenv.2003.11.004

Bauer MR, Hultman NE, Panek JA, & Goldstein AH (2000). Ozone deposition to a ponderosa pine plantation in the Sierra Nevada Mountains (CA): a comparison of two different climatic years. Journal of Geophysical Research: Atmospheres, 105(D17), 22123–22136. 10.1029/2000JD900168

Beddows AV, Kitwiroon N, Williams ML, & Beevers SD (2017). Emulation and sensitivity analysis of the community multiscale air quality model for a UK Ozone pollution episode. Environmental Science & Technology, 51(11), 6229–6236. [PubMed: 28443333]

Bela MM, Longo KM, Freitas SR, Moreira DS, Beck V, Wofsy SC, et al. (2015). Ozone production and transport over the Amazon Basin during the dry-to-wet and wet-to-dry transition seasons. Atmospheric Chemistry and Physics, 15, 757–782. 10.5194/acp-15-757-2015

Bocquet F, Helmig D, & Oltmans SJ (2007). Ozone in interstitial air of the mid-latitude, seasonal snowpack at Niwot Ridge, Colorado. Arctic Antarctic and Alpine Research, 39, 375–387

Bocquet F, Helmig D, Van Dam BA, & Fairall CW (2011). Evaluation of the flux gradient technique for measurement of ozone surface fluxes over snowpack at Summit, Greenland. Atmospheric Measurement Techniques, 4, 2305–2321. 10.5194/amt-4-2305-2011

Bonan GB, Patton EG, Harman IN, Oleson KW, Finnigan JJ, Lu YQ, & Burakowski EA (2018). Modeling canopy-induced turbulence in the Earth system: a unified parameterization of turbulent exchange within plant canopies and the roughness sublayer (CLM-ml v0). Geoscientific Model Development, 11, 1467–1496. 10.5194/gmd-11-1467-2018

Bonan GB, Williams M, Fisher RA, & Oleson KW (2014). Modeling stomatal conductance in the earth system: linking leaf water-use efficiency and water transport along the soil–plant–atmosphere continuum. Geoscientific Model Development, 7(5), 2193–2222.

Bottenheim JW, Fuentes JD, Tarasick DW, & Anlauf KG (2002). Ozone in the Arctic lower troposphere during winter and spring 2000 (ALERT2000). Atmospheric Environment, 36, 2535–2544. 10.1016/s1352-2310(02)00121-8

Bourtsoukidis E, Behrendt T, Yañez-Serrano AM, Hellén H, Diamantopoulos E, Catão E, et al. (2018). Strong sesquiterpene emissions from Amazonian soils. Nature Communications, 9(1).

Bouvier-Brown NC, Goldstein AH, Gilman JB, Kuster WC, & de Gouw JA (2009). In-situ ambient quantification of monoterpenes, sesquiterpenes, and related oxygenated compounds during BEARPEX: implications for gas- and particle-phase chemistry. Atmospheric Chemistry and Physics, 9, 5505–5518.

Breuninger C, Oswald R, Kesselmeier J, & Meixner FX (2012). The dynamic chamber method: trace gas exchange fluxes (NO, NO2, O3) between plants and the atmosphere in the laboratory and in the field. Atmospheric Measurement Techniques, 5(5), 955–989.

Bryan AM, Bertman SB, Carroll MA, Dusanter S, Edwards GD, Forkel R, et al. (2012). In-canopy gas-phase chemistry during CABINEX 2009: sensitivity of a 1-D canopy model to vertical mixing and isoprene chemistry. Atmospheric Chemistry and Physics, 12, 8829–8849.

Brutsaert W (1979). Heat and Mass Transfer to and from Surfaces with Dense Vegetation or Similar Permeable Roughness. Boundary-Layer Meteorology, 16, 365–388.

Buckley TN, & Mott KA (2013). Modelling stomatal conductance in response to environmental factors. Plant, Cell & Environment, 36(9), 1691–1699.

Burkhardt J (2010). Hygroscopic particles on leaves: Nutrients or desiccants? Ecological Monographs, 80(3), 369–399. 10.1890/09-1988.1

Burkhardt J, & Eiden R (1994). Thin water films on coniferous needles. Atmospheric Environment. 10.1016/1352-2310(94)90469-3

Burkhardt J, & Hunsche M (2013). "Breath figures" on leaf surfaces — formation and effects of microscopic leaf wetness. Frontiers in Plant Science, 4(422). 10.3389/fpls.2013.00422

Buschhaus C, & Jetter R (2012). Composition and Physiological Function of the Wax Layers Coating Arabidopsis Leaves: β-Amyrin Negatively Affects the Intracuticular Water Barrier. Plant Physiology, 160(2), 1120–1129. 10.1104/pp.112.198473 [PubMed: 22885935]

Businger JA (1986). EVALUATION OF THE ACCURACY WITH WHICH DRY DEPOSITION CAN BE MEASURED WITH CURRENT MICROMETEOROLOGICAL TECHNIQUES. Journal of Climate and Applied Meteorology, 25(8), 1100–1124.

Businger JA, Wyngaard JC, Izumi Y, & Bradley EF (1971). Flux-profile relationships in the atmospheric surface layer. Journal of the Atmospheric Sciences, 28(2), 181–189.

Buzorius G, Rannik Ü, Makela JM, Vesala T, & Kulmala M (1998). Vertical aerosol particle fluxes measured by eddy covariance technique using condensational particle counter. Journal of Aerosol Science, 29(1–2), 157–171.

Büker P, Emberson LD, Ashmore MR, Cambridge. HM, Jacobs CMJ, Massman WJ, et al. (2007). Comparison of different stomatal conductance algorithms for ozone flux modelling. Environmental Pollution, 146, 736–735. 10.1016/j.envpol.2006.04.007 [PubMed: 16781803]

Büker P, Morrissey T, Briolat A, Falk R, Simpson D, Tuovinen J-P, et al. (2012). DO3SE modelling of soil moisture to determine ozone flux to forest trees. Atmospheric Chemistry and Physics, 12(12), 5537–5562. 10.5194/acp-12-5537-2012

Calatayud V, Cerveró J, & Sanz MJ (2007). Foliar, physiological and growth responses of four maple species exposed to ozone. Water, Air, and Soil Pollution, 185, 239–254.

Calogirou A, Larsen BR, & Kotzias D (1999). Gas-phase terpene oxidation products: a review. Atmospheric Environment, 33, 1423–1439.

Campbell PC, Bash JO, & Spero TL (2019). Updates to the Noah Land Surface Model in WRF-CMAQ to improve simulated meteorology, air quality, and deposition. Journal of Advances in Modeling Earth Systems, 11, 231–256. 10.1029/2018MS001422 [PubMed: 31007838]

Cape JN, Hamilton R & Heal MR (2009). Reactive uptake of ozone at simulated leaf surfaces: Implications for "non-stomatal" ozone flux. Atmospheric Environment. 10.1016/j.atmosenv.2008.11.007

Cavicchioli C, Manzi G, Catenacci G, Brusasca, & Borgarello M (1997). Dry Deposition Inferential Meaesurement in a Rural Region of Northern Italy. In Slanina S (Ed.), Transport and Chemical Transformation of Pollutants in the Troposphere: Experimental and Theoretical Studies of Biogenic Emissions and of Pollutant Deposition (pp. 457–466). Berlin: Springer.

Cellier P, & Brunet Y (1992). Flux-gradient relationships above tall plant canopies. Agricultural and Forest Meteorology, 58, 93–117.

Centoni F (2017). Global scale modelling of ozone deposition processes and interactions between surface ozone and climate change (Doctoral dissertation). Edinburgh, United Kingdom: The University of Edinburgh.

Cernusak LA, Ubierna N, Jenkins MW, Garrity SR, Rahn T, Powers HH, et al. (2018). Unsaturation of vapour pressure inside leaves of two conifer species. Scientific Reports. 10.1038/s41598-018-25838-2

Chang K-Y, Paw U KT, & Chen S-H (2018). Canopy profile sensitivity on surface layer simulations evaluated by a multiple canopy layer higher order closure land surface model. Agricultural and Forest Meteorology, 252, 192–207. 10.1016/j.agrformet.2018.01.027

Chapleski RC, Zhang Y, Troya D, & Morris JR (2016). Heterogeneous chemistry and reaction dynamics of the atmospheric oxidants, O3, NO3, and OH, on organic surfaces. Chemical Society Reviews. 10.1039/c5cs00375j

Charusombat U, Niyogi D, Kumar A, & Wang X (2010). Evaluating a new deposition velocity module in the Noah land-surface model. Boundary-Layer Meteorology, 137, 271–290. 10.1007/s10546-010-9531-y

Choi W, Faloona IC, Bouvier-Brown NC, McKay M, Goldstein AH, Mao J, et al. (2010). Observations of elevated formaldehyde over a forest canopy suggest missing sources from rapid oxidation of boreal hydrocarbons. Atmospheric Chemistry and Physics, 10(18), 8761–8781.

Choudhury BJ, & Monteith JL (1988). A four-layer model for the heat budget of homogeneous land surfaces. Quarterly Journal of the Royal Meteorological Society, 114(480), 373–398.

Chu H, Baldocchi DD, John R, Wolf S, & Reichstein M (2017). Fluxes all of the time? A primer on the temporal representativeness of FLUXNET. Journal of Geophysical Research: Biogeosciences, 122(2), 289–307. 10.1002/2016JG003576

Cieslik SA (2004). Ozone uptake by various surface types: a comparison between dose and exposure. Atmospheric Environment, 38(15), 2409–2420.

Cieslik S (2009). Ozone fluxes over various plant ecosystems in Italy: A review, Environmental Pollution, 157, 1487–1496. 10.1016/j.envpol.2008.09.050 [PubMed: 19027210]

Cieslik S, & Labatut A (1997). Ozone and heat fluxes over a Mediterranean pseudosteppe. Atmospheric Environment, 31, 177–184.

Clark DB, Mercado LM, Sitch S, Jones CD, Gedney N, Best MJ, et al. (2011). The Joint UK Land Environment Simulator (JULES), model description–Part 2: carbon fluxes and vegetation dynamics. Geoscientific Model Development, 4(3), 701–722.

Clifton OE (2018). Constraints on ozone removal by land and implications for 21st Century ozone pollution (Doctoral dissertation). New York, New York: Columbia University in the City of New York. 10.7916/D8709J8T

Clifton OE, Fiore AM, Munger JW, Malyshev S, Horowitz LW, Shevliakova E, et al. (2017). Interannual variability in ozone removal by a temperate deciduous forest. Geophysical Research Letters, 44(1), 542–552. 10.1002/2016GL070923

Clifton OE, Fiore AM, Munger JW, & Wehr R (2019). Spatiotemporal controls on observed daytime ozone deposition velocity over Northeastern U.S. forests during summer. Journal of Geophysical Research: Atmospheres. 10.1029/2018JD029073

Coe H, Gallagher MW, Choularton TW, & Dore C (1995). Canopy scale measurements of stomatal and cuticular O3 uptake by Sitka spruce. Atmospheric Environment, 29(12), 1413–1423.

Colbeck I, & Harrison RM (1985). DRY DEPOSITION OF OZONE - SOME MEASUREMENTS OF DEPOSITION VELOCITY AND OF VERTICAL PROFILES TO 100-METRES. Atmospheric Environment, 19, 1807–1818. 10.1016/0004-6981(85)90007-1

Commane R, Meredith LK, Baker IT, Berry JA, Munger JW, Montzka SA, et al. (2015). Seasonal fluxes of carbonyl sulfide in a midlatitude forest. Proceedings of the National Academy of Sciences, 112(46), 14162–14167.

Cook GD, & Viskanta R (1968). Mutual Diffusional Interference Between Adjacent Stomata of a Leaf. Plant Physiology, 43, 1017–1022. [PubMed: 16656876]

Cooter EJ, & Schwede DB (2000). Sensitivity of the National Oceanic and Atmospheric Administration multilayer model to instrument error and parameterization uncertainty. Journal of Geophysical Research, 105(D5), 6695–6707. 10.1029/1999JD901080

Cowan IR, & Farquhar GD (1977). Stomatal function in relation to leaf metabolism and environment. In Jennings DH (Ed.), Integration of Activity in the Higher Plant (pp. 471–505). Cambridge, United Kingdom: Cambridge University Press.

Coyle M (2005). The gaseous exchange of ozone at terrestrial surfaces: nonstomatal deposition to grassland (Doctoral dissertation). Edinburgh, United Kingdom: The University of Edinburgh.

Coyle M, Nemitz E, Storeton-West R, Fowler D and Cape JN (2009). Measurements of ozone deposition to a potato canopy. Agricultural and Forest Meteorology, 149, 655–666. 10.1016/j.agrformet.2008.10.020

Crawford JH, Davis DD, Chen G, Buhr M, Oltmans S, Weller R, et al. (2001). Evidence for photochemical production of ozone at the South Pole surface. Geophysical Research Letters, 28, 3641–3644. 10.1029/2001gl013055

Cristofanelli P, Putero D, Bonasoni P, Busetto M, Calzolari F, Camporeale G, et al. (2018). Analysis of multi-year near-surface ozone observations at the WMO/GAW "Concordia" station (75°06'S, 123°20'E, 3280 m a.s.l. - Antarctica). Atmospheric Environment, 177, 54–63. 10.1016/j.atmosenv.2018.01.007

Cros B, Delon C, Affre C, Marion T, Druilhet A, Perros PE, & Lopez A (2000). Sources and sinks of ozone in savanna and forest areas during EXPRESSO: Airborne turbulent flux measurements. Journal of Geophysical Research: Atmospheres, 105(D24), 29347–29358. 10.1029/2000JD900451

Damköhler G (1940). Der einfluss der turbulenz auf die flammengeschwindigkeit in gasgemischen. Zeitschrift für Elektrochemie und angewandte physikalische Chemie, 46(11), 601–626.

Daudet FA, Le Roux X, Sinoquet H, & Adam B (1999). Wind speed and leaf boundary layer conductance variation within tree crown Consequences on leaf-to-atmosphere coupling and tree functions. Agricultural and Forest Meteorology, 97, 171–185.

D'Anna B, Jammoul A, George C, Stemmler K, Fahrni S, Ammann M, & Wisthaler A (2009). Light-induced ozone depletion by humic acid films and submicron aerosol particles. Journal of Geophysical Research: Atmospheres. 10.1029/2008JD011237

Deckmyn G, De Beeck MO, Löw M, Then C, Verbeeck H, Wipfler P, & Ceulemans R (2007). Modelling ozone effects on adult beech trees through simulation of defence, damage, and repair costs: implementation of the CASIROZ ozone model in the ANAFORE forest model. Plant Biology, 9(02), 320–330. [PubMed: 17357024]

Delaria ER, Vieira M, Cremieux J, & Cohen RC (2018). Measurements of NO and NO2 exchange between the atmosphere and *Quercus agrifolia*. Atmospheric Chemistry and Physics, 18(19), 14161–14173.

De Miguel A, & Bilbao J (1999). Ozone dry deposition and resistances onto green grassland in summer in central Spain. Journal of Atmospheric Chemistry, 34(3), 321–338.

Desjardins RL, MacPherson JI, Neumann H, den Hartog G, & Schuepp PH (1995). Flux Estimates of Latent and Sensible Heat, Carbon Dioxide, and Ozone using an Aircraft-Tower Combination. Atmospheric Environment, 29(21), 3147–3158.

Dias-Júnior CQ, Luís Dias N, Santos RMN, Sörgel M, Araújo S, Tsokankunku A, et al. (2019). Is there a classical inertial sublayer over the Amazon forest? Geophysical Research Letters, 46, 5614–5622. 10.1029/2019GL083237

Disselkamp RS, Carpenter MA, Cowin JP, Berkowitz CM, Chapman EG, Zaveri RA, & Laulainen NS (2000). Ozone loss in soot aerosols. Journal of Geophysical Research: Atmospheres, 105(D8), 9767–9771. 10.1029/1999JD901189

Dorsey JR, Duyzer JH, Gallagher MW, Coe H, Pilegaard K, Westrate JH, Jensen NO, & Walton S (2004). Oxidized nitrogen and ozone interaction with forests. I: Experimental observations and analysis of exchange with Douglas fir. Quarterly Journal of the Royal Meteorological Society, 130, 1941–1955. 10.1256/qj.03.124

Droppo JG (1985). Concurrent measurements of ozone dry deposition using eddy correlation and profile flux methods. Journal of Geophysical Research: Atmospheres, 90(D1), 2111–2118. 10.1029/JD090iD01p02111

Drummond JW, Topham LA, Mackay GI, & Schiff HI (1991). Use of chemiluminescence techniques in portable, lightweight, highly sensitive instruments for measuring NO2, NOx, and O3. In Measurement of Atmospheric Gases (Vol. 1433, pp. 224–232). International Society for Optics and Photonics.

Ducker JA, Holmes CD, Keenan TF, Fares S, Goldstein AH, Mammarella I, Munger JW, & Schnell J (2018) Synthetic ozone deposition and stomatal uptake at flux tower sites. Biogeosciences, 15, 5395–5413. 10.5194/bg-15-5395-2018

Dupont S, & Patton EG (2012). Momentum and scalar transport within a vegetation canopy following atmospheric stability and seasonal canopy changes: the CHATS experiment. Atmospheric Chemistry and Physics, 12, 5913–5935.

Duyzer J, Deinum G, & Baak J (1995). The interpretation of measurements of surface exchange of nitrogen oxides: correction for chemical reactions. Philosophical Transactions of the Royal Society of London A, 351, 231–248.

Duyzer JH, Dorsey JR, Gallagher MW, Pilegaard K, & Walton S (2004). Oxidized nitrogen and ozone interaction with forests. II: Multi-layer process-oriented modelling results and a sensitivity study for Douglas fir. Quarterly Journal of the Royal Meteorological Society, 130, 1957–1971. 10.1256/qj.03.125

Duyzer JH, Meyer GM, & van Aalst RM (1983). Measurement of dry deposition velocities of NO, NO2, and O3 and the influence of chemical reactions. Atmospheric Environment, 17(10), 2117–2120.

Duyzer J, & Westrate H (1995). The use of the gradient method to monitor trace gas fluxes over forest: Flux-profile functions for ozone and heat. In Heij GJ & Erisman JW (Eds.), Acid Rain Research: Do we have enough answers? (pp. 21–30). Elsevier Science BV.

Eastman JA, & Stedman DH (1977). A fast response sensor for ozone eddy-correlation flux measurements. Atmospheric Environment, 11(12), 1209–1211.

Eiden R, Burkhardt J, & Burkhardt O (1994). Atmospheric aerosol particles and their role in the formation of dew on the surface of plant leaves. Journal of Aerosol Science, 25(2), 367–376. 10.1016/0021-8502(94)90087-6

Eller AS, & Sparks JP (2006). Predicting leaf-level fluxes of O3 and NO2: the relative roles of diffusion and biochemical processes. Plant, Cell & Environment, 29(9), 1742–1750.

El-Madany T, Niklasch K, & Klemm O (2017). Stomatal and non-stomatal turbulent deposition flux of ozone to a managed peatland. Atmosphere, 8(9), 175.

Emberson LD, Nitwiroon N, Beevers S, Büker P, & Cinderby S (2013). Scorched Earth: how will changes in the strength of the vegetation sink to ozone deposition affect human health and ecosystems? Atmospheric Chemistry and Physics,13, 6741–6755. 10.5194/acp-13-6741-2013

Emberson LD, Pleijel H, Ainsworth EA, Van den Berg M, Ren W, Osborne S, et al. (2018). Ozone effects on crops and consideration in crop models. European Journal of Agronomy, 100, 19–34.

Emberson LD, Simpso D, Tuovine J-P, Ashmor MR, & Cambridg HM. (2000). Towards a model of ozone deposition and stomatal uptake over Europe (Research Note No. 42). Norwegian Meteorological Institute.

Enders G (1992). Deposition of ozone to a mature spruce forest: measurements and comparison to models. Environmental Pollution, 75, 61–67. [PubMed: 15092050]

Enders G, Dlugi R, Steinbrecher R, Clement B, Daiber R, Eijk J. v., et al. (1992). Biosphere/atmosphere interactions: Integrated research in a European coniferous forest ecosystem. Atmospheric Environment, 26A(1), 171–189.

Erisman JW, Van Pul A, & Wyers P (1994). Parameterization of surface resistance for the quantification of atmospheric deposition of acidifying pollutants and ozone. Atmospheric Environment, 28, 2595–2607.

Ermel M, Oswald R, Mayer J-C, Moravek A, Song G, Beck. M, et al. (2013). Preparation methods to optimize the performance of sensor discs for fast chemiluminescence ozone analyzers. Environmental Science & Technology, 47, 1930–1936. 10.1021/es3040363 [PubMed: 23343053]

Ewert F, & Porter JR (2000). Ozone effects on wheat in relation to CO2: modelling short-term and long-term responses of leaf photosynthesis and leaf duration. Global Change Biology, 6(7), 735–750.

Falk S, & Søvde Haslerud A (2019). Update and evaluation of the ozone dry deposition in Olso CTM3 v1.0. Geoscientific Model Development, 12, 4705–4728. 10.5194/gmd-12-4705-2019

Faloona I, Tan D, Brune W, Hurst J, Barket D, Couch TL, et al. (2001). Nighttime observations of anomalously high levels of hydroxyl radicals above a deciduous forest canopy. Journal of Geophysical Research: Atmospheres, 106(D20), 24315–24333. 10.1029/2000JD900691

Fan SM, Wofsy SC, Bakwin PS, Jacob DJ, & Fitzjarrald DR (1990). Atmosphere-biosphere exchange of CO2 and O3 in the central Amazon forest. Journal of Geophysical Research: Atmospheres, 95(D10), 16851–16864. 10.1029/JD095iD10p16851

Farage PK, Long SP, Lechner EG, & Baker NR (1991). The sequence of change within the photosynthetic apparatus of wheat following short-term exposure to ozone. Plant Physiology, 95(2), 529–535. [PubMed: 16668016]

Fares S, Loreto F, Kleist E, & Wildt J (2007). Stomatal uptake and stomatal deposition of ozone in isoprene and monoterpene emitting plants. Plant Biology. 10.1055/s-2007-965257

Fares S, Matteucci G, Scarascia Mugnozza G, Morani A, Calfapietra C, Salvatori E, Fusaro L, Manes F, & Loreto F (2013). Testing of models of stomatal ozone fluxes with field measurements in a mixed Mediterranean forest. Atmospheric Environment. 10.1016/j.atmosenv.2012.11.007

Fares S, McKay M, Holzinger R, & Goldstein AH (2010). Ozone fluxes in a Pinus ponderosa ecosystem are dominated by non-stomatal processes: Evidence from long-term continuous measurements. Agricultural and Forest Meteorology, 150(3), 420–431.

Fares S, Park J-H, Ormeno E, Gentner DR, McKay M, Loreto F, Karlik J, & Goldstein AH (2010). Ozone uptake by citrus trees exposed to a range of ozone concentrations. Atmospheric Environment, 44, 3404–3412. 10.1016/j.atmosenv.2010.06.010

Fares S, Savi F, Muller J, Matteucci G, & Paoletti E (2014). Simultaneous measurements of above and below canopy ozone fluxes help partitioning ozone deposition between its various sinks in a Mediterranean Oak Forest. Agricultural and Forest Meteorology, 198, 181–191.

Fares S, Weber R, Park J-H, Gentner D, Karlik J, & Goldstein AH (2012). Ozone deposition to an orange orchard: partitioning between stomatal and non-stomatal sinks. Environmental Pollution, 169, 258–266. [PubMed: 22341155]

Farmer DK, & Cohen RC (2008). Observations of HNO3, SAN, SPN and NO2 fluxes: evidence for rapid HOx chemistry within a pine forest canopy. Atmospheric Chemistry and Physics, 8(14), 3899–3917.

Farmer DK, Kimmel JR, Phillips G, Docherty KS, Worsnop DR, Sueper D, et al. (2011). Eddy covariance measurements with high-resolution time-of-flight aerosol mass spectrometry: a new approach to chemically resolved aerosol fluxes. Atmospheric Measurement Techniques, 4(6), 1275–1289.

Finco A, Coyle M, Nemitz E, Marzuoli R, Chiesa M, Loubet B, et al. (2018). Characterization of ozone deposition to mixed oak-hornbeam forest – flux measurements at five levels above and inside the canopy and their interactions with nitric oxide. Atmospheric Chemistry and Physics, 18, 17945–17961. 10.5194/acp-18-17945-2018

Finkelstein PL (2001). Deposition velocities of SO2 and O3 over agricultural and forest ecosystems. Water, Air and Soil Pollution: Focus, 1(5–6), 49–57.

Finkelstein PL, Ellestad TG, Clarke JF, Meyers TP, Schwede DB, Hebert EO, & Neal JA (2000). Ozone and sulfur dioxide dry deposition to forests: Observations and model evaluation. Journal of Geophysical Research, 105(D12), 15365–15377. 10.1029/2000JD900185

Finkelstein PL, & Sims PF (2001). Sampling error in eddy correlation flux measurements. Journal of Geophysical Research: Atmospheres, 106(D4), 3503–3509. 10.1029/2000JD900731

Finnigan JJ, Shaw RH, & Patton EG (2009). Turbulence structure above a vegetation canopy. Journal of Fluid Mechanics, 637, 387–424.

Fiscus EL, Booker FL, & Burkey KO (2005). Crop responses to ozone: uptake, modes of action, carbon assimilation and partitioning. Plant, Cell & Environment, 28, 997–1011. 10.1111/J.1365-3040.2005.01349.X

Fitzjarrald DR, & Lenschow DH (1983). MEAN CONCENTRATION AND FLUX PROFILES FOR CHEMICALLY REACTIVE SPECIES IN THE ATMOSPHERIC SURFACE-LAYER. Atmospheric Environment, 17(12), 2505–2512.

Foken T, Mauder M, Liebethal C, Wimmer F, Beyrich F, Leps JP, et al. (2010). Energy balance closure for the LITFASS-2003 experiment. Theoretical and Applied Climatology, 101(1–2), 149–160.

Fowler D, Flechard C, Cape JN, Storeton-West RL, & Coyle M (2001). Measurements of ozone deposition to vegetation quantifying the flux, the stomatal and non-stomatal components. Water, Air, and Soil Pollution, 130, 63–74. 10.1023/A:1012243317471

Fowler D, Nemitz E, Misztal P, Di Marco C, Skiba U, Ryder J, et al. (2011). Effects of land use on surface-atmosphere exchanges of trace gases and energy in Borneo: comparing fluxes over oil palm plantations and a rainforest. Philosophical Transactions of the Royal Society B: Biological Sciences, 366(1582), 3196–3209.

Fowler D, Pilegaard K, Sutton MA, Ambus P, Raivonen M, Duyzer J, et al. (2009). Atmospheric composition change: Ecosystems-Atmosphere interactions. Atmospheric Environment, 43, 5193–5267. 10.1016/j.atmosenv.2009.07.068

Franks PJ, Bonan GB, Berry JA, Lombardozzi DL, Holbrook NM, Herold N, & Oleson KW (2018). Comparing optimal and empirical stomatal conductance models for application in Earth system models. Global Change Biology, 1–16. 10.1111/gcb.14445

Franz M, Simpson D, Arneth A, & Zaehle S (2017). Development and evaluation of an ozone deposition scheme for coupling to a terrestrial biosphere model. Biogeosciences, 14, 45–71. 10.5194/bg-14-45-2017

Freer-Smith PH, & Dobson MC (1989). Ozone flux to Picea sitchensis (bong) carr and Picea abies (l) karst during short episodes and the effects of these on transpiration and photosynthesis. Environmental Pollution, 59(2), 161–176. [PubMed: 15092411]

Freire LS, Gerken T, Ruiz-Plancarte J, Wei D, Fuentes JD, Katul GG, Dias NL, Acevedo OC, & Chamecki M (2017). Turbulent mixing and removal of ozone within an Amazon rainforest canopy. Journal of Geophysical Research: Atmospheres, 122, 2791–2811. 10.1002/2016JD026009

Fuentes JD, Chamecki M, Nascimento dos Santos RM, Von Randow C, Stoy PC, Katul G, et al. (2016). Linking meteorology, turbulence, and air chemistry in the Amazon rain forest. Bulletin of the American Meteorological Society, 97(12), 2329–2342.

Fuentes JD, den Hartog G, Neumann HH, & Gillespie TJ (1994). Measurements and modelling of ozone deposition to wet foliage. In Air Pollutants and the Leaf Cuticle (pp. 239–253). Berlin, Germany: Springer.

Fuentes JD, & Gillespie TJ (1992). A gas exchange system to study the effects of leaf surface wetness on the deposition of ozone. Atmospheric Environment, 26A(6), 1165–1173. 10.1016/0960-1686(92)90048-P

Fuentes JD, Gillespie TJ, den Hartog G, & Neumann HH (1992). Ozone deposition onto a deciduous forest during dry and wet conditions. Agricultural and Forest Meteorology, 62, 1–18.

Fumagalli I, Gruening C, Marzuoli R, Cieslik S, & Gerosa G (2016). Long-term measurements of NOx and O3 soil fluxes in a temperate deciduous forest. Agricultural and Forest Meteorology, 228, 205–216. 10.1016/j.agrformet.2016.07.011

Fung PK (2018). Ozone deposition over a boreal lake by the eddy covariance method (Masters dissertation). Helsinki, Finland: University of Helsinki.

Galbally IE (1971). Ozone Profiles and Ozone Fluxes in Atmospheric Surface Layer. Quarterly Journal of the Royal Meteorological Society, 97. 10.1002/qj.49709741103

Galbally I, & Allison I (1972). Ozone fluxes over snow surfaces. Journal of Geophysical Research, 77. 10.1029/JC077i021p03946

Galbally IE, & Roy CR (1980). Destruction of Ozone at the Earth's surface. Quarterly Journal of the Royal Meteorological Society, 106, 599–620.

Gallagher MW, Beswick KM, & Coe H (2001). Ozone deposition to coastal waters. Quarterly Journal of the Royal Meteorological Society, 127, 539–558.

Galmarini S, de Arellano JVG, & Duyzer J (1997). Fluxes of chemically reactive species inferred from mean concentration measurements. Atmospheric Environment, 31(15), 2371–2374.

Ganzeveld L, Ammann C & Loubet B (2015). Modelling atmosphere-biosphere exchange of ozone and nitrogen oxides. In Massad R-S & Loubet B (Eds.), Review and Integration of Biosphere-Atmosphere Modelling of Reactive Trace Gases and Volatile Aerosols (pp. 85–105). Netherlands: Springer.

Ganzeveld L, Helmig D, Fairall CW, Hare J, & Pozzer A (2009). Atmosphere-ocean ozone exchange: A global modeling study of biogeochemical, atmospheric and waterside turbulence dependencies. Global Biogeochemical Cycles, 23(GB4021). 10.1029/2008GB003301

Ganzeveld LN, Lelieveld J, Dentener FJ, Krol MC, & Roelofs GJ (2002). Atmosphere-biosphere trace gas exchanges simulated with a single-column model. Journal of Geophysical Research: Atmospheres, 107(D16). 10.1029/2001JD000684

Gao W, Shaw RH, & Paw U KT (1989). Observation of organized structure in turbulent flow within and above a forest canopy. Boundary-Layer Meteorology, 47, 349–377.

Gao W, Wesely ML, Cook DR, & Hart RL (1992). Air-surface exchange of H2O, CO2, and O3 at a tallgrass prairie in relation to remotely sensed vegetation indices. Journal of Geophysical Research: Atmospheres, 97(D17), 18,663–18,671. 10.1029/91JD03175

Garland JA, & Penkett SA (1976). Absorption of peroxy acetyl nitrate and ozone by natural surfaces. Atmospheric Environment, 10, 1127–1131.

Georgii H-W (Ed.) (1989). Mechanisms and Effects of Pollutant-Transfer into Forests. Dordrecht: Kluwer Academic Publishers. 10.1007/978-94-009-1023-2

Gerosa GA, Vitale M, Finco A, Manes F, Ballarin Denti. A, & Cieslik S (2005). Ozone uptake by an evergreen Mediterranean forest (Quercus ilex) in Italy. Part I: Micrometeorological flux measurements and flux partitioning. Atmospheric Environment, 39(18), 3255–3266. 10.1016/j.atmosenv.2005.01.056

Gerosa G, Cieslik S, & Ballarin-Denti A (2003). Micrometeorological determination of time-integrated stomatal ozone fluxes over wheat: a case study in Northern Italy. Atmospheric Environment, 37(6), 777–788. 10.1016/S1352-2310(02)00927-5

Gerosa G, Cieslik S, & Derghi F (2007). Comparison of Different Algorithms for Stomatal Ozone Flux Determination from Micrometeorological Measurements. Water, Air, and Soil Pollution, 179(1–4), 309–321. 10.1007/s11270-006-9234-7

Gerosa G, Finco A, Mereu S, Vitale M, Manes F, & Ballarin Denti A (2009a). Comparison of seasonal variations of ozone exposure and fluxes in a Mediterranean Holm oak forest between the exceptionally dry 2003 and the following year. Environmental Pollution, 157, 1737–1744. 10.1016/j.envpol.2007.11.025 [PubMed: 18180087]

Gerosa G, Finco A, Mereu S, Marzuoli R, & Ballarin-Denti A (2009b). Interactions among vegetation and ozone, water and nitrogen fluxes in a coastal Mediterranean maquis ecosystem. Biogeosciences, 6, 1783–1798.

Godowitch JM (1990). Vertical ozone fluxes and related deposition parameters over agricultural and forested landscapes. Boundary-Layer Meteorology, 50, 375–404.

Goldstein AH (2003). Ozone uptake by a ponderosa pine in the Sierra Nevada: A measurement perspective. Developments in Environmental Science, 2, 83–109.

Goldstein AH, Koven CD, Heald CL, & Fung IY (2009). Biogenic carbon and anthropogenic pollutants combine to form a cooling haze over the southeastern United States. Proceedings of the National Academy of Sciences, 106(22), 8835–8840.

Goldstein AH, McKay M, Kurpius MR, Schade GW, Lee A, Holzinger R, & Rasmussen RA (2004). Forest thinning experiment confirms ozone deposition to forest canopy is dominated by reaction with biogenic VOCs. Geophysical Research Letters, 31(22). 10.1029/2004GL021259

Gong SL, Walmsley JL, Barrie LA, & Hopper JF (1997). Mechanisms for surface ozone depletion and recovery during polar sunrise. Atmospheric Environment, 31(7), 969–981.

Grantz DA, Zhang XJ, Massman WJ, Delany A, & Pederson JR (1997). Ozone deposition to a cotton (Gossypium hirsutum L.) field: stomatal and surface wetness effects during the California Ozone Deposition Experiment. Agricultural and Forest Meteorology, 85(1–2), 19–31.

Grantz DA, Zhang X,J, Massman WJ, den Hartog G, Neumann HH, & Pederson JR (1995). Effects of stomatal conductance and surface wetness on ozone deposition in field-grown grape. Atmospheric Environment, 29(21), 3189–3198.

Grøntoft T, Henriksen JF, & Seip HM (2004). The humidity dependence of ozone deposition onto a variety of building surfaces. Atmospheric Environment, 38(1), 59–68

Gut A, Van Dijk S, Scheibe M, Rummel U, Welling M, Ammann C, et al. (2002). NO emission from an Amazonian rain forest soil: continuous measurements of NO flux and soil concentration. Journal of Geophysical Research: Atmospheres, 107. 10.1029/2001JD000521

Güsten H, & Heinrich G (1996). On-line measurements of ozone surface fluxes. 1. Methodology and instrumentation. Atmospheric Environment, 30(6), 897–909.

Güsten H, Heinrich G, Mönnich E, Sprung D, and Weppner J (1997). On-line measurements of Ozone Surface Fluxes: Instrumentation and Methodology. In Slanina S (Ed.), Transport and Chemical Transformation of Pollutants in the Troposphere: Experimental and Theoretical Studies of Biogenic Emissions and of Pollutant Deposition (p. 201–215). Berlin: Springer.

Güsten H, Heinrich G, Mönnich E, Sprung D, Weppner J, Ramadan AB, et al. (1996). On-line measurements of ozone surface fluxes: Part II. Surface-level ozone fluxes onto the Sahara desert. Atmospheric Environment, 30(6), 911–918.

Güsten H, Heinrich G, Schmidt RWH, & Schurath U (1992). A Novel Ozone Sensor for Direct Eddy Flux Measurements. Journal of Atmospheric Chemistry, 14(1–4), 73–84.

Hanisch F, & Crowley JN (2003). Ozone decomposition on Saharan dust: An experimental investigation. Atmospheric Chemistry and Physics. 10.5194/acp-3-119-2003

Hardacre C, Wild O, & Emberson L (2015). An evaluation of ozone dry deposition in global scale chemistry climate models. Atmospheric Chemistry and Physics, 15(11), 6419–6436. 10.5194/acp-15-6419-2015

Hargreaves KJ, Fowler D, Storeton-West RL, & Duyzer JH (1992). The exchange of nitric oxide, nitrogen dioxide and ozone between pasture and the atmosphere. Environmental Pollution, 75(1), 53–59. [PubMed: 15092049]

Harman IN, & Finnigan JJ (2007). A simple unified theory for flow in the canopy and roughness sublayer. Boundary-Layer Meteorology, 123(2), 339–363.

Harman IN, & Finnigan JJ (2008). Scalar concentration profiles in the canopy and roughness sublayer. Boundary-Layer Meteorology, 129(3), 323–351.

Hassan IA, Ashmore MR, & Bell JNB (1994). Effects of O3 on the stomatal behavior of Egyptian varieties of radish (Raphanus sativus L. cv. Baladey) and turnip (Brassica rapa L. cv. Sultani). New Phytologist, 128, 243–249.

Helmig D, Bocquet F, Cohen L, & Oltmans SJ (2007). Ozone uptake to the polar snowpack at Summit, Greenland. Atmospheric Environment, 41, 5061–5076. 10.1016/j.atmosenv.2006.06.064

Helmig D, Cohen LD, Bocquet F, Oltmans S, Grachev A, & Neff W (2009). Spring and summertime diurnal surface ozone fluxes over the polar snow at Summit, Greenland. Geophysical Research Letters, 36, 1–5. 10.1029/2008gl036549

Helmig D, Ganzeveld L, Butler T, & Oltmans SJ (2007). The role of ozone atmosphere-snow gas exchange on polar, boundary-layer tropospheric ozone - a review and sensitivity analysis. Atmospheric Chemistry and Physics, 7. 10.5194/acp-7-15-2007

Helmig D, Johnson B, Oltmans SJ, Neff W, Eisele F, & Davis DD (2008). Elevated ozone in the boundary layer at South Pole. Atmospheric Environment, 42, 2788–2803. 10.1016/j.atmosenv.2006.12.032

Helmig D, Lang EK, Bariteau L, Boylan P, Fairall CW, Ganzeveld L, et al. (2012). Atmosphere-ocean ozone fluxes during the TexAQS 2006, STRATUS 2006, GOMECC 2007, GasEx 2008, and AMMA 2008 cruises. Journal of Geophysical Research: Atmospheres, 117(D4). 10.1029/2011JD015955

Helmig D, Ortega J, Guenther A, Herrick JD, & Geron C (2006). Sesquiterpene emissions from loblolly pine and their potential contribution to biogenic aerosol formation in the Southeastern US. Atmospheric Environment, 40(22), 4150–4157.

Helmig D, Seok B, Williams MW, Hueber J, & Sanford R (2009). Fluxes and chemistry of nitrogen oxides in the Niwot Ridge, Colorado, snowpack. Biogeochemistry, 95, 115–130. 10.1007/s10533-009-9312-1

Herbinger K, Then C, Haberer K, Alexou M, Low M, Remele K, Rennenberg H, Matyssek R, Grill D, Wieser G, & Tausz M (2007). Gas exchange and antioxidative compounds in young beech trees under free-air ozone exposure and comparisons to adult trees. Plant Biology, 9, 288–297. [PubMed: 17357021]

Herwehe JA, Otte TL, Mathur R, & Rao ST (2011). Diagnostic analysis of ozone concentrations simulated by two regional-scale air quality models. Atmospheric Environment, 45(33), 5957–5969.

Hicks BB, Kolb CE, & Lenschow DH (1989). New opportunities for flux measurement. In Lenschow DH & Hicks BB (Eds.), Global Tropospheric Chemistry: Chemical Fluxes in the Global Atmosphere (pp. 83–85). Boulder, Colorado: National Center for Atmospheric Research.

Hicks BB, Wesely ML, & Durham JL (1980) Critique of methods to measure dry deposition workshop summary. United States.

Hillel D (1980). Fundamentals of Soil Physics. New York, NY: Academic Press.

Hogg A (2007). Stomatal and non-stomatal fluxes of ozone, NOx, and NOy to a northern mixed hardwood forest (Doctoral dissertation). Ann Arbor, Michigan: The University of Michigan.

Hogg A, Uddling J, Ellsworth D, Carroll MA, Pressley S, Lamb B, & Vogel C (2007). Stomatal and non-stomatal fluxes of ozone to a northern mixed hardwood forest. Tellus Series B, 59(3), 514–525

Hogrefe C, Liu P, Pouliot G, Mathur R, Roselle S, Flemming J, Lin M, & Park RJ (2018). Impacts of different characterizations of large-scale background on simulated regional-scale ozone over the continental United States. Atmospheric Chemistry and Physics, 18, 3839–3864. 10.5194/acp-18-3839-2018 [PubMed: 30079085]

Hole LR, Semb A, & Tørseth K (2004). Ozone deposition to a temperate coniferous forest in Norway; gradient method measurements and comparison with the EMEP deposition module. Atmospheric Environment, 38(15), 2217–2223

Hollaway MJ, Arnold SR, Collins WJ, Folberth G, & Rap A (2016). Sensitivity of midnineteenth century tropospheric ozone to atmospheric chemistry-vegetation interactions. Journal of Geophysical Research: Atmospheres, 122. 10.1002/2016JD025462

Holzinger R, Lee A, Paw U KT, & Goldstein AH (2005). Observations of oxidation products above a forest imply biogenic emissions of very reactive compounds. Atmospheric Chemistry and Physics, 5, 67–75.

Hopper JF, Barrie LA, Silis A, Hart W, Gallant AJ, & Dryfhout H (1998). Ozone and meteorology during the 1994 Polar Sunrise Experiment. Journal of Geophysical Research: Atmospheres, 103(D1), 1481–1492. 10.1029/97JD02888

Horváth L, Führer E, & Lajtha K (2006). Nitric oxide and nitrous oxide emission from Hungarian forest soils; linked with atmospheric N-deposition. Atmospheric Environment, 40, 7786–7795.

Horváth L, Koncz P, Móring A, Nagy Z, Pintér K, & Weidinger T (2018). An attempt to partition stomatal and non-stomatal ozone deposition parts on a short grassland. Boundary-Layer Meteorology, 167(2), 303–326.

Horváth L, Nagy Z, & Weidinger T (1998). Estimation of dry deposition velocities of nitric oxide, sulfur dioxide, and ozone by the gradient method above short vegetation during the TRACT campaign. Atmospheric Environment, 32(7), 1317–1322.

Horváth L, Weidinger T, Nagy Z, & Führer E (1997). Measurement of Dry Deposition Velocity of Ozone, Sulfur Dioxide and Nitrogen Oxides above Pine Forest and Low Vegetation in Different Seasons by the Gradient Method. In Slanina S (Ed.), Transport and Chemical Transformation of Pollutants in the Troposphere: Experimental and Theoretical Studies of Biogenic Emissions and of Pollutant Deposition (pp. 304–310). Berlin: Springer.

Hoshika Y, Fares S, Savi F, Gruening C, Goded I, De Marco A, et al. (2017). Stomatal conductance models for ozone risk assessment at canopy level in two Mediterranean evergreen forests. Agricultural and Forest Meteorology, 234, 212–221.

Hoshika Y, Katata G, Deushi M, Watanabe M, Koike T, & Paoletti E (2015). Ozone-induced stomatal sluggishness changes carbon and water balance of temperate deciduous forests. Scientific Reports, 5, 9871. [PubMed: 25943276]

Hosker RP, & Lindberg SE (1982). Review: Atmospheric deposition and plant assimilation of gases and particles. Atmospheric Environment, 16(5), 889–910.

Högström U (1988). Non-dimensional wind and temperature profiles in the atmospheric surface layer: A re-evaluation. Boundary-Layer Meteorology, 42, 55–78.

Huang L, McDonald-Buller EC, McGaughey G, Kimura Y, & Allen DT (2016). The impact of drought on ozone dry deposition over eastern Texas. Atmospheric Environment, 127, 176–186. 10.1016/j.atmosenv.2015.12.022

Jacob DJ (2000). Heterogenous chemistry and tropospheric ozone. Atmospheric Environment, 34, 2131–2159.

Jacob DJ, Fan SM, Wofsy SC, Spiro PA, Bakwin PS, Ritter JA, et al. Moore KE (1992). Deposition of ozone to tundra. Journal of Geophysical Research: Atmospheres, 97(D15), 16473–16479. 10.1029/91JD02696

Jammoul A, Gligorovski S, George C, & D'Anna B (2008). Photosensitized heterogeneous chemistry of ozone on organic films. Journal of Physical Chemistry A. 10.1021/jp074348t

Jardine K, Yañez Serrano A, Arneth A, Abrell L, Jardine A, van Haren J, et al. (2011). Within-canopy sesquiterpene ozonolysis in Amazonia. Journal of Geophysical Research: Atmospheres, 116(D19). 10.1029/2011JD016243

Jarvis PG (1976). The Interpretation of the Variations in Leaf Water Potential and Stomatal Conductance Found in Canopies in the Field. Philosophical Transactions of the Royal Society of London. Series B. Biological Sciences, 273, 593–610.

Jensen NO, & Hummelshøj P (1995). Derivation of canopy resistance for water vapour fluxes over a spruce forest, using a new technique for the viscous sublayer resistance. Agricultural and Forest Meteorology, 73(3–4), 339–352.

Jensen NO, & Hummelshøj P (1997). Derivation of canopy resistance for water vapor fluxes over a spruce forest, using a new technique for the viscous sublayer resistance (correction to vol. 73, pp. 339, 1995). Agricultural and Forest Meteorology, 85(3–4), 289.

Jetter R, Kunst L, & Samuels AL (2006). Composition of Plant Cuticular Waxes. In Riederer M & Müller C (Eds.), Biology of the Plant Cuticle, Annual Plant Reviews (Vol. 23, pp. 145–181). Oxford: Blackwell.

Joss U, & Graber WK (1996). Profiles and simulated exchange of H2O, O3, NO2 between the atmosphere and the HartX Scots pine plantation. Theoretical and Applied Climatology, 53(1–3), 157–172.

Jud W, Fischer L, Canaval E, Wohlfahrt G, Tissier A, & Hansel A (2016). Plant surface reactions: an ozone defence mechanism impacting atmospheric chemistry. Atmospheric Chemistry and Physics. 10.5194/acpd-15-19873-2015

Jurá S, Šigut L, Holub P, Fares S, Klem K, Grace J, & Urban O (2019). Ozone flux and ozone deposition in a mountain spruce forest are modulated by sky conditions. Science of The Total Environment. 10.1016/j.scitotenv.2019.03.491

Kabata-Pendias A (2004). Soil–plant transfer of trace elements—an environmental issue. Geoderma, 122(2–4), 143–149.

Kanagendran A, Pazouki L, Li S, Liu B, Kännaste A, & Niinemets Ü (2018). Ozone-triggered surface uptake and stress volatile emissions in Nicotiana tabacum 'Wisconsin'. Journal of Experimental Botany, 69(3), 681–697. 10.1093/jxb/erx431 [PubMed: 29301045]

Kaplan WA, Wofsy SC, Keller M, & Da Costa JM (1988). Emission of NO and deposition of O3 in a tropical forest system. Journal of Geophysical Research: Atmospheres, 93(D2), 1389–1395. 10.1029/JD093iD02p01389

Karagulian F, & Rossi MJ (2006). The heterogeneous decomposition of ozone on atmospheric mineral dust surrogates at ambient temperature. International Journal of Chemical Kinetics. 10.1002/kin.20175

Kavassalis SC, & Murphy JG (2017), Understanding ozone-meteorology correlations: A role for dry deposition. Geophysical Research Letters, 44, 2922–2931. 10.1002/2016GL071791

Kelliher FM, Leuning R, Raupach MR, & Schulze ED (1995). Maximum conductances for evaporation from global vegetation types. Agricultural and Forest Meteorology, 73(1–2), 1–16.

Kennedy D, Swenson S, Oleson KW, Lawrence DM, Fisher R, Lola da Costa AC, & Gentine P (2019). Implementing plant hydraulics in the Community Land Model, version 5. Journal of Advances in Modeling Earth Systems, 11, 485–513. 10.1029/2018MS001500

Keronen P, Reissell A, A., Rannik Ü, Pohja T, Siivola E, Hiltunen V, et al. (2003). Ozone flux measurements over a Scots pine forest using eddy covariance method: performance evaluation and comparison with flux-profile method. Boreal Environment Research, 8(4), 425–443.

Kim Y, Still CJ, Hanson CV, Kwon H, Greer BT, & Law BE (2016). Canopy skin temperature variations in relation to climate, soil temperature, and carbon flux at a ponderosa pine forest in central Oregon. Agricultural and Forest Meteorology, 226, 161–173.

Kirchhoff VWJH, Browell EV, & Gregory GL (1988). Ozone measurements in the troposphere of an Amazonian rain forest environment. Journal of Geophysical Research: Atmospheres, 93(D12), 15850–15860. 10.1029/JD093iD12p15850

Kirkman G, Gut A, Ammann C, Gatti L, Cordova A, Moura M, Andreae M, & Meixner F (2002). Surface exchange of nitric oxide, nitrogen dioxide, and ozone at a cattle pasture in Rondônia, Brazil. Journal of Geophysical Research: Atmospheres, 107. 10.1029/2001JD000523

Koch JR, Scherzer AJ, Eshita SM, & Davis KR (1998). Ozone sensitivity in hybrid poplar is correlated with a lack of defense-gene activation. Plant Physiology, 118(4), 1243–1252. [PubMed: 9847098]

Kramm G, Dlugi R, Dollard GJ, Foken T, Mölders N, Müller H, et al. (1995). On the dry deposition of ozone and reactive nitrogen species. Atmospheric Environment, 29(21), 3209–3231.

Kramm G, Müller H, Fowler D, Höfken KD, Meixner FX, & Schaller E (1991). A Modified Profile Method for Determining the Vertical Fluxes of NO, NO2, Ozone, and HNO3 in the Atmospheric Surface Layer. Journal of Atmospheric Chemistry, 13(3), 265–288.

Kurpius MR, & Goldstein AH (2003). Gas-phase chemistry dominates O3 loss to a forest, implying a source of aerosols and hydroxyl radicals to the atmosphere. Geophysical Research Letters, 30(7). 10.1029/2002GL016785

Kurpius MR, McKay M, & Goldstein AH (2002). Annual ozone deposition to a Sierra Nevada ponderosa pine plantation. Atmospheric Environment, 36(28), 4503–4515.

Kvalevåg MM, & Myhre G (2013). The effect of carbon-nitrogen coupling on the reduced land carbon sink caused by tropospheric ozone. Geophysical Research Letters, 40, 3227–3231. 10.1002/grl.50572

Laisk A, Kull O, & Moldau H (1989). Ozone Concentration in Leaf Intercellular Air Spaces Is Close to Zero. Plant Physiology. 10.1104/pp.90.3.1163

Lamaud E, Carrara A, Brunet Y, López A, & Druilhet A (2002). Ozone fluxes above and within a pine forest canopy in dry and wet conditions. Atmospheric Environment, 36, 77–88.

Lamaud E, Loubet B, Irvine M, Stella P, Personne E, & Cellier P (2009). Partitioning of ozone deposition over a developed maize crop between stomatal and non-stomatal uptakes, using eddy-covariance flux measurements and modelling. Agricultural and Forest Meteorology, 149, 1385–1396. 10.1016/j.agrformet.2009.03.017

Launiainen S, Katul GG, Grönholm T, & Vesala T (2013). Partitioning ozone fluxes between canopy and forest floor by measurements and a multi-layer model. Agricultural and Forest Meteorology, 173, 85–99. 10.1016/j.agrformet.2012.12.009

Lee X, Massman W, & Law B (Eds.). (2004). Handbook of micrometeorology: a guide for surface flux measurement and analysis (Vol. 29). Springer Science & Business Media.

Legrand M, Preunkert S, Jourdain B, Gallee H, Goutail F, Weller R, & Savarino J (2009). Year-round record of surface ozone at coastal (Dumont d'Urville) and inland (Concordia) sites in East Antarctica. Journal of Geophysical Research: Atmospheres, 114. 10.1029/2008jd011667

Legrand M, Preunkert S, Savarino J, Frey MM, Kukui A, Helmig D, Jourdain B, Jones AE, Weller R, Brough N, & Gallée H (2016). Inter-annual variability of surface ozone at coastal (Dumont d'Urville, 2004–2014) and inland (Concordia, 2007–2014) sites in East Antarctica. Atmospheric Chemistry and Physics, 16, 8053–8069. 10.5194/acp-16-8053-2016

Le Morvan-Quéméner A, Coll I, Kammer J, Lamaud E, Loubet B, Personne E, & Stella P (2018). Impact of parameterization choices on the restitution of ozone deposition over vegetation. Atmospheric Environment, 178, 49–65.

Lenschow DH (1982). Reactive trace species in the boundary layer from a micrometeorological perspective. Journal of the Meteorological Society of Japan, 60(1), 472–480. 10.2151/jmsj1965.60.1_472

Lenschow DH, & Delany AC (1987). An analytic formulation for NO and NO2 flux profiles in the atmospheric surface layer. Journal of Atmospheric Chemistry, 5(3), 301–309.

Lenschow DH, Delany AC, Stankov BB, & Stedman DH (1980). Airborne measurements of the vertical flux of ozone in the boundary layer. Boundary-Layer Meteorology, 19(2), 249–265. 10.1007/bf00117223

Lenschow DH, & Hicks BB (Eds.) (1989). Global Tropospheric Chemistry: Chemical Fluxes in the Global Atmosphere. Boulder, CO: National Center for Atmospheric Research.

Lenschow DH, Pearson R Jr., & Stankov. BB (1981). Estimating the ozone budget in the boundary layer by use of aircraft measurements of ozone eddy flux and mean concentration. Journal of Geophysical Research, 86(C8), 7291–7297. 10.1029/JC086iC08p07291

Lenschow DH, & Raupach MR (1991). The attenuation of fluctuations in scalar concentrations through sampling tubes. Journal of Geophysical Research: Atmospheres, 96(D8), 15259–15268. 10.1029/91JD01437

Leuning R (1995). A critical appraisal of a combined stomatal-photosynthesis model for C3 plants. Plant, Cell & Environment, 18(4), 339–355.

Leuning R, Neumann HH, & Thurtell GW (1979). Ozone uptake by corn (Zea mays L.): A general approach. Agricultural Meteorology, 20(2), 115–135.

Leuning R, Unsworth MH, Neuman HN, & King KM (1979). Ozone fluxes to tobacco and soil under field conditions. Atmospheric Environment, 13, 1155–1163.

Li J, Mahalov A, & Hyde P (2016). Simulating the impacts of chronic ozone exposure on plant conductance and photosynthesis, and on the regional hydroclimate using WRF/Chem. Environmental Research Letters, 11. 10.1088/1748-9326/11/11/114017

Li J, Mahalov A, & Hyde P (2018). Simulating the effects of chronic ozone exposure on hydrometeorology and crop productivity using a fully coupled crop, meteorology and air quality modeling system. Agricultural and Forest Meteorology, 260–261, 287–299. 10.1016/j.agrformet.2018.06.013

Li J, Duan Q, Wang YP, Gong W, Gan Y, & Wang C (2018). Parameter optimization for carbon and water fluxes in two global land surface models based on surrogate modelling. International Journal of Climatology, 38, e1016–e1031.

Li Q, Gabay M, Rubin Y, Fredj E, & Tas E (2018). Measurement-based investigation of ozone deposition to vegetation under the effects of coastal and photochemical air pollution in the Eastern Mediterranean. Science of the Total Environment, 645, 1579–1597. 10.1016/j.scitotenv.2018.07.037

Lin C, Gentine P, Huang Y, Guan K, Kimm H, & Zhou S (2018). Diel ecosystem conductance response to vapor pressure deficit is suboptimal and independent of soil moisture. Agricultural and Forest Meteorology, 250–251, 24–34. 10.1016/j.agrformet.2017.12.078

Lin J-T, Youn D, Liang X-Z, & Wuebbles DJ (2008). Global model simulation of summertime U.S. ozone diurnal cycle and its sensitivity to PBL mixing, spatial resolution, and emissions. Atmospheric Environment, 42, 8470–8483.

Lin M, Horowitz LW, Payton R, Fiore AM, & Tonnesen G (2017). US surface ozone trends and extremes from 1980 to 2014: Quantifying the roles of rising Asian emissions, domestic controls, wildfires, and climate. Atmospheric Chemistry and Physics, 17, 2943–2970. 10.5194/acp-17-2943-2017

Lin M, Malyshev S, Shevliakova E, Paulot F, Horowitz LW, Fares S, Mikkelsen TN, and Zhang L (2019). Sensitivity of ozone dry deposition to ecosystem-atmosphere-interactions: A critical appraisal of observations and simulations. Global Biogeochemical Cycles. 10.1029/2018GB006157

Lin YS, Medlyn BE, Duursma RA, Prentice IC, Wang H, Baig S, Eamus D, de Dios VR, Mitchell P, Ellsworth DS, & de Beeck MO (2015). Optimal stomatal behaviour around the world. Nature Climate Change, 5(5), 459–464. 10.1038/nclimate2550

Lombardozzi D, Levis S, Bonan G, & Sparks JP (2012). Predicting photosynthesis and transpiration responses to ozone: decoupling modeled photosynthesis and stomatal conductance. Biogeosciences, 9, 3113–3130. 10.5194/bg-9-3113-2012

Lombardozzi D, Levis S, Bonan G, Hess PG, & Sparks JP (2015). The Influence of Chronic Ozone Exposure on Global Carbon and Water Cycles. Journal of Climate, 28, 292–305. 10.1175/Jcli-D-14-00223.1

Lombardozzi D, Sparks JP, & Bonan G (2013). Integrating O3 influences on terrestrial processes: photosynthetic and stomatal response data available for regional and global modeling. Biogeosciences, 10, 6815–6831. 10.5194/bg-10-6815-2013

Lombardozzi D, Sparks JP, Bonan G, & Levis S (2012). Ozone exposure causes a decoupling of conductance and photosynthesis: implications for the Ball-Berry stomatal conductance model. Oecologia, 169, 651–659. [PubMed: 22218943]

Loreto F, & Fares S (2007). Is ozone flux inside leaves only a damage indicator? Clues from volatile isoprenoid studies. Plant Physiology, 143(3), 1096–1100. [PubMed: 17344434]

Loubet B, Cellier P, Fléchard C, Zurfluh O, Irvine M, Lamaud E, et al. (2013). Investigating discrepancies in heat, CO2 fluxes, and O3 deposition velocity over maize as measured by the eddy-covariance and the aerodynamic gradient methods. Agricultural and Forest Meteorology, 169, 35–50. 10.1016/j.agrformet.2012.09.010

MacPherson JI, Desjardins RL, Schuepp PH, & Pearson R Jr. (1995). Aircraft-Measured Ozone Deposition in the San Joaquin Valley of California. Atmospheric Environment, 29(21), 3133–3145.

Mahrt L, Lenschow DH, Sun J, Weil JC, MacPherson JI, & Desjardins RL (1995). Ozone fluxes over a patchy cultivated surface. Journal of Geophysical Research, 100(D11), 23125–23131. 10.1029/95JD02599

Maier-Maercker U, & Koch W (1991). Experiments on the control capacity of stomata of Picea abies (l) karst after fumigation with ozone and in environmentally damaged material. Plant, Cell & Environment, 14, 175–184.

Makar PA, Fuentes JD, Wang D, Staebler RM, & Wiebe HA (1999). Chemical processing of biogenic hydrocarbons within and above a temperate deciduous forest. Journal of Geophysical Research: Atmospheres, 104(D3), 3581–3603. 10.1029/1998JD100065

Manes F, Donato E, & Vitale M (2001). Physiological response of Pinus halepensis needles under ozone and water stress conditions. Physiologia Plantarum, 113, 249–257. [PubMed: 12060303]

Manes F, Vitale M, Donato E, & Paoletti E (1998). O3 and O3+CO2 effects on a Mediterranean evergreen broadleaf tree, holm oak (Quercus ilex L.). Chemosphere, 36, 801–806.

Martin MJ, Host GE, Lenz KE, & Isebrands JG (2001). Simulating the growth response of aspen to elevated ozone: a mechanistic approach to scaling a leaf-level model of ozone effects on photosynthesis to a complex canopy architecture. Environmental Pollution, 115(3), 425–436. [PubMed: 11789923]

Massman WJ (1993). Partitioning ozone fluxes to sparse grass and soil and the inferred resistances to dry deposition. Atmospheric Environment, 27A(2), 167–174.

Massman WJ (1998). A review of the molecular diffusivities of H2O, CO2, CH4, CO, O3, SO2, NH3, N2O, NO, and NO2 in air, O2 and N2 near STP. Atmospheric Environment, 32(6), 1111–1127.

Massman WJ (1999). A model study of kBH−1 for vegetated surfaces using 'localized near-field' Lagrangian theory. Journal of Hydrology, 223(1–2), 27–43.

Massman WJ (2004). Toward an ozone standard to protect vegetation based on effective dose: a review of deposition resistances and a possible metric. Atmospheric Environment, 38, 2323–2337.

Massman WJ, Musselman RC, & Lefohn AS (2000). A conceptual ozone dose-response model to develop a standard to protect vegetation. Atmospheric Environment, 34(5), 745–759

Massman WJ, Pederson J, Delany A, Grantz D, Den Hartog G, Neumann HH, et al. (1994). An evaluation of the regional acid deposition model surface module for ozone uptake at three sites in the San Joaquin Valley of California. Journal of Geophysical Research: Atmospheres, 99(D4), 8281–8294. 10.1029/93JD03267

Matichuk R, Tonnesen G, Luecken D, Gilliam R, Napelenok SL, Baker KR, et al. (2017). Evaluation of the Community Multiscale Air Quality Model for simulating winter ozone formation in the Uinta Basin. Journal of Geophysical Research: Atmospheres, 122(24), 13545–13572. 10.1002/2017JD027057

Matsuda K, Watanabe I, Wingpud V, Theramongkol P, Khummongkol P, Wangwongwatana S, & Totsuka T (2005). Ozone dry deposition above a tropical forest in the dry season in northern Thailand. Atmospheric Environment, 39(14), 2571–2577.

Matsuda K, Watanabe I, Wingpud V, Theramongkol P, & Ohizumi T (2006). Deposition velocity of O3 and SO2 in the dry and wet season above a tropical forest in northern Thailand. Atmospheric Environment, 40(39), 7557–7564.

Matyssek R, Sandermann H, Wieser G, Booker F, Cieslik S, Musselman R, & Ernst D (2008). The challenge of making ozone risk assessment for forest trees more mechanistic. Environmental Pollution, 156(3), 567–582. [PubMed: 18571819]

Matyssek R, Wieser G, Nunn AJ, Kozovits AR, Reiter IM, et al. (2004). Comparison between AOT40 and ozone uptake in forest trees of different species, age and site conditions. Atmospheric Environment, 38, 2271–2281. 10.1016/j.atmosenv.2003.09.078

Mayer J-C, Bargsten A, Rummel U, Meixner FX, & Foken T (2011). Distributed Modified Bowen Ratio method for surface layer fluxes of reactive and non-reactive trace gases. Agricultural and Forest Meteorology, 151(6), 655–668.

McCabe J, & Abbatt JPD (2009). Heterogeneous loss of gas-phase ozone on n-hexane soot surfaces: Similar kinetics to loss on other chemically unsaturated solid surfaces. The Journal of Physical Chemistry C, 113(6), 2120–2127. 10.1021/jp806771q

McLaughlin SB, Wullschleger SD, Sun G, & Nosal M (2007). Interactive effects of ozone and climate on water use, soil moisture content and streamflow in a southern Appalachian forest in the USA. New Phytologist, 174, 125–136.

Medlyn BE, Duursma RA, Eamus D, Ellsworth DS, Prentice IC, Barton CV, Crous KY, de Angelis P, Freeman M, & Wingate L (2011). Reconciling the optimal and empirical approaches to modelling stomatal conductance. Global Change Biology, 17(6), 2134–2144.

Meixner F, Fickinger T, Marufu L, Serca D, Nathaus F, Makina E, Mukurumbira L, & Andreae M (1997). Preliminary results on nitric oxide emission from a southern African savanna ecosystem. Nutrient Cycling in Agroecosystems, 48, 123–138.

Meyers TP, & Baldocchi DD (1993). Trace gas exchange above the floor of a deciduous forest: 2. SO2 and O3 deposition. Journal of Geophysical Research: Atmospheres, 98(D7), 12631–12638. 10.1029/93JD00720

Meyers TP, & Baldocchi DD (2005). Current Micrometeorological Flux Methodologies with Applications in Agriculture. Publications, Agencies and Staff of the U.S. Department of Commerce (500).

Meyers TP, Finkelstein P, Clarke J, Ellestad TG, & Sims PF (1998). A multilayer model for inferring dry deposition using standard meteorological measurements. Journal of Geophysical Research, 103(D17), 22645–22661. 10.1029/98JD01564

Mészáros R, Horváth L, Weidinger T, Neftel A, Nemitz E, Dammgen U, Cellier P, & Loubet B (2009). Measurement and modelling ozone fluxes over a cut and fertilized grassland. Biogeosciences, 6(10), 1987–1999

Mészáros R, Zsély I. Gy., Szinyei D, Vincze Cs., & Lagzi I (2009). Sensitivity analysis of an ozone deposition model. Atmospheric Environment, 43, 663–672. 10.1016/j.atmosenv.2008.09.058

Michou M, Laville P, Serça D, Fotiadi A, Bouchou P, & Peuch VH (2005). Measured and modeled dry deposition velocities over the ESCOMPTE area. Atmospheric Research, 74(1–4), 89–116.

Mikkelsen TN, Ro-Poulsen H, Hovmand MF, Jensen NO, Pilegaard K, & Egeløv AH (2004). Five-year measurements of ozone fluxes to a Danish Norway spruce canopy. Atmospheric Environment, 38, 2361–2371. 10.1016/j.atmosenv.2003.12.036

Mikkelsen TN, Ro-Poulsen H, Pilegaard K, Hovmand MF, Jensen NO, Christensen CS, & Hummgelshoej P (2000). Ozone uptake by an evergreen forest canopy: temporal variation and possible mechanisms. Environmental Pollution, 109, 423–429. [PubMed: 15092875]

Mills G, Hayes F, & Wilkinson S (2009). Chronic exposure to increasing background ozone impairs stomatal functioning in grassland species. Global Change Biology, 15, 1522–1533. 10.1111/j.1365-2486.2008.01798.x

Mills G, Pleijel H, Malley CS, Sinha B, Cooper OR, Schultz MG, et al. (2018). Tropospheric Ozone Assessment Report: Present-day tropospheric ozone distribution and trends relevant to vegetation. Elementa: Science of the Anthropocene, 6(47). 10.1525/elementa.302

Min KE, Pusede SE, Browne EC, LaFranchi BW, & Cohen RC (2014). Eddy covariance fluxes and vertical concentration gradient measurements of NO and NO2 over a ponderosa pine ecosystem: observational evidence for within-canopy chemical removal of NOx. Atmospheric Chemistry and Physics, 14(11), 5495–5512.

Min KE, Pusede SE, Browne EC, LaFranchi BW, Wooldridge PJ, Wolfe GM, Harrold SA, Thornton JA, & Cohen RC (2012). Observations of atmosphere-biosphere exchange of total and speciated peroxynitrates: nitrogen fluxes and biogenic sources of peroxynitrates. Atmospheric Chemistry and Physics, 12(20), 9763–9773.

Miner GL, Bauerle WL, & Baldocchi DD (2017). Estimating the sensitivity of stomatal conductance to photosynthesis: a review. Plant, Cell & Environment, 40(7), 1214–1238.

Morrison GC, & Nazaroff WW (2002). The rate of ozone uptake on carpet: mathematical modeling. Atmospheric Environment, 36, 1749–1756.

Muller JBA, Coyle M, Fowler D, Gallagher MW, Nemitz EG, & Percival CJ (2009). Comparison of ozone fluxes over grassland by gradient and eddy covariance technique. Atmospheric Science Letters, 10, 164–169. 10.1002/asl.226

Muller JBA, Percival CJ, Gallagher MW, Fowler D, Coyle M, & Nemitz E (2010). Sources of uncertainty in eddy covariance ozone flux measurements made by dry chemiluminescence fast response analysers. Atmospheric Measurement Techniques, 3(1), 163–176.

Munger JW, Wofsy SC, Bakwin PS, Fan S-M, Goulden ML, Daube BC, Goldstein AH, Moore KE, & Fitzjarrald DR (1996). Atmospheric deposition of reactive nitrogen oxides and ozone in a temperate deciduous forest and a subarctic woodland 1. Measurements and mechanisms. Journal of Geophysical Research, 101(D7), 12639–12657. 10.1029/96JD00230

Murray KA, Kramer LJ, Doskey PV, Ganzeveld L, Seok B, Van Dam B, & Helmig D (2015). Dynamics of ozone and nitrogen oxides at Summit, Greenland. II. Simulating snowpack chemistry during a spring high ozone event with a 1-D process-scale model. Atmospheric Environment, 117, 110–123. 10.1016/j.atmosenv.2015.07.004

Musselman RC, Lefohn AS, Massman WJ, & Heath RL (2006). A critical review and analysis of the use of exposure-and flux-based ozone indices for predicting vegetation effects. Atmospheric Environment, 40(10), 1869–1888.

National Academies of Sciences, Engineering, and Medicine (NASEM) (2016). The Future of Atmospheric Chemistry Research: Remembering Yesterday, Understanding Today, Anticipating Tomorrow. National Academies Press. 10.17226/23573

Neirynck J, Gielen B, Janssens IA, & Ceulemans R (2012). Insights into ozone deposition patterns from decade-long ozone flux measurements over a mixed temperate forest. Journal of Environmental Monitoring, 14(6), 1684–1695. [PubMed: 22622798]

Neirynck J, & Verstraeten A (2018). Variability of Ozone Deposition Velocity Over a Mixed Suburban Temperate Forest, Frontiers in Environmental Science, 6. 10.3389/fenvs.2018.00082

Nicolini G, Aubinet M, Feigenwinter C, Heinesch B, Lindroth A, Mamadou O, et al. (2018). Impact of CO2 storage flux sampling uncertainty on net ecosystem exchange measured by eddy covariance. Agricultural and Forest Meteorology, 248, 228–239.

Noormets A, Sôber A, Pell EJ, Dickson RE, Podila GK, Sôber J, Isebrands JG, & Karnosky DF (2001). Stomatal and non-stomatal limitation to photosynthesis in two trembling aspen (Populus tremuloides michx.) clones exposed to elevated CO2 and/or O3. Plant, Cell & Environment, 24, 327–336.

Nunn AJ, Cieslik S, Metzger U, Wieser G, & Matyssek R (2010). Combining sap flow and eddy covariance approaches to derive stomatal and non-stomatal O3 fluxes in a forest stand. Environmental Pollution, 158, 2014–2022. 10.1016/j.envpol.2009.11.034 [PubMed: 20056523]

Oliver RJ, Mercado LM, Sitch S, Simpson DM, Medlyn BE, Lin Y, & Folberth GA (2018). Large but decreasing effect of ozone on the European carbon sink. Biogeosciences, 15(13), 4245–4269.

Omasa K, Tobe K, Hosomi M, & Kobayashi M (2000). Absorption of ozone and seven organic pollutants by Populus nigra and Camellia sasanqua. Environmental Science & Technology, 34(12), 2498–2500.

Padro J (1993). Seasonal Contrasts in Modeled and Observed Dry Deposition Velocities of O3, SO2 and NO2 over 3 Surfaces. Atmospheric Environment, 27, 807–814. 10.1016/0960-1686(93)90002-G

Padro J (1994). Observed characteristics of the dry deposition velocity of O3 and SO2 above a wet deciduous forest. Science of the Total Environment, 146, 395–400.

Padro J (1996). Summary of ozone dry deposition velocity measurements and model estimates over vineyard, cotton, grass and deciduous forest in summer. Atmospheric Environment, 30(13), 2363–2369.

Padro J, Den Hartog G, & Neumann HH (1991). An investigation of the ADOM dry deposition module using summertime O3 measurements above a deciduous forest. Atmospheric Environment. Part A. General Topics, 25(8), 1689–1704.

Padro J, Massman WJ, Den Hartog G, & Neumann HH (1994). Dry deposition velocity of O3 over a vineyard obtained from models and observations: The 1991 California ozone deposition experiment. Water, Air, and Soil Pollution, 75(3–4), 307–323.

Padro J, Massman WJ, Shaw RH, Delany A, & Oncley SP (1994). A comparison of some aerodynamic resistance methods using measurements over cotton and grass from the 1991 California ozone deposition experiment. Boundary-Layer Meteorology, 71(4), 327–339.

Padro J, Neumann HH, & Den Hartog G (1992). Modelled and observed dry deposition velocity of O3 above a deciduous forest in the winter. Atmospheric Environment. Part A. General Topics, 26(5), 775–784.

Paoletti E (2005). Ozone slows stomatal response to light and leaf wounding in a Mediterranean evergreen broadleaf, Arbutus unedo. Environmental Pollution, 134, 439–445. 10.1016/j.envpol.2004.09.011 [PubMed: 15620589]

Paoletti E, & Grulke NE (2005). Does living in elevated CO2 ameliorate tree response to ozone? A review on stomatal responses. Environmental Pollution, 137(3), 483–493. [PubMed: 16005760]

Paoletti E, & Grulke NE (2010). Ozone exposure and stomatal sluggishness in different plant physiognomic classes. Environmental Pollution, 158(8), 2664–2671. [PubMed: 20537773]

Pape L, Ammann C, Nyfelder-Brunner A, Spirig C, Hans K, & Meixner FX (2009). An automated dynamic chamber system for surface exchange measurement of non-reactive and reactive trace gases of grassland ecosystem. Biogeosciences, 6, 405–429.

Park RJ, Hong SK, Kwon HA, Kim S, Guenther A, Woo JH, & Loughner CP (2014). An evaluation of ozone dry deposition simulations in East Asia. Atmospheric Chemistry and Physics, 14(15), 7929–7940.

Patton EG, & Finnigan JJ (2013). Canopy Turbulence. In Fernando HJS (Ed.), Handbook of Environmental Fluid Dynamics (Vol. 1, pp. 311–327). CRC Press/Taylor & Francis Group

Patton EG, Horst TW, Sullivan PP, Lenschow DH, Oncley SP, Brown WO, et al. (2011). The canopy horizontal array turbulence study. Bulletin of the American Meteorological Society, 92(5), 593–611.

Patton EG, Sullivan PP, Shaw RH, Finnigan JJ, & Weil JC (2016). Atmospheric Stability Influences on Coupled Boundary Layer and Canopy Turbulence. Journal of the Atmospheric Sciences, 73, 1621–1647.

Paulot F, Malyshev S, Nguyen T, Crounse JD, Shevliakova E, & Horowitz LW (2018). Representing sub-grid scale variations in nitrogen deposition associated with land use in a global Earth system model: implications for present and future nitrogen deposition fluxes over North America. Atmospheric Chemistry and Physics, 18(24), 17963–17978.

Paw U KT, & Meyers TP (1989). Investigations with a higher-order canopy turbulence model into mean source-sink levels and bulk canopy resistances. Agricultural and Forest Meteorology, 47, 259–271.

Pearson R (1990). MEASURING AMBIENT OZONE WITH HIGH-SENSITIVITY AND BANDWIDTH. Review of Scientific Instruments, 61(2), 907–916.

Peterson MC, & Honrath RE (2001). Observations of rapid photochemical destruction of ozone in snowpack interstitial air. Geophysical Research Letters, 28, 511–514.

Pilegaard K (2001). Air-soil exchange of NO, NO2 and O3 in forests. Water, Soil, and Air Pollution: Focus, 1, 79–88.

Pilegaard K, Hummelshøj P, & Jensen NO (1998). Fluxes of ozone and nitrogen dioxide measured by eddy correlation over a harvested wheat field. Atmospheric Environment, 32(7), 1167–1177.

Pilegaard K, Jensen NO, & Hummelshøj P (1995). Seasonal and diurnal variation in the deposition velocity of ozone over a spruce forest in Denmark. Water, Air, and Soil Pollution, 85(4), 2223–2228.

Pio CA, & Feliciano MS (1996). Dry deposition of ozone and sulphur dioxide over low vegetation in moderate southern European weather conditions. Measurements and modelling. Physics and Chemistry of the Earth, 21(5–6), 373–377.

Pio CA, Feliciano MS, Vermeulen AT, & Sousa EC (2000). Seasonal variability of ozone dry deposition under southern European climate conditions, in Portugal. Atmospheric Environment, 34(2), 195–205.

Plake D, Sörgel M, Stella P, Held A, & Trebs I (2015). Influence of meteorology and anthropogenic pollution on chemical flux divergence of the NO–NO2-O3 triad above and within a natural grassland canopy. Biogeosciences, 12(4), 945–959.

Plake D, Stella P, Moravek A, Mayer J-C, Amman C, Held A, & Trebs I (2015). Comparison of ozone deposition measured with the dynamic chamber and the eddy covariance method. Agricultural and Forest Meteorology, 206, 97–112. 10.1016/j.agrformet.2015.02.014

Plake D, & Trebs I (2013). An automated system for selective and continuous measurements of vertical thoron profiles for the determination of transport times near the ground. Atmospheric Measurement Techniques, 6, 1017–1030. 10.5194/amt-6-1017-2013

Pleijel H, Pihl Karlsson G, Danielsson H, & Selldén G (1995). Surface wetness enhances ozone deposition to a pasture canopy. Atmospheric Environment, 29(22), 3391–3393.

Pleim J, & Ran L (2011). Surface Flux Modeling for Air Quality Applications. Atmosphere, 2, 271–302. 10.3390/atmos2030271

Pleim JE, Xiu A, Finkelstein PL, & Otte TL (2001). A coupled land-surface and dry deposition model and comparison to field measurements of surface heat, moisture, and ozone fluxes. Water, Air, and Soil Pollution: Focus, 1(5–6), 243–252.

Plöchl M, Lyons T, Ollerenshaw J, & Barnes J (2000). Simulating ozone detoxification in the leaf apoplast through the direct reaction with ascorbate. Planta, 210(3), 454–467. [PubMed: 10750904]

Popek R, Gawro ska H, Wrochna M, Gawro ski SW, & Sæbø A (2013). Particulate Matter on Foliage of 13 Woody Species: Deposition on Surfaces and Phytostabilisation in Waxes – a 3-Year Study. International Journal of Phytoremediation. 10.1080/15226514.2012.694498

Potier E, Loubet B, Durand B, Flura D, Bourdat-Deschamps M, Ciuraru R, & Ogée J (2017). Chemical reaction rates of ozone in water infusions of wheat, beech, oak and pine leaves of different ages. Atmospheric Environment, 151, 176–187. 10.1016/j.atmosenv.2016.11.069

Potier E, Ogée J, Jouanguy J, Lamaud E, Stella P, Personne E, Durand B, Mascher N, & Loubet B (2015). Multilayer modelling of ozone fluxes on winter wheat reveals large deposition on wet senescing leaves. Agricultural and Forest Meteorology, 211, 58–71. 10.1016/j.agrformet.2015.05.006

Poyatos R, Granda V, Molowny-Horas R, Mencuccini M, Steppe K, & Martínez-Vilalta(2016). SAPFLUXNET: towards a global database of sap flow measurements. Tree Physiology, 36, 1449–1455. 10.1093/treephys/tpw110 [PubMed: 27885171]

Pöschl U, & Shiraiwa M (2015). Multiphase chemistry at the atmosphere-biosphere interface influencing climate and public health in the Anthropocene. Chemical Reviews, 115, 4440–4475. 10.1021/cr500487s [PubMed: 25856774]

Pyles RD, Weare BC, & Paw U KT (2000). The UCD Advanced Canopy-Atmosphere-Soil Algorithm: Comparisons with observations from different climate and vegetation regimes. Quarterly Journal of the Royal Meteorological Society, 126, 2951–2980.

Ran L, Pleim J, Song C, Band L, Walker JT, & Binkowski FS (2017). A photosynthesis-based two-leaf canopy stomatal conductance model for meteorology and air quality modeling with WRF/CMAQ PX LSM. Journal of Geophysical Research: Atmospheres, 122(3), 1930–1952. 10.1002/2016JD025583

Rannik Ü, Altimir N, Mammarella I, Bäck J, Rinne J, Ruuskanen TM, Hari P, Vesala T, & Kulmala M (2012). Ozone deposition into a boreal forest over a decade of observations: Evaluating deposition partitioning and driving variables. Atmospheric Chemistry and Physics, 12. 10.5194/acp-12-12165-2012

Rannik Ü, Mammarella I, Keronen P & Vesala T (2009). Vertical advection and nocturnal deposition of ozone over a boreal pine forest. Atmospheric Chemistry and Physics, 9, 2089–2095.

Raoult NM, Jupp TE, Cox PM, & Luke CM (2016). Land-surface parameter optimisation using data assimilation techniques: the adJULES system V1.0. Geoscientific Model Development, 9(8). 10.5194/gmd-9-2833-2016

Raupach MR (1979). Anomalies in flux-gradient relationships over forest. Boundary-Layer Meteorology, 16(3), 467–486.

Raupach MR (1989). Applying Lagrangian fluid mechanics to infer scalar source distributions from concentration profiles in plant canopies. Agricultural and Forest Meteorology, 47, 85–108.

Raupach MR, & Finnigan JJ (1987). 'Single-layer models of evaporation from plant canopies are incorrect but useful, whereas multilayer models are correct but useless': Discuss. Australian Journal of Plant Physiology, 15, 705–716.

Raupach MR, Finnigan JJ, & Brunet Y (1996). Coherent eddies and turbulence in vegetation canopies: the mixing-layer analogy. Boundary-Layer Meteorology, 78, 351–382.

Ray JD, Stedman DH, & Wendel GJ (1986). Fast chemiluminescent method for measurement of ambient ozone. Analytical Chemistry, 58(3), 598–600.

Regener VH (1957). The vertical flux of atmospheric ozone. Journal of Geophysical Research, 62(2), 221–228. 10.1029/JZ062i002p00221

Reich PB (1987). Quantifying plant response to ozone: a unifying theory. Tree Physiology, 3(1), 63–91. [PubMed: 14975835]

Remde A, Ludwig J, Meixner FX, & Conrad R (1993). A study to explain the emission of nitric oxide from a marsh soil. Journal of Atmospheric Chemistry, 17, 249–275.

Rich S (1964). Ozone Damage to Plants. Annual Review of Phytopathology, 2, 253–266.

Rich S, Waggoner PE, & Tomlinson H (1970). Ozone update by bean leaves. Science, 169(3940), 79–80. 10.1126/science.169.3940.79 [PubMed: 5447535]

Rischbieter E, Stein H, & Schumpe A (2000). Ozone solubilities in water and aqueous salt solutions. Journal of Chemical and Engineering Data, 45(2), 338–340.

Rondón A (1993). Atmosphere-surface exchange of nitrogen oxides and ozone (Doctoral dissertation. Stockholm, Sweden: Stockholm University.

Rondón A, Johansson C, & Granat L (1993). Dry deposition of nitrogen dioxide and ozone to coniferous forests. Journal of Geophysical Research, 98(D3), 5159–5172. 10.1029/92JD02335

Ro-Poulsen H, Mikkelsen TN, Hovamand MF, Hummelsehøj P, & Jensen NO (1998). Ozone deposition in relation to canopy physiology in a mixed conifer forest in Denmark. Chemosphere, 36(4–5), 669–674

Rummel U, Ammann C, Gut A, Meixner FX, & Andreae MO (2002). Eddy covariance measurements of nitric oxide flux within an Amazonian rain forest. Journal of Geophysical Research: Atmospheres, 107(D20). 10.1029/2001JD000520

Rummel U, Ammann C, Kirkman GA, Moura MAL, Foken T, Andreae MO, & Meixner FX (2007). Seasonal variation of ozone deposition to a tropical rain forest in southwest Amazonia. Atmospheric Chemistry and Physics, 7, 5415–5435. 10.5194/acp-7-5415-2007

Rydsaa JH, Stordal F, Gerosa G, Finco A, & Hodnebrog Ø (2016). Evaluating stomatal ozone fluxes in WRF-Chem: Comparing ozone uptake in Mediterranean ecosystems. Atmospheric Environment, 143, 237–248.

Sadiq M, Tai APK, Lombardozzi D, & Val Martin M (2017). Effects of ozone-vegetation coupling on surface ozone air quality via biogeochemical and meteorological feedbacks. Atmospheric Chemistry and Physics, 17, 3055–3066. 10.5194/acp-17-3055-2017

Sander R (1999). Modeling atmospheric chemistry: Interactions between gas-phase species and liquid phase cloud/aerosol particles. Surveys in Geophysics, 20, 2–31.

Sander R (2015). Compilation of Henry's law constants (version 4.0) for water as solvent. Atmospheric Chemistry and Physics, 15, 4399–4981. 10.5194/acp-15-4399-2015

Savi F, & Fares S (2014). Ozone dynamics in a Mediterranean Holm oak forest: comparison among transition periods characterized by different amounts of precipitation. Annals of Silvicultural Research, 38(1), 1–6.

Sæbø A, Popek R, Nawrot B, Hanslin HM, Gawronska H, & Gawronski SW (2012). Plant species differences in particulate matter accumulation on leaf surfaces. Science of the Total Environment. 10.1016/j.scitotenv.2012.03.084

Sánchez ML, Rodríguez R & López A (1997). Ozone Dry Deposition in a Semi-Arid Steppe and in a Coniferous Forest in Southern Europe. Journal of the Air & Waste Management Association, 47(7), 792–799. 10.1080/10473289.1997.10463939

Schobesberger S, Lopez-Hilfiker FD, Taipale D, Millet DB, D'Ambro EL, Rantala P, et al. (2016). High upward fluxes of formic acid from a boreal forest canopy. Geophysical Research Letters, 43(17), 9342–9351. 10.1002/2016GL069599

Schuepp PH (1993). Tansley Review No. 69. Leaf Boundary Layers. New Phytologist, 125(3), 477–507.

Schwede DB, Leduc SK, & Otte TL (2001). Using meteorological model output as a surrogate for on-site observations to predict deposition velocity. Water, Air, and Soil Pollution: Focus, 1, 59–66.

Schwede D, Zhang L, Vet R, & Lear G (2011). An intercomparison of the deposition models used in the CASTNET and CAPMoN networks. Atmospheric Environment, 45, 1337–1346. 10.1016/j.atmosenv.2010.11.050

Seinfeld JH, & Pandis SN (2006). Atmospheric Chemistry and Physics. Hoboken, New Jersey: Wiley.

Seok B, Helmig D, Liptzin D, Williams MW, & Vogel CS (2015). Snowpack-atmosphere gas exchanges of carbon dioxide, ozone, and nitrogen oxides at a hardwood forest site in northern Michigan. Elementa-Science of the Anthropocene, 3, 1–20. 10.12952/journal.elementa.000040

Shen J, &. Gao Z (2018). Ozone removal on building material surface: A literature review. Building and Environment. 10.1016/j.buildenv.2018.02.046

Shu Y, & Atkinson R (1994). Rate constants for the gas-phase reactions of O3 with a series of terpenes and OH radical formation from the O3 reactions with sesquiterpenes at 296±2 K. International Journal of Chemical Kinetics, 26, 1192–1205.

Silva S, & Heald C (2018). Investigating Dry Deposition of Ozone to Vegetation. Journal of Geophysical Research: Atmospheres, 123, 559–573. 10.1002/2017JD027278

Silva SJ, Heald CL, Ravela S, Mammarella I, & Munger JW (2019). A Deep Learning Parameterization for Ozone Dry Deposition Velocities. Geophysical Research Letters, 46(2), 983–989. 10.1029/2018GL081049

Simpson D, Tuovinen JP, Emberson L, & Ashmore MR (2001). Characteristics of an ozone deposition module. Water, Air and Soil Pollution: Focus, 1(5–6), 253–262.

Simpson D, Tuovinen JP, Emberson L, & Ashmore MR (2003). Characteristics of an ozone deposition module II: Sensitivity analysis. Water, Air, and Soil Pollution, 143(1–4), 123–137.

Sitch S, Cox PM, Collins WJ, & Huntingford C (2007). Indirect radiative forcing of climate change through ozone effects on the land-carbon sink. Nature. 10.1038/nature06059

Solberg S, Hov Ø, Søvdee A, Isaksen ISA, Coddevillee P, De Backer H, Forster C, Orsolini Y, & Uhse K (2008). European surface ozone in the extreme summer 2003. Journal of Geophysical Research, 113(D07307). 10.1029/2007JD009098

Sorimachi A, & Sakamoto K (2007) Laboratory Measurement of Dry Deposition of Ozone onto Northern Chinese Soil Samples. In Brimblecombe P, Hara H, Houle D, & Novak M (Eds.), Acid Rain - Deposition to Recovery (pp. 181–186). Dordrecht: Springer. 10.1007/978-1-4020-5885-1_20

Sorimachi A, Sakamoto K, Ishihara H, Fukuyama T, Utiyama M, Liu H, et al. (2003). Measurements of sulfur dioxide and ozone dry deposition over short vegetation in northern China—a preliminary study. Atmospheric Environment, 37(22), 3157–3166.

Sperry JS, Venturas MD, Anderegg WR, Mencuccini M, Mackay DS, Wang Y, & Love DM (2017). Predicting stomatal responses to the environment from the optimization of photosynthetic gain and hydraulic cost. Plant, Cell & Environment, 40(6), 816–830.

Stedman DH, Daby E, Stuhl F, & Niki H (1972). Analysis of ozone and nitric oxide by a chemiluminescent method. Journal of the Air Pollution Control Association, 22, 260–263.

Steiner AL, Pressley SN, Botros A, Jones E, Chung S,H, & Edburg SL (2011). Analysis of coherent structures and atmosphere-canopy coupling strength during the CABINEX field campaign. Atmospheric Chemistry and Physics, 11, 11921–11936. 10.5194/acp-11-11921-2011

Stella P, Loubet B, de Berranger C, Charrier X, Ceschia E, Gerosa G, Finco A, Lamaud E, Serça D, George C, & Ciuraru R (2019). Soil ozone deposition: Dependence of soil resistance to soil texture. Atmospheric Environment, 119, 202–209. 10.1016/j.atmosenv.2018.11.036

Stella P, Loubet B, Lamaud E, Laville P, & Cellier P (2011). Ozone deposition onto bare soil: A new parameterisation. Agricultural and Forest Meteorology, 151, 669–681. 10.1016/j.agrformet.2011.01.015

Stella P, Loubet B, Laville P, Lamaud E, Cazaunau M, Laufs S, et al. (2012). Comparison of methods for the determination of NO-O3-NO2 fluxes and chemical interactions over a bare soil. Atmospheric Measurement Techniques, 5(6), 1241–1257.

Stella P, Personne E, Lamaud E, Loubet B, Trebs I, & Cellier P (2013). Assessment of the total, stomatal, cuticular, and soil 2 year ozone budgets of an agricultural field with winter wheat and maize crops. Journal of Geophysical Research: Biogeosciences, 118(3), 1120–1132. 10.1002/jgrg.20094

Stella P, Personne E, Loubet B, Lamaud E, Ceschia E, Béziat P, et al. (2011). Predicting and partitioning ozone fluxes to maize crops from sowing to harvest: the Surfatm-O3 model. Biogeosciences, 8, 2869–2886. 10.5194/bg-8-2869-2011

Stevenson DS, Dentener FJ, Schultz MG, Ellingsen K, van Noije TPC, Wild O, et al. (2006). Multimodel ensemble simulations of present-day and near-future tropospheric ozone. Journal of Geophysical Research, 111(D08301). 10.1029/2005JD006338

Stocker DW, Stedman DH, Zeller KF, Massman WJ, & Fox DG (1993). Fluxes of nitrogen oxides and ozone measured by eddy correlation over a shortgrass prairie. Journal of Geophysical Research: Atmospheres, 98(D7), 12619–12630. 10.1029/93JD00871

Stocker DW, Zeller KF, & Stedman DH (1995). O3 and NO2 fluxes over snow measured by eddy-correlation. Atmospheric Environment, 29, 1299–1305.

Stokes VJ, Morecroft MD, & Morison JIL (2006). Boundary layer conductance for contrasting leaf shapes in a deciduous broadleaved forest canopy. Agricultural and Forest Meteorology, 139, 40–54.

Stoy PC, El-Madany T, Fisher JB, Gentine P, Gerken T, Good SP, et al. (2019). Reviews and syntheses: Turning the challenges of partitioning ecosystem evaporation and transpiration into opportunities. Biogeosciences, 16, 3747–3775. 10.5194/bg-16-3747-2019

Stroud C, Makar P, Karl T, Guenther A, Geron C, Turnipseed A, et al. (2005). Role of canopy-scale photochemistry in modifying biogenic-atmosphere exchange of reactive terpene species: Results from the CELTIC field study. Journal of Geophysical Research, 110(D17303). 10.1029/2005JD005775

Stull RB (1988). An Introduction to Boundary Layer Meteorology. Springer.

Subke J-A, Toet S, D'Haese D, Crossman Z, Emberson LD, Barnes JD, Ashmore MR, Evershed RP, & Ineson P (2009). A new method using 18O to trace ozone deposition. Rapid Communications in Mass Spectrometry, 23, 980–984. 10.1002/rcm.3961 [PubMed: 19241413]

Sun G, McLaughlin SB, Porter JH, Uddling J, Mulholland PJ, Adams MB, & Pederson N (2012). Interactive influences of ozone and climate on streamflow of forested watersheds. Global Change Biology, 18, 3395–3409. 10.1111/j.1365-2486.2012.02787.x

Sun S, Moravek A, Trebs I, Kesselmeier J, & Sörgel M (2016). Investigation of the influence of liquid surface films on O3 and PAN deposition to plant leaves coated with organic/inorganic solution. Journal of Geophysical Research: Atmospheres, 121(23). 10.1002/2016JD025519

Sun S, Moravek A, von der Heyden L, Held A, Sörgel M, & Kesselmeier J (2016). Twin-cuvette measurement technique for investigation of dry deposition of O3 and PAN to plant leaves under controlled humidity conditions. Atmospheric Measurement Techniques, 9, 599–617. 10.5194/amt-9-599-2016

Super I, Vilá-Guerau de Arellano J, & Krol MC (2016). Cumulative ozone effect on canopy stomatal resistance and thee impact on boundary layer dynamics and CO2 assimilation at the diurnal scale: A case study for grassland in the Netherlands. Journal of Geophysical Research: Biogeosciences, 120, 1348–1365. 10.1002/2015JG002996

Tang W, Cohan DS, Morris GA, Byun DW, & Luke WT (2011). Influence of vertical mixing uncertainties on ozone simulation in CMAQ. Atmospheric Environment, 45, 2898–2909. 10.1016/j.atmosenv.2011.01.057

Tao F, Feng Z, Tang H, Chen Y, & Kobayashi K (2017). Effects of climate change, CO2 and O3 on wheat productivity in Eastern China, singly and in combination. Atmospheric Environment, 153, 182–193.

Thom AS (1975). Momentum, mass, and heat exchange of plant communities. In Monteith JL (Ed.), Vegetation and the Atmosphere (pp. 57–109). London: Academic Press.

Thomas C, & Foken T (2007). Flux contribution of coherent structures and its implications for the exchange of energy and matter in a tall spruce canopy. Boundary-Layer Meteorology, 123(2), 317–337.

Thomas JL, Stutz J, Lefer B, Huey LG, Toyota K, Dibb JE, & von Glasow R (2011). Modeling chemistry in and above snow at Summit, Greenland - Part 1: Model description and results. Atmospheric Chemistry and Physics, 11, 4899–4914. 10.5194/acp-11-4899-2011

Toet S, Subke J-A, D'Haese D, Ashmore MR, Emberson LD, Crossman Z, Evershed RP, Barnes JD, & Ineson P (2009). A new stable isotope approach identifies the fate of ozone in plant-soil systems. New Phytologist, 182, 85–90.

Tong L, Wang X, Geng C, Wang W, Lu F, Song W, et al. (2011). Diurnal and phenological variations of O3 and CO2 fluxes of rice canopy exposed to different O3 concentrations. Atmospheric Environment, 45(31), 5621–5631.

Torsethaugen G, Pell E, & Assmann S (1999). Ozone inhibits guard cell K+ channels implicated in stomatal opening. Proceedings of the National Academy of Sciences, 96, 13577–13582.

Toyota K, Dastoor AP, & Ryzhkov A (2016). Parameterization of gaseous dry deposition in atmospheric chemistry models: Sensitivity to aerodynamic resistance formulations under statically stable conditions. Atmospheric Environment, 147, 409–422. 10.1016/j.atmosenv.2016.09.055

Travis KR, & Jacob DJ (2019). Systematic bias in evaluating chemical transport models with maximum daily 8 h average (MDA8) surface ozone for air quality applications: a case study with GEOS-Chem v9.02. Geoscientific Model Development, 12, 3641–3648. 10.5194/gmd-12-3641-2019

Tuovinen J-P, Ashmore MR, Emberson LD, & Simpson D (2004). Testing and improving the EMEP ozone deposition module. Atmospheric Environment, 38(15), 2373–2385.

Tuovinen J-P, Aurela M, & Laurila T (1998). Resistances to ozone deposition to a flark fen in the northern aapa mire zone. Journal of Geophysical Research: Atmospheres, 103(D14), 16953–16966. 10.1029/98JD01165

Tuovinen J-P, Emberson L, & Simpson D (2009). Modelling ozone fluxes to forests for risk assessment: status and prospects. Annals of Forest Science, 66.

Tuovinen J-P, Simpson D, Mikkelsen TN, Emberson LD, Ashmore MR, Aurela M, et al. (2001). Comparisons of measured and modelled ozone deposition to forests in Northern Europe. Water, Air, and Soil Pollution: Focus, 1(5–6), 263–274.

Turner NC, Rich S, & Waggoner PE (1973). Removal of ozone by soil. Journal of Environmental Quality, 2(2), 259–263.

Turner NC, Waggoner PE, & Rich S (1974). Removal of ozone from the atmosphere by soil and vegetation. Nature, 250, 486–489.

Turnipseed AA, Burns SP, Moore DJ, Hu J, Guenther AB, & Monson RK (2009). Controls over ozone deposition to a high elevation subalpine forest. Agricultural and Forest Meteorology, 149(9), 1447–1459. 10.1016/j.agrformet.2009.04.001

Turnipseed AA, Huey LG, Nemitz E, Stickel R, Higgs J, Tanner DJ, Slusher DL, Sparks JP, Flocke F, & Guenther A (2006). Eddy covariance fluxes of peroxyacetyl nitrates (PANs) and NOy to a coniferous forest. Journal of Geophysical Research: Atmospheres, 111(D9). 10.1029/2005JD006631

Tuzet A, Perrier A, Loubet B, & Cellier P (2011). Modeling ozone deposition fluxes: The relative roles of deposition and detoxification processes. Agricultural and Forest Meteorology, 151, 480–492. 10.1016/j.agrformet.2010.12.004

U.S. Environmental Protection Agency (EPA). (2006). Air Quality Criteria for Ozone and Related Photochemical Oxidants, Vol. 1.

Uddling J, Matyssek R, Pettersson JBC, & Wieser G (2012). To what extent do molecular collisions arising from water vapour efflux impede stomatal O3 influx? Environmental Pollution, 170, 39–42. [PubMed: 22763329]

Unsworth M, Heagle A, & Heck W (1984). Gas exchange in open-top field chambers – I. Measurement and analysis of atmospheric resistances to gas exchange. Atmospheric Environment, 18, 373–380.

Val Martin M, Heald CL, & Arnold SR (2014). Coupling dry deposition to vegetation phenology in the Community Earth System Model: Implications for the simulation of surface O3. Geophysical Research Letters, 41, 2988–2996. 10.1002/2014GL059651

Van Aalst RM (1982). Air Pollution by Nitrogen Oxides Dry Deposition of NOx. Studies in Environmental Science. 10.1016/B978-0-444-42127-2.50028-2

Van Dam B, Helmig D, Doskey PV, & Oltmans SJ (2016). Summertime surface O3 behavior and deposition to tundra in the Alaskan Arctic. Journal of Geophysical Research: Atmospheres, 121(13), 8055–8066. 10.1002/2015JD023914

Van Dam B, Helmig D, Honrath R, Hueber J, Seok B, Toro C, Kramer L, Ganzeveld L, & Neff W (2010). Exchange of ozone at the atmosphere-snowpack interface at Summit, Greenland. 2010 State of the Arctic Meeting, 16–19 March, Miami, Florida, Poster Presentation.

Van Dam B, Helmig D, Toro C, Doskey P, Kramer L, Murray K, Ganzeveld L, & Seok B (2015). Dynamics of ozone and nitrogen oxides at Summit, Greenland: I. Multi-year observations in the snowpack. Atmospheric Environment, 123, 268–284. 10.1016/j.atmosenv.2015.09.060

Van Pul WAJ, & Jacobs AFG (1994). The conductance of a maize crop and the underlying soil to ozone under various environmental conditions. Boundary-Layer Meteorology, 69(1–2), 83–99.

Vautard R, Honore C, Beekmann M, & Rouil L (2005). Simulation of ozone during the August 2003 heat wave and emission control scenarios. Atmospheric Environment, 39(16), 2957–2967.

Verhoef A, & Egea G (2014). Modeling plant transpiration under limited soil water: Comparison of different plant and soil hydraulic parameterizations and preliminary implications for their use in land surface models. Agricultural and Forest Meteorology, 191, 22–32. 10.1016/j.agrformet.2014.02.009

Vieno M, Dore AJ, Stevenson DS, Doherty R, Heal MR, Reis S, et al. (2010). Modelling surface ozone during the 2003 heat-wave in the UK. Atmospheric Chemistry and Physics, 10(16), 7963–7978.

Vilá-Guerau de Arellano J (2003). Bridging the gap between atmospheric physics and chemistry in studies of small-scale turbulence. Bulletin of the American Meteorological Society, 51–56.

Vilá-Guerau de Arellano J, & Duynkerke PG (1992). Influence of chemistry on the flux-gradient relationships for the NO2-O3-NO system. Boundary-Layer Meteorology, 61, 375–387.

Vilá-Guerau de Arellano J, Duynkerke PG, & Builtjes PJH (1993) The divergence of the turbulent diffusion flux in the surface layer due to chemical reactions: the NO-O3-NO2 system. Tellus B: Chemical and Physical Meteorology, 45(1), 23–33. 10.3402/tellusb.v45i1.15576

Vitale M, Gerosa G, Ballarin-Denti A, & Manes F (2005). Ozone uptake by an evergreen mediterranean forest (Quercus ilex L.) in Italy—Part II: flux modelling. Upscaling leaf to canopy ozone uptake by a process-based model. Atmospheric Environment, 39(18), 3267–3278.

Vuolo RM, Loubet B, Mascher N, Gueudet JC, Durand B, Laville, et al. (2017). Nitrogen oxides and ozone fluxes from an oilseed-rape management cycle: The influence of cattle slurry application. Biogeosciences, 14, 2225–2244. 10.5194/bg-14-2225-2017

Walker TW (2014). Applications of adjoint modelling in chemical composition: Studies of tropospheric ozone at middle and high northern latitudes (Doctoral dissertation). Retrieved from University of Toronto. (https://tspace.library.utoronto.ca). Toronto, Canada: University of Toronto.

Walton S, Gallagher MW, Choularton TW, & Duyzer J (1997). Ozone and NO2 exchange to fruit orchards. Atmospheric Environment, 31(17), 2767–2776.

Walton S, Gallagher MW, & Duyzer JH (1997). Use of a detailed model to study the exchange of NOx and O3 above and below a deciduous canopy. Atmospheric Environment, 31(18), 2915–2931.

Wang D, Hinckley TM, Cumming AB, & Braatne J (1995). A comparison of measured and modeled ozone uptake into plant leaves. Environmental Pollution, 89(3), 347–254.

Warrick AW, & Nielsen DR (1980). Spatial Variability of Soil Physical Properties in the Field. In: Hillel D (Ed.), Applications of Soil Physics (pp. 319–344). New York: Academic Press.

Wehr R, Commane R, Munger JW, McManus JB, Nelson DD, Zahniser MS, Saleska SR, & Wofsy SC (2017). Dynamics of canopy stomatal conductance, transpiration, and evaporation in a temperate deciduous forest, validated by carbonyl sulfide uptake. Biogeosciences, 14, 389–401. 10.5194/bg-14-389-2017

Wehr R, Munger JW, McManus JB, Nelson DD, Zahniser MS, Davidson EA, Wofsy SC, & Saleska SR (2016). Seasonality of temperate forest photosynthesis and daytime respiration. Nature, 534, 680–683. [PubMed: 27357794]

Wehr R, & Saleska SR (2015). An improved isotopic method for partitioning net ecosystem-atmosphere CO2 exchange. Agricultural and Forest Meteorology, 214–215, 515–531. 10.1016/j.agrformet.2015.09.009

Weinheimer AJ (2006). Chemical methods: chemiluminescence, chemical amplification, electrochemistry, and derivatization. In Heard DE (Ed.), Analytical Techniques for Atmospheric Measurement (pp. 311–354). Oxford, UK: Blackwell Publishing Ltd.

Wesely ML (1989). Parameterization of surface resistances to gaseous dry deposition in regional-scale numerical models. Atmospheric Environment, 23(6), 1293–1304.

Wesely ML, Cook DR, & Williams RM (1981). Field measurements of small ozone fluxes to snow, wet bare soil, and lake water. Boundary-Layer Meteorology, 20, 459–471.

Wesely ML, Eastman JA, Cook DR, & Hicks BB (1978). Daytime variations of ozone eddy fluxes to maize. Boundary-Layer Meteorology, 15, 361–373. 10.1007/bf02652608

Wesely ML, & Hicks BB (1977). Some factors that affect the deposition rates of sulfur dioxide and similar gases on vegetation. Journal of the Air Pollution Control Association, 27(11), 1110–1116.

Wesely ML, & Hicks BB (2000). A review of the current status of knowledge on dry deposition. Atmospheric Environment, 34, 2261–2282.

Whelan ME, Lennartz ST, Gimeno TE, Wehr R, Wohlfahrt G, Wang Y, et al. (2018). Reviews and syntheses: Carbonyl sulfide as a multi-scale tracer for carbon and water cycles. Biogeosciences, 15(12), 3625–3657. 10.5194/bg-15-3625-2018

Wieser G, Luis VC, & Cuevas E (2006). Quantification of ozone uptake at the stand level in a Pinus canariensis forest in Tenerife, Canary Islands: An approach based on sap flow measurements. Environmental Pollution, 140, 383–386. 10.1016/j.envpol.2005.12.003 [PubMed: 16457921]

Wieser G, Matyssek R, Götz B, & Grünhage L (2012). Branch cuvettes as means of ozone risk assessment in adult forest tree crowns: combining experimental and modelling capacities. Trees, 26(6), 1703–1712.

Wieser G, Matyssek R, Köstner B, & Oberhuber W (2003). Quantifying ozone uptake at the canopy level of spruce, pine and larch trees at the alpine timberline: an approach based on sap flow measurement. Environmental Pollution, 126, 5–8. [PubMed: 12860097]

Wild O (2007). Modelling the tropospheric ozone budget: exploring the variability in current models. Atmospheric Chemistry and Physics, 7, 2643–2660.

Wilson KB, & Baldocchi DD (2000). Seasonal and interannual variability of energy fluxes over a broadleaved temperate deciduous forest in North America. Agricultural and Forest Meteorology, 100, 1–18.

Wofsy S, Goulden M, Munger JW, Fan S, Bakwin P, Daube B, Bassow S, & Bazzaz F (1993). Net exchange of CO2 in a mid-latitude forest. Science, 260, 1314–1317. [PubMed: 17755426]

Wohlfahrt G, Haslwanter A, Hörtnagl L, Jasoni RL, Fenstermaker LF, Arnone III JA, & Hammerle A (2009). On the consequences of the energy imbalance for calculating surface conductance to water vapor. Agricultural and Forest Meteorology, 149, 1556–1559. 10.1016/j.agrformet.2009.03.015 [PubMed: 24465070]

Wohlfahrt G, Hörtnagl L, Hammerle A, Graus M, & Hansel A (2009). Measuring eddy covariance fluxes of ozone with a slow-response analyser. Atmospheric Environment, 43, 4570–4576. 10.1016/j.atmosenv.2009.06.031

Wolf A, Anderegg WR, & Pacala SW (2016). Optimal stomatal behavior with competition for water and risk of hydraulic impairment. Proceedings of the National Academy of Sciences, 113(46), E7222–E7230.

Wolfe GM, Hanisco TF, Arkinson HL, Bui TP, Crounse JD, Dean-Day J, et al. (2015). Quantifying sources and sinks of reactive gases in the lower atmosphere using airborne flux observations. Geophysical Research Letters, 42. 10.1002/2015GL065839

Wolfe GM, & Thornton JA (2011). The Chemistry of Atmosphere-Forest Exchange (CAFE) Model - Part 1: Model description and characterization. Atmospheric Chemistry and Physics, 11, 77–101.

Wolfe GM, Thornton JA, McKay M, & Goldstein AH (2011). Forest-atmosphere exchange of ozone: sensitivity to very reactive biogenic VOC emissions and implications for in-canopy photochemistry. Atmospheric Chemistry and Physics, 11(15), 7875–7891. 10.5194/acp-11-7875-2011

Wolfe GM, Thornton JA, Yatavelli RLN, McKay M, Goldstein AH, LaFranchi B, et al. (2009). Eddy covariance fluxes of acyl peroxy nitrates (PAN, PPN and MPAN) above a Ponderosa pine forest. Atmospheric Chemistry and Physics, 9(2), 615–634.

Wong SC, Cowan IR, & Farquhar GD (1979). Stomatal conductance correlates with photosynthetic capacity. Nature, 282, 424–426.

Wong AYH, Geddes JA, Tai APK, & Silva SJ (2019). Importance of dry deposition parameterization choice in global simulations of surface ozone. Atmospheric Chemistry and Physics, 19, 14365–14385. 10.5194/acp-19-14365-2019

Wu Y, Brashers B, Finkelstein PL, & Pleim JE (2003). A multilayer biochemical dry deposition model 2. Model evaluation. Journal of Geophysical Research: Atmospheres, 108(D1). 10.1029/2002JD002306

Wu ZY, Zhang L, Wang XM, & Munger JW (2015). A modified micrometeorological gradient method for estimating O3 dry depositions over a forest canopy. Atmospheric Chemistry and Physics. 10.5194/acp-15-7487-2015

Wu Z, Schwede DB, Vet R, Walker JT, Shaw M, Staebler R, & Zhang L (2018). Evaluation and intercomparison of five North American dry deposition algorithms at a mixed forest site. Journal of Advances in Modeling Earth Systems. 10.1029/2017MS001231

Wu Z, Staebler R, Vet R & Zhang L (2016). Dry deposition of O3 and SO2 estimated from gradient measurements above a temperate mixed forest. Environmental Pollution, 210, 202–210. 10.1016/j.envpol.2015.11.052 [PubMed: 26735165]

Wu Z, Wang X, Chen F, Turnipseed AA, Guenther AB, Niyogi D, et al. (2011). Evaluating the calculated dry deposition velocities of reactive nitrogen oxides and ozone from two community models over a temperate deciduous forest. Atmospheric Environment, 45(16), 2663–2674.

Xu X, Zhang Z, Bao L, Mo L, Yu X, Fan D, & Lun X (2017). Influence of rainfall duration and intensity on particulate matter removal from plant leaves. Science of the Total Environment, 609, 11–16.

Yeats TH, & Rose JK (2013). The formation and function of plant cuticles. Plant Physiology, 163(1), 5–20. [PubMed: 23893170]

Yee LD, Isaacman-VanWertz G, Wernis RA, Meng M, Rivera V, Kreisberg NM, et al. (2018). Observations of sesquiterpenes and their oxidation products in central Amazonia during the wet and dry seasons. Atmospheric Chemistry and Physics, 18. 10.5194/acp-18-10433-2018

Young PJ, Archibald AT, Bowman KW, Lamarque J-F, Naik V, Stevenson DS, et al. (2013). Pre-industrial to end 21st century projections of tropospheric ozone from the Atmospheric Chemistry and Climate Model Intercomparison Project (ACCMIP). Atmospheric Chemistry and Physics, 13, 2063–2090. 10.5194/acp-13-2063-2013

Young PJ, Naik V, Fiore AM, Gaudel A, Guo J, Lin ML, et al. (2018). Tropospheric Ozone Assessment Report: Assessment of global-scale model performance for global and regional ozone distributions, variability, and trends. Elementa: Science of the Anthropocene, 6(10). 10.1525/elementa.265

Yue X & Unger N (2014). Ozone vegetation damage effects on gross primary productivity in the United States. Atmospheric Chemistry and Physics, 14, 9137–9153. 10.5194/acp-14-9137-2014

Zahn A, Weppner J, Widmann H, Schlote-Holubek K, Burger B, Kuehner T, & Franke H (2012). A fast and precise chemiluminescence ozone detector for eddy flux and airborne application. Atmospheric Measurement Techniques, 5(2), 363–375.

Zapletal M, Cudlín P, Chroust P, Urban O, Pokorný R, Edwards-Jonášová M, et al. (2011). Ozone flux over a Norway spruce forest and correlation with net ecosystem production. Environmental Pollution, 159(5), 1024–1034. [PubMed: 21177010]

Zeller K (2000). Wintertime ozone fluxes and profiles above a subalpine spruce–fir forest. Journal of Applied Meteorology, 39(1), 92–101.

Zeller K, & Hehn T (1995). Ozone deposition in a snow-covered subalpine spruce-fir forest environment. In Biogeochemistry of Seasonally Snow-Covered Catchments (International Association of Hydrological Sciences Publication No. 228). Boulder, CO.

Zeller K, & Hehn T (1996). Measurements of upward turbulent ozone fluxes above a subalpine spruce-fir forest. Geophysical Research Letters, 23, 841–844. 10.1029/96GL00786

Zeller KF, & Nikolov NT (2000). Quantifying simultaneous fluxes of ozone, carbon dioxide and water vapor above a subalpine forest ecosystem. Environmental Pollution, 107, 1–20. [PubMed: 15093004]

Zenone T, Hendriks C, Brilli F, Fransen E, Gioli B, Portillo-Estrada M, et al. (2016). Interaction between isoprene and ozone fluxes in a poplar plantation and its impact on air quality at the European level. Scientific Reports, 6, 32676. [PubMed: 27615148]

Zhang L, Brook JR, & Vet R (2002). On ozone dry deposition – with emphasis on non-stomatal uptake and wet canopies. Atmospheric Environment, 36, 4787–4799.

Zhang L, Brook JR, & Vet R (2003). A revised parameterization for gaseous dry deposition in air-quality models. Atmospheric Chemistry and Physics, 3, 2067–2082. 10.5194/acpd-3-1777-2003

Zhang L, Brook JR, Vet R, Shaw M, & Finkelstein PL (2001). Evaluation and improvement of a dry deposition model using SO2 and O3 measurements over a mixed forest. Water, Air, and Soil Pollution: Focus, 1, 67–78.

Zhang L, Vet R, Brook JR, & Legge A,H (2006). Factors affecting stomatal uptake of ozone by different canopies and a comparison between dose and exposure. Science of the Total Environment, 370, 117–132.

Zhang L, Zhang Z, Chen L, & McNulty S (2019). An investigation on the leaf accumulation-removal efficiency of atmospheric particulate matter for five urban plant species under different rainfall regimes. Atmospheric Environment. 10.1016/j.atmosenv.2019.04.010

Zhang S, Chen X, Hara H, HORIE K, AOKI M, MATSUDA K, et al. (2005). Diurnal and Seasonal Variations of the O3 Dry Deposition Velocity on a Red Pine Forest and its Relationship with Microclimate Factors. Journal of Agricultural Meteorology, 60(5), 1053–1056.

Zhou PT, Ganzeveld L, Rannik Ü, Zhou LX, Gierens R, Taipale D, Mammarella I, & Boy M (2017). Simulating ozone dry deposition at a boreal forest with a multi-layer canopy deposition model. Atmospheric Chemistry and Physics, 17, 1361–1379. 10.5194/acp-17-1361-2017

Zhou S, Duursma RA, Medlyn BE, Kelly JW, & Prentice IC (2013). How should we model plant responses to drought? An analysis of stomatal and non-stomatal responses to water stress. Agricultural and Forest Meteorology, 182, 204–214. 10.1016/j.agrformet.2013.05.009

Zhou SS, Tai AP, Sun S, Sadiq M, Heald CL, & Geddes JA (2018). Coupling between surface ozone and leaf area index in a chemical transport model: strength of feedback and implications for ozone air quality and vegetation health. Atmospheric Chemistry and Physics, 18(19), 14133–14148.

Zhu Z (2019). Effects of Environmental Factors on Ozone Flux over a Wheat Field Modeled with an Artificial Neural Network. Advances in Meteorology. 10.1155/2019/1257910

Zhu Z, Sun X, Dong Y, Zhao F, & Meixner FX (2014). Diurnal variation of ozone flux over corn field in Northwestern Shandong Plain of China. Science China Earth Sciences, 57(3), 503–511.

Zhu Z, Zhao F, Voss L, Xu L, Sun X, Yu G, & Meixner FX (2015). The effects of different calibration and frequency response correction methods on eddy covariance ozone flux measured with a dry chemiluminescence analyzer. Agricultural and Forest Meteorology, 213, 114–125.

Zona D, Gioli B, Fares S, De Groote T, Pilegaard K, Ibrom A, & Ceulemans R (2014). Environmental controls on ozone fluxes in a poplar plantation in Western Europe. Environmental Pollution, 184, 201–210. [PubMed: 24060739]

Key Points

- Ozone dry deposition occurring through pathways other than plant stomata is critical for describing the total terrestrial ozone sink

- Process-level knowledge of ozone deposition pathways is missing from the models used to quantify deposition impacts on the earth system

- Long-term ozone flux and related measurements are key for establishing relative importance of individual pathways
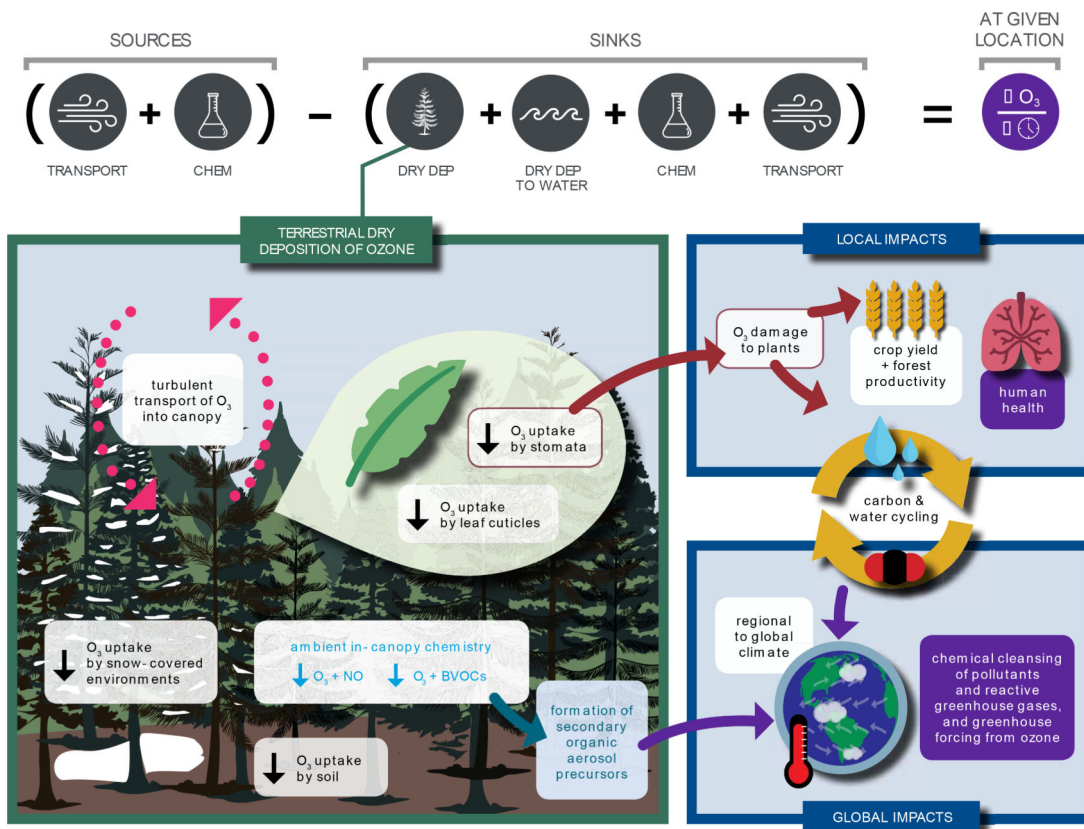
Figure 1.
Processes contributing and related to terrestrial ozone dry deposition and its impacts on tropospheric chemistry, air pollution, ecosystems, and climate, both directly (red and blue arrows) and indirectly (purple boxes and arrows) through changes in tropospheric ozone. Yellow arrows indicate that carbon and water cycling connect the local impact of ozone plant damage to global impacts on climate. Processes included on the left-hand panel in white boxes are reviewed in this paper; downward black arrows represent ozone deposition pathways. Figure illustrated by Simmi Sinha.
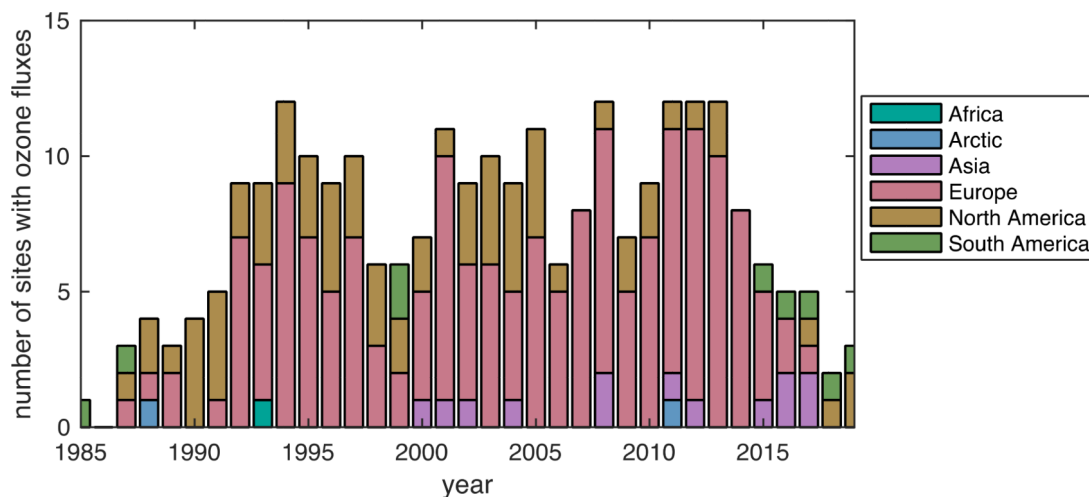
Figure 2.
No growth in the number of sites that measure ozone fluxes since the mid-1990s as shown by the number of sites per year with ozone flux measurements from 1985 to 2019. Table A1 contains the full list of ozone flux datasets and relevant details. In brief, included datasets are for terrestrial surfaces and represent the ecosystem scale (both flux gradient and eddy covariance fluxes). Not all datasets reported are in the peer-reviewed literature, some are included following personal communication. Most sites included do not have a full year of data for a given year (e.g., 57 out of 114 sites have two months of data or less). Very low numbers after 2014 may reflect the time needed to report and analyze data.
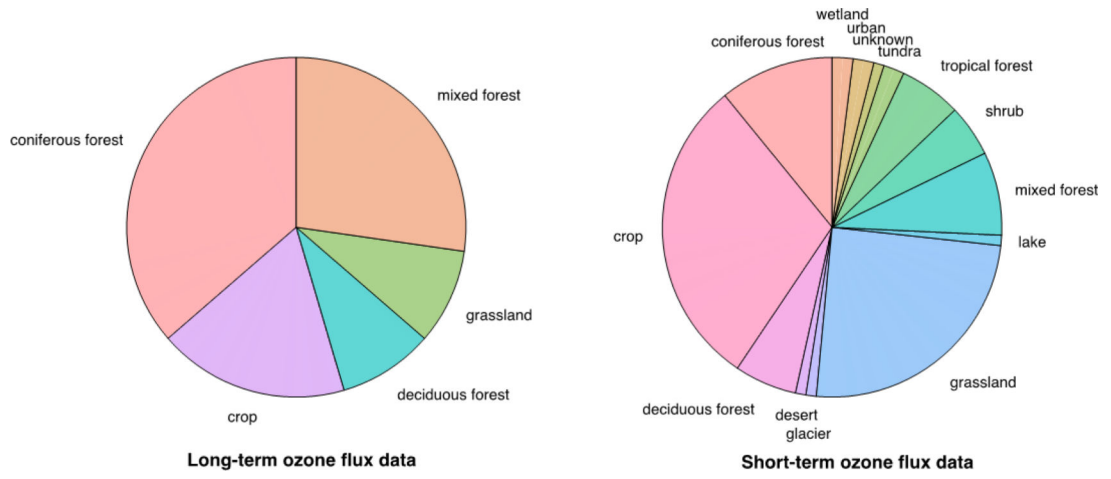
Figure 3.
Land use/land cover types represented in ozone flux datasets. Long-term data is defined as more than five years of annual records. Table A1 contains the full list of datasets.
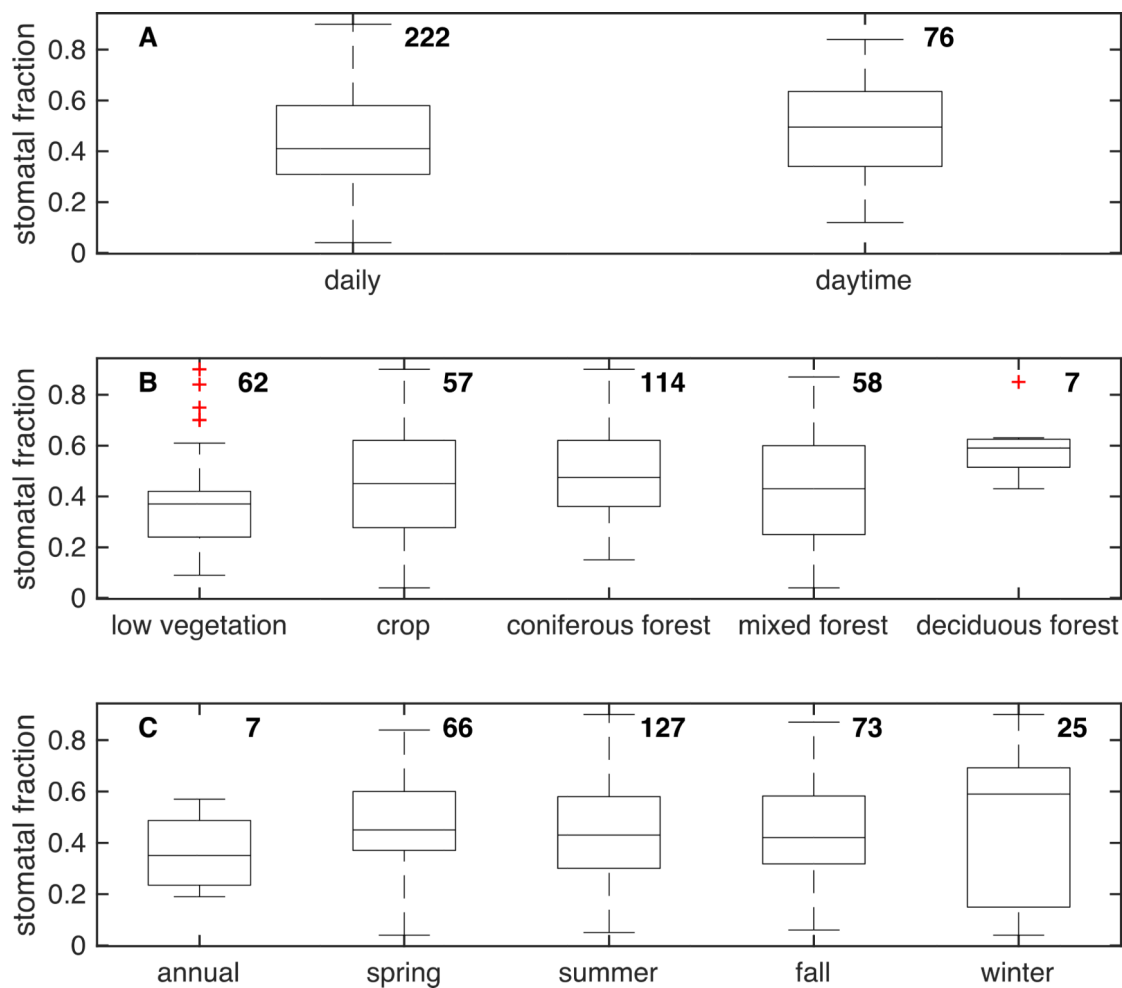
Figure 4.

The stomatal fraction of ozone dry deposition aggregated from estimates from field sites in previous literature. The number of data points in each composite is to the right of the respective box and whiskers plot. Not all datasets reporting spring, summer, fall, or winter stomatal fraction estimates provide an annual estimate, and thus the annual estimate is lower than the estimate for each season. The bottom of the box is the 25th percentile of the data, middle is the median, and the top is the 75th percentile. The error bars indicate maximum and minimum values not considering outliers (red symbols). Outliers are defined as values >1.5x the interquartile range of the 25th to 75th percentiles. Sites and references included are Auchencorth Moss (Fowler et al., 2001), Bergamo (Gerosa et al., 2003), Bily Kriz (Jurá̆ et al., 2019; Zapletal et al., 2011), Blodgett Forest (Ducker et al., 2018; Fares, McKay, Holzinger, et al., 2010; Goldstein, 2003; Kurpius & Goldstein, 2003), Bondville (Zhang, L., et al., 2006), Braunscheig (Mészáros, Horváth, Weidinger, et al., 2009), Bugacpuszta (Horváth et al., 2017), Burriana (Cieslik, 2004), Cadenazzo (Bassin et al., 2004), Cala Violina (Cieslik, 2009), Camp Borden (Fuentes et al., 1992), Castelporziano (Cieslik, 2004, 2009; Gerosa et al., 2005; Gerosa, Finco, Mereu, et al., 2009a,b; Fares et al., 2014; Hoshika et al., 2017; Savi & Fares, 2014), California Ozone Deposition Experiment (CODE) cotton (Grantz et al., 1997), CODE vineyard (Grantz et al., 1995), Comun Nuovo (Bassin et al.,

2004; Cieslik, 2009), Cuatro Vientos (Cieslik, 2004), Diepoholz (El-Madany et al., 2017), Flanders (Neirynck et al., 2012), Gilchriston Farm (Coyle et al., 2009), GLEES Brooklyn Lake (Zeller & Nikolov, 2000), Grignon (Stella, Personne, Lamaud, et al., 2011; Stella et al., 2013), Hartheim (Joss & Graber, 1996), Harvard Forest (Clifton et al., 2017; Ducker et al., 2018), Hyytiälä (Altimir et al., 2006; Ducker et al., 2018; Launiainen et al., 2013; Rannik et al., 2012; Zhou, P. T., et al., 2017), Ispra (Cieslik, 2004), Kaamanen (Tuovinen et al., 1998), Kane Experimental Forest (Zhang, L., et al., 2006), Klippeneck (Cieslik, 2004), Kranzberger Forst (Nunn et al., 2010), La Cape Sud (Stella, Personne, Lamaud, et al., 2011), Le Dézert (Cieslik, 2004), Les Landes (Lamaud et al., 2002), Lincove (Fares et al., 2012), Lochristi (Zona et al., 2014), Central Plains Experimental Range (Massman et al., 1993), Nashville (Zhang, L., et al., 2006), Niwot Ridge (Turnipseed et al., 2009), Polder Piloto de Sarazola (Pio et al., 2000), Ramat Hanadiv Nature Park (Li, Q., et al., 2018), Rhineland-Palatinate (Plake, Stella, Moravek, et al., 2015), Rivox (Coe et al., 1995), S. Pietro Capofiume (Cieslik, 2004, 2009), San Rossore (Hoshika et al., 2017), Sand Flats State Forest (Zhang, L., et al., 2006), Sand Mountain (Zhang, L., et al., 2006), Sinderhoeve (Van Pul & Jacobs, 1994), Speulderbos (Dorsey et al., 2004), Ulborg (Mikkelsen et al., 2004), UMBS Prophet (Hogg, 2007; Hogg et al., 2007), Viols-en-Laval (Cieslik, 2004), and Voghera (Cieslik, 2004, 2009; Gerosa et al., 2007).
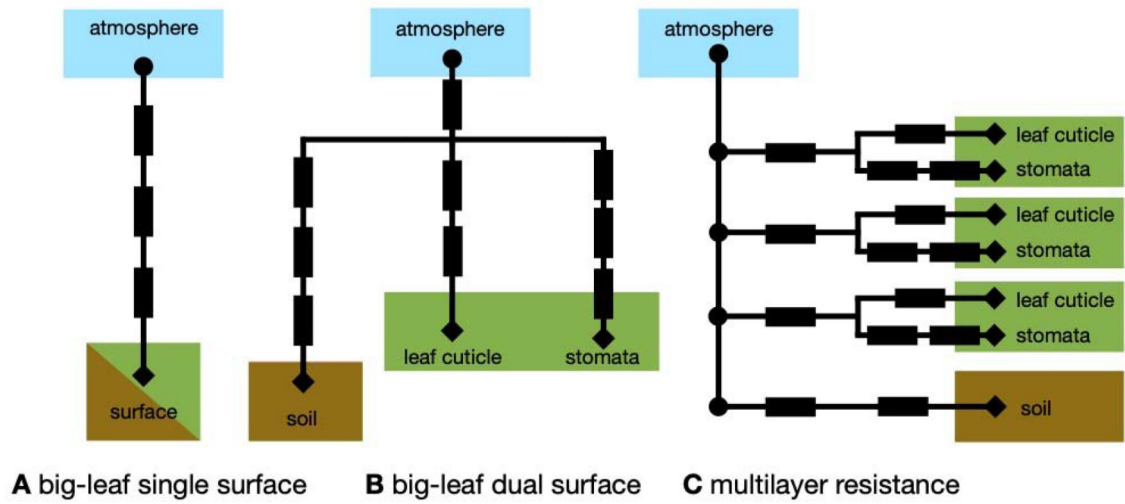
Figure 5.
Resistance networks for modeling ozone dry deposition. Circles and diamonds show where ozone concentration is needed as input for a given network. For the diamonds, the ozone concentration is typically assumed to be zero. Rectangles indicate resistances.
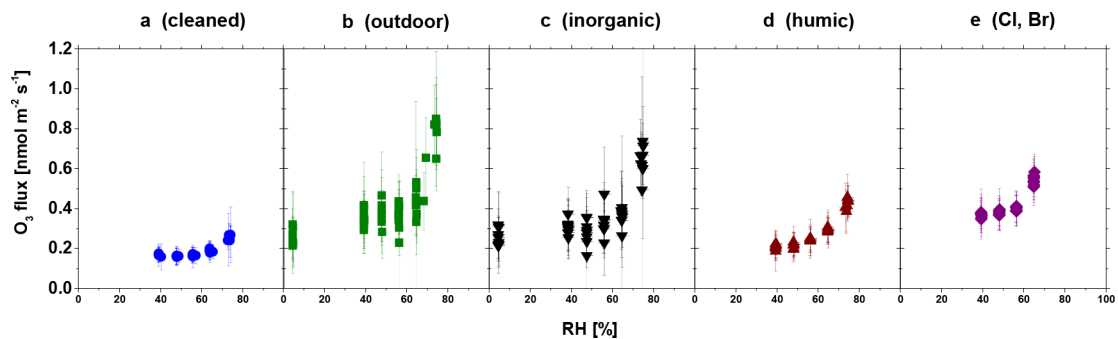
Figure 6.
Differences in cuticular ozone flux to Quercus ilex leaves treated with various compounds (see panel labels) and abscisic acid to induce stomatal closure in the laboratory. Cuticular ozone fluxes are a function of relative humidity (RH). Error bars represent the random error calculated according to Sun, S., Moravek, von der Heyden, et al. (2016). Figure is adapted from Figure 6 of Sun, S., Moravek, Trebs, et al. (2016) with permission. © 2016. American Geophysical Union. All Rights Reserved.
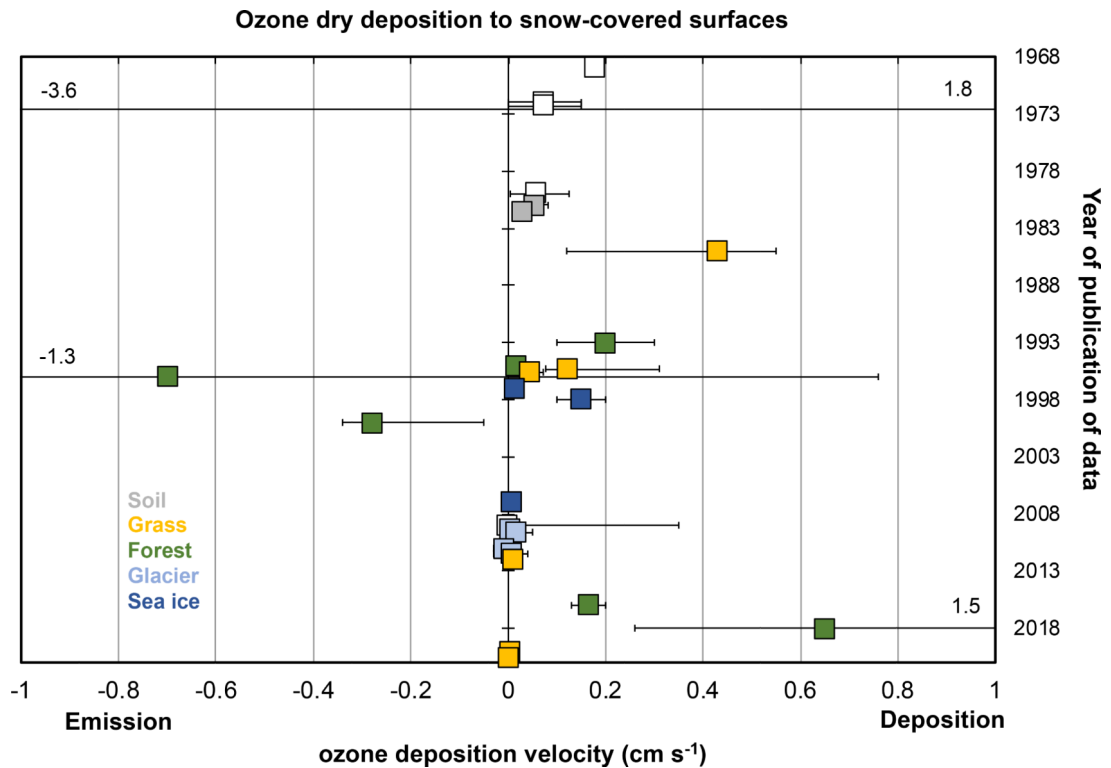
Figure 7.

Range of ozone deposition velocities observed or inferred from observations over snow-covered surfaces. The vertical order of symbols reflects the year of the publication featuring the data (we impose small y-axis shifts for multiple years with publications). Colors indicate land use/land cover type underneath the snow. Symbols without color indicate unspecified underlying land use/land cover type or laboratory measurements. Error bars are the range of reported values, except for the forest point with 0.017 cm s^{-1} for which the error bars are one standard deviation. Numbers represent the value of the error bar cut off by the x-axis range. Figure is adapted from Helmig, Ganzeveld, Butler, et al. (2007). Data included are laboratory studies (Aldaz, 1969; Galbally & Roy, 1980) and field studies from Mawson, Antarctica (Galbally & Allison, 1972), Mt. Buller, Australia (Galbally & Allison, 1972), Illinois (Wesely et al., 1981), Lancaster, England (Colbeck & Harrison, 1985), Camp Borden (Padro, 1993; Padro et al., 1992; Wu, Z., et al., 2016), GLEES Brooklyn Lake (Zeller, 2000; Zeller & Hehn, 1995, 1996), Central Plains Experimental Range (Stocker et al., 1995), Ice Camp Narwahl (Gong et al., 1997), Alert, Canada (Hopper et al., 1998), Arctic (Helmig, Bocquet, Cohen, et al., 2007), Bruneck in the Southern Alps (Cieslik, 2009), Summit Greenland (Bocquet et al., 2011; Helmig, Cohen, Bocquet, et al., 2009), Flanders (Neirynck & Verstaeten, 2018), and Horsepool in the Uintah Basin (unpublished).
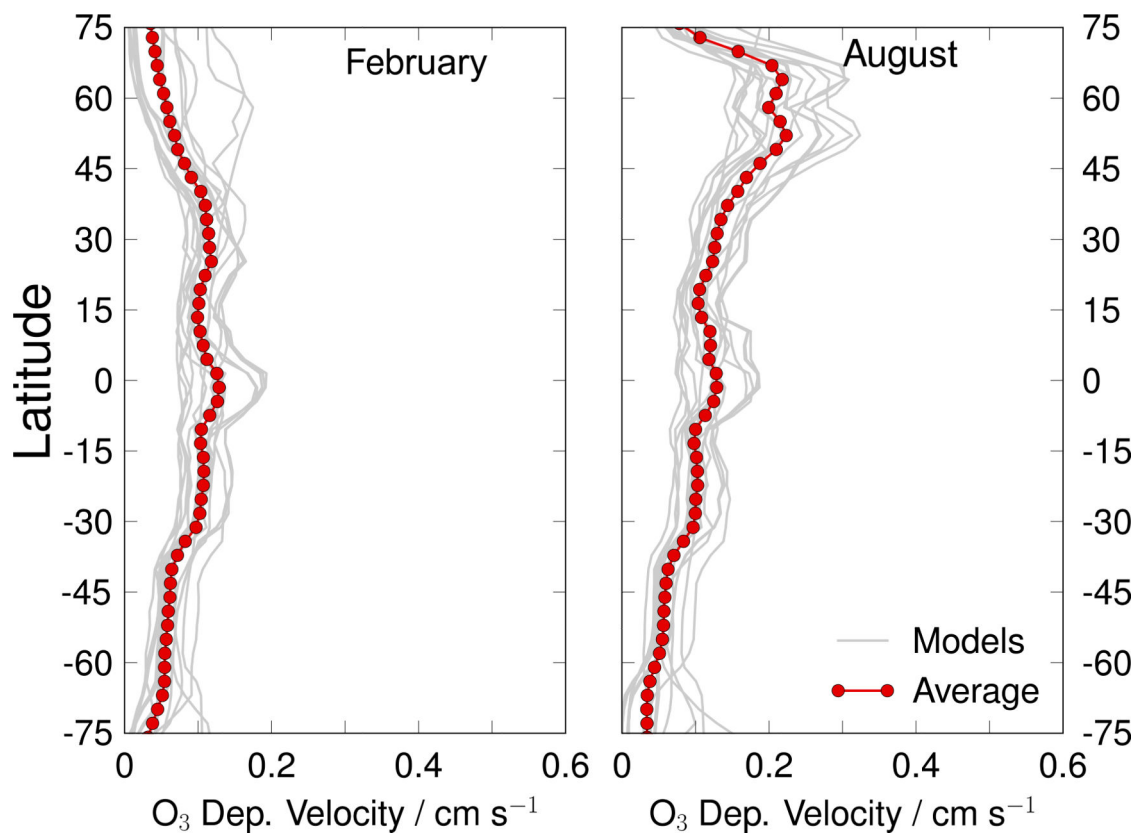
Figure 8.
Variation in ozone deposition velocity across an ensemble of global models, most of which identify as using the Wesely (1989) scheme. Latitudinal averages per three degrees latitude band are shown. Grey lines indicate individual models participating in the Task Force on Hemispheric Transport of Air Pollution model intercomparison. Red circles show the multimodel average. Figure is from Hardacre et al. (2015).
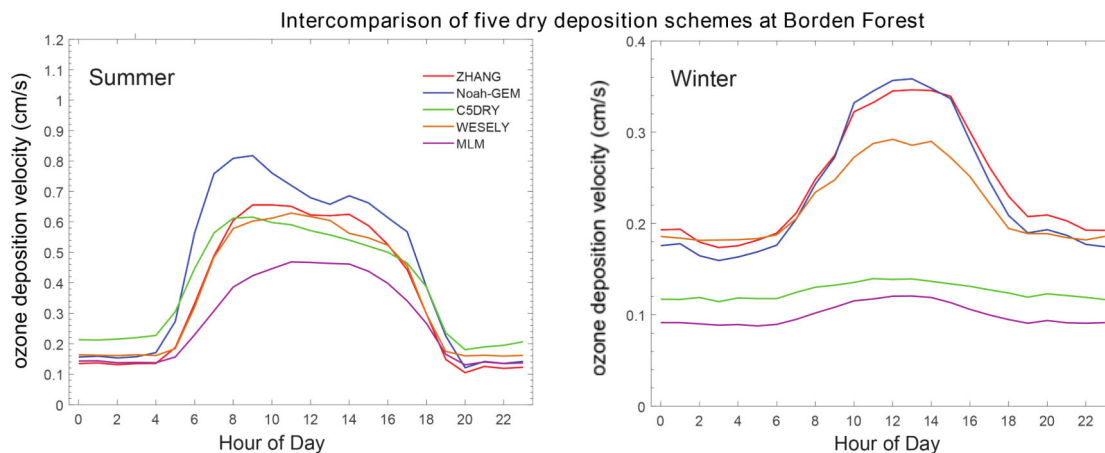
Figure 9.

Variation in simulated ozone deposition velocity across single-point models all driven by the same forcing data from Borden Forest in Ontario, Canada. Figure is adapted from Figure 1 of Z. Wu et al. (2018) with permission. © 2018. The Authors and Her Majesty the Queen in Right of Canada. This article has been contributed to by US Government employees and their work is in the public domain in the USA. This is an open access article under the terms of the Creative Commons Attribution-NonCommercial-NoDerivs License, which permits use and distribution in any medium, provided the original work is properly cited, the use is non-commercial and no modifications or adaptations are made.
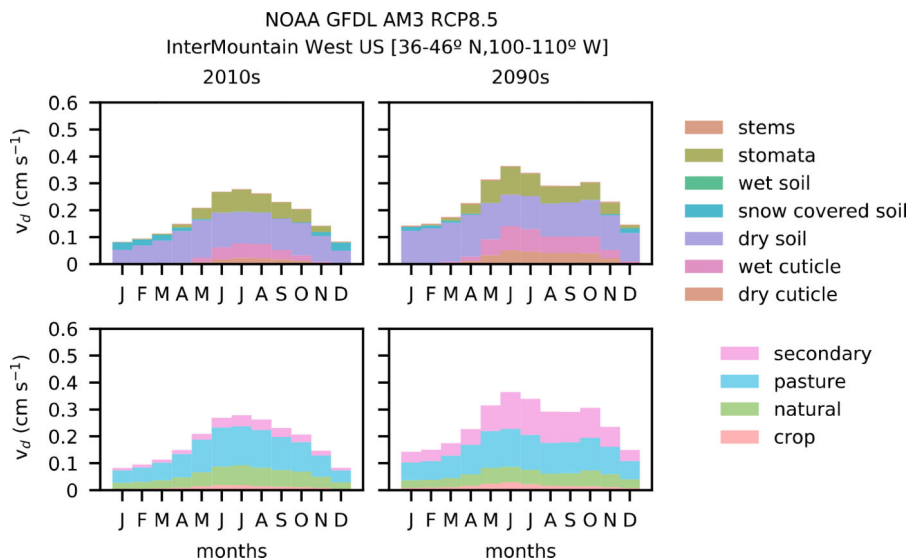
NOAA GFDL AM3 RCP8.5
InterMountain West US [36-46º N,100-110º W]

Figure 10.

Model diagnostics for process understanding of simulated ozone deposition velocity (v_d) as illustrated by regional monthly daily mean v_d for the InterMountain West United States at the beginning and end of the 21st century under RCP8.5 (a climate and emissions scenario designed for the Coupled Model Intercomparison Project 5, or CMIP5), as simulated by the NOAA GFDL atmospheric model version 3 (AM3) with dry deposition calculated in the land component of the model (Paulot et al., 2018; Clifton, 2018). Colors indicate contributions from deposition pathways (top panel) and land use/land cover types (bottom panel). The order of the labels on the legend reflects the order in which the corresponding v_d contribution is included on the figure.

Table 1

Commercially-Available Fast Ozone Analyzers.

Manufacturer or research group	Model	Type	Response time (approximate)	References
Enviscope GmbH	Schnelle Ozon Sonde (SOS)	Solid	10 Hz	Zahn et al., 2012; Zhu et al., 2015
Sextant	FOS	Solid	10 Hz	Stella et al., 2012; Li, Q., et al., 2018
Ecometrics	Chemiluminescence Ozone Fast Analyser (COFA)	Solid	10 Hz	(GFAS clone) https://www.ecometrics.it/cosa-facciamo/338-2/, date of access July 10, 2019
Ecophysics	CLD88	Gas (NO)	10 Hz	https://www.ecophysics-us.com/atmospheric-research-products, date of access July 10, 2019

Table 2

Summary of Field Studies Reporting Changes in Ozone Dry Deposition After Rain and Dew.

Site name	Measurement period and type	Site description	Sign of response to rain	Sign of response to dew	Reference
Bondville (40.05°N, 88.37°W)	two months of ozone EC fluxes	maize	increase	increase	Zhang, L., et al., 2002
Camp Borden (44°19'N, 79°56'W)	five days of ozone EC fluxes	temperate deciduous forest	increase[a]	Increase[a]	Fuentes et al., 1992
	two months of ozone EC fluxes		decrease (day), no change (night)	increase (episodic), no change (systematic)	Padro, 1994
CODE cotton (36°48'50"N, 120°40'38"W)	one month of ozone EC fluxes	cotton field		no change[a]	Massman et al., 1994
				decrease	Grantz et al., 1997
CODE vineyard (36°51'36"N, 120°6'7"W)	one month of ozone EC fluxes	vineyard		no change[a]	Massman et al., 1994
				increase	Grantz et al., 1995
Flanders (51°18'N, 4°31'E)	ten years of ozone fluxes from flux gradient technique	temperate deciduous forest	increase	increase	Neirynck & Verstraeten, 2018
Grignon (48.84422°N, 1.95191°E)	five months of ozone EC fluxes from three years each	wheat	increase	increase	Potier et al., 2015
Harvard Forest (42.53°N, 72.18°W)	four months of ozone EC fluxes from eleven years each	temperate deciduous forest	increase[b]		Clifton et al., 2019
Hyytiälä (61.85°N, 24.28°E)	six months of ozone EC fluxes from two years each	boreal forest	increase		Altimir et al., 2006
Kane Experimental Forest (41.595°N, 78.766°W)	four months of ozone EC fluxes	temperate deciduous forest	increase[b]		Clifton et al., 2019
	seven months of ozone EC fluxes		decrease (day), increase (night)	increase (day), no change (night)	Finkelstein et al., 2000
			increase	increase	Zhang, L., et al., 2002
Les Landes (44°12'N, 0°42'W)	two months of ozone EC fluxes from two years	temperate coniferous forest		increase	Lamaud et al., 2002
Nashville (36.65°N, 87.03°W)	five months of ozone EC fluxes	soybean	decrease		Zhang, L., et al., 2002
Niwot Ridge (40.03°N, 105.55°W)	three to seven months of ozone EC fluxes from four years each	subalpine coniferous forest	increase		Turnipseed et al., 2009
Rush	one day of ozone EC fluxes	senescent maize		decrease[a]	Wesely et al., 1978
Sand Flats State Forest (43.565°N, 75.238°W)	four months of ozone EC fluxes	temperate mixed forest	increase[b]		Clifton et al., 2019

Site name	Measurement period and type	Site description	Sign of response to rain	Sign of response to dew	Reference
	six months of ozone EC fluxes		increase (day), no change (night; high LAI), increase (night low LAI)	increase (day), no change (night; high LAI), increase (night; low LAI)	Finkelstein et al., 2000
			increase	increase	Zhang, L., et al., 2002
Sand Mountain (34.29°N, 85.97°W)	two months of ozone EC fluxes	pasture	decrease (day), increase (night)	increase	Zhang, L., et al., 2002
Sangamon, Illinois	two days of ozone EC fluxes	healthy maize		decrease[a]	Wesely et al., 1978

[a]findings may be particularly uncertain due to low signal-to-noise ratio or authors do not calculate systematic differences (e.g., average over composites)

[b]study does not attribute changes, or all changes, to cuticular uptake

Table 3

Summary of Field Studies Examining the Response of Soil Ozone Dry Deposition to Soil Moisture (or a Related Quantity).

Site name	Measurement period and type	Site description	Sign of change for ozone dry deposition	Details	Reference
Braunschweig (53°18'N, 10°26'E)	one month of ozone EC fluxes	cut and fertilized grassland	decrease	inferred from increases in ozone deposition following decrease in soil moisture	Mészáros, Horváth, Weidinger, et al., 2009
Castelporziano (41.42°N, 12.21°E)	two months of sub-canopy ozone EC fluxes	urban forest	decrease	inferred from correlation between measured and modeled ozone flux below the canopy for mean diel cycle (model includes effect of soil water content on ozone dry deposition to soil)	Fares et al., 2014
Central Plains Experimental Range (40°28'23"N, 104°45'15"W)	two years of ozone EC fluxes	grassland	decrease	inferred based on comparison between two different years (one with wetter soil, one with drier soil)	Massman, 1993; Stocker et al., 1993; Massman, 2004
Grignon (48.84422°N, 1.95191°E)	three months of ozone EC fluxes	bare agricultural soil	decrease	inferred from correlation between soil water content and r_{soil}[a]	Stella, Loubet, Lamaud, et al., 2011
	one month of ozone EC fluxes	bare agricultural soil	increase	increased ozone uptake by soil after rainfall (attributed increases to tillage and slurry application)	Vuolo et al., 2017
Flanders (51°18'N, 4°31'E)	ten years of ozone fluxes from flux gradient technique	temperate mixed forest	decrease	inferred from correlation between v_d and ground water table depth	Neirynck & Verstraeten, 2018
Harvard Forest (42.53°N, 72.18°W)	nine years of ozone EC fluxes	temperate deciduous forest	decrease	inferred from anticorrelation between summertime mean v_d and cumulative rain over summer and modeling	Clifton et al., 2019
Ispra (45.8126°N, 8.6336°E)	one year of ozone chamber flux measurements	temperate deciduous forest	decrease	inferred from correlation between soil water content and r_{soil}	Fumagalli et al., 2016
Sinderhoeve (51.58°N, 5.42°E)	ten days of ozone EC fluxes	cornfield	decrease	inferred based on decreases in nonstomatal deposition with soil moisture	Van Pul & Jacobs, 1994
Walker Branch Watershed (35°57'30"N, 84°17'15"W)	two weeks in spring and two weeks in fall 1988 of ozone EC fluxes above soil	mixed forest	no change	data not shown; only concluded	Meyers & Baldocchi, 1993
Huntington Forest (43°59'N, 74°14'W)	ten days in July 1990 of ozone EC fluxes above soil	temperate deciduous forest	no change	data not shown; only concluded	Meyers & Baldocchi, 1993

[a]r_{soil} is the resistance to ozone dry deposition to soil

Table 4

Recommendations for Ecosystem-Scale Field Measurement Setups Including Ozone Eddy Covariance Flux and Ozone Concentration Profiles, organized by the scientific question that determines the highest-priority other measurements.

Scientific Question	Other measurements (long term)	Other measurements (short term)
What is the contribution of stomatal uptake to ozone dry deposition?*	water vapor flux, carbon dioxide flux, friction velocity	other independent tracers of stomatal conductance (e.g., carbonyl sulfide flux), canopy skin temperature
What is the contribution of leaf cuticular uptake to ozone dry deposition?	humidity, leaf/canopy wetness, leaf area index, dew point temperature, precipitation, same as * to obtain residual ecosystem-scale nonstomatal conductance	chamber fluxes for ozone around branches including tracers of stomatal conductance to isolate cuticular uptake, composition of cuticles
What is the contribution of soil uptake to ozone dry deposition?	soil moisture and temperature, same as * to obtain residual ecosystem-scale nonstomatal conductance	lower canopy ozone fluxes, fluxes of NO, NO_2, and highly reactive BVOC emission from soil, chambers measuring ozone uptake by soil, soil properties (e.g., organic content, clay content, porosity, hydraulic conductivity)
What is the contribution of chemistry in the canopy air space to ozone dry deposition?	NO and NO_2 fluxes, highly reactive BVOC fluxes, same as * to obtain residual ecosystem-scale nonstomatal conductance	fluxes of oxidation products
How do snow-covered surfaces influence ozone dry deposition?	horizontal and vertical extent of snow cover, snow age	snow impurities and NO content of snowpack